Examination of alternative splice code of Neurexins for synaptic specification

Inauguraldissertation

zur
Erlangung der Würde eines Doktors der Philosophie
vorgelegt der
Philosophisch-Naturwissenschaftlichen Fakultät
der Universität Basel

von

Thi-Minh Nguyen
aus Freiburg im Üechtland, Schweiz

Basel, 2016

Genehmigt von der Philosophisch-Naturwissenschaftlichen Fakultät

Auf Antrag von:

Prof. Dr. Peter Scheiffele

Prof. Dr. Silvia Arber

Basel, den 22.März2016

Prof. Dr. Jörg Schibler

Dekan der Philosophish-

Naturwissenschaftlichen Fakultät

Table of content

Summary

The brain is composed of a large number of cells types that assemble together into highly specific circuits. Precise connectivity is crucial to ensure proper brain functions and requires mechanisms that generate molecular diversity to encode certain aspects of neuronal wiring. One possible mechanism to generate molecular diversity is alternative splicing. For example through alternative splicing *Neurexin* (*Nrxn1-2-3)* genes have the potential to give rise to more than 12'000 protein isoforms (Tabuchi and Sudhof, 2002). Neurexin has been demonstrated to be involved in synapse formation and functions (Reissner et al., 2013). Importantly, studies have reported that alternative splicing plays a pivotal role in the function of Neurexin as it regulates their interaction with a large variety of ligands (Reissner et al., 2013). This in turn can promote the differentiation of distinct postsynaptic structures (Chih et al., 2006). Therefore, Neurexins constitute ideal candidates to encode certain parameters of synaptic connectivity. However, a central question has remained unraveled. Indeed, the spatial logic of Neurexin isoforms expression in the brain is not well understood.

Here, I report that by using bichromatic reporters, alternative splicing is differentially regulated between neuronal and non-neuronal cell populations and that the alternative splicing activity within a cell population can exhibit different levels of cell-to-cell variations. By profiling *Nrxn* mRNA repertoires in genetically-defined neuronal cell populations, I have identified highly divergent splice insert incorporation choices in two fundamentally different neurons populations in the hippocampus. Indeed, exon 21 which encodes for splice insert at alternative splice segment 4 (AS4) in *Nrxn* is predominantly incorporated in mRNA in Parvalbumin interneurons compared to excitatory Camk2 pyramidal neurons. Finally I investigated the function of Neurexin isoforms containing the exon 21 *in vivo* by conditionally deleting them in Parvalbumin interneurons population. Anatomical analyses indicated that synaptic density and vesicle docking were unaltered. However, mice in which isoforms containing splice insert at AS4 in *Nrxn 1* and *3* were deleted, displayed an impaired short-term memory formation.

Thus, my study has provided evidences that alternative splicing regulation of *Nrxn genes* is genetically encoded and that deletion of cell-type specific isoforms impairs neuronal functions. This highlights the relevance of cell-type specific regulation of alternative splicing.

1.Introduction

1.1. General introduction

The brain is a central networks system that processes neuronal information within diverse neuronal circuits to control the vital and cognitive functions of organisms. In those circuits, neurons exhibit a large number of different cell types which communicate with each other through specialized structures called synapses. The synapses formed by different neuronal cell populations display different transmission properties. Recent genome-wide studies have revealed that mutations in molecules expressed at synapses are linked with cognitive diseases such as autism spectrum disorder or schizophrenia. This highlights the importance of correct synaptic connectivity und function between neurons. Molecular mechanisms that instruct the formation of synapses have been identified. However, the mechanisms that specify synapse functions in different neuronal cell populations are currently not well understood. In order to gain more insights into the pathophysiology underlying cognitive diseases, it is crucial to investigate how synapses with specialized functions are generated.

1.2. Neuronal diversity

The brain is composed of a myriad of neuron cell types which are assembled into distinct circuits to perform neuronal information processing. It is believed that each neuronal cell population due to its intrinsic molecular and functional properties contributes to distinct aspects of information processing. An example for this is the firing patterns of distinct neuronal populations in the hippocampus during the theta oscillations (Klausberger et al., 2003). It is believed that those oscillations ranging from 4 to 10Hz are important for spatial navigation in rodents or during certain phases of sleep (Buzsaki and Moser, 2013). By recording the firing patterns of three distinct neuronal populations, it was observed that they exhibit different discharge timing (Klausberger et al., 2003). For example, one population was found to preferentially fire in the descending phase of the oscillations whereas the other would discharge right after the peak of the theta oscillations. This finding strongly suggests that distinct neuronal populations are involved in various aspects of neuronal coding. In consequence, it remains to determine how to define a neuronal population.

Historically, neuronal cell populations were defined by their anatomy. Ramon y Cajal's pioneer works put into light that neuronal cells exhibit distinct cellular shapes and that they present highly organized connection patterns in diverse brain areas. Now after decades of research it has becoming clear that defining a cell population relies additionally on the molecular markers they express and also on their processing capabilities. Nonetheless, recent works have reported that within a defined cell type, those neurons were not entirely identical as they can be recruited by distinct neuronal pathways, indicating that additional criteria might be required for distinguishing subpopulations. In this first part, I will discuss on possible molecular markers used to identify neuronal cell populations and also their functional properties.

Neurotransmitters are essential small molecules to transmit neuronal information at neuronal chemical synapses. The principal neurotransmitters employed in the central nervous system are glutamate, γ- aminobutyric acid (GABA) and glycine. Glutamate and GABA are the most widely used and permit to distinguish between two major populations of neurons. Glutamate is an excitatory neurotransmitter and neurons that use glutamate (=glutamatergic neurons) are often referred as principal cells. These neurons make predominantly long-range connections with different brain areas and account for circa 80% of total neuronal population. In contrast, GABA is an inhibitory neurotransmitter which is used by approximatively 20% of the total neuronal population. GABAergic interneurons usually make local projections but long range projections have also been described (Kepecs and Fishell, 2014).

Glutamate or GABA release induces two fundamental opposite effects at the postsynaptic membrane. The binding of neurotransmitter to their cognate receptors trigger distinct postsynaptic responses. Glutamatergic synapses induce depolarization which activates postsynaptic cells whereas GABAergic synapses generate hyperpolarization of the postsynaptic neurons. Moreover, glutamatergic neurons relay neuronal information across different brain areas while GABAergic interneurons through their inhibition modulate locally neuronal information transmission by controlling the coordination of neuronal networks activity and the gating of information (Kepecs and Fishell, 2014).

Glutamatergic excitatory and GABAergic inhibitory neurons have large diversity of cells which can be identified by molecular antigens. For example calcium buffer proteins or neuropeptides have been used to identify different cell types of

interneurons. Those are parvalbumin (PV), somatostatin (SOM), vasoactive intestinal peptide, cholecystokin (CCK) calretinin, neuropeptide Y and nitric oxide synthetase. PV, SOM and vasoactive intestinal peptide positive interneurons together account for 85% of total interneurons and can build non-overlapping classes (Kepecs and Fishell, 2014). In contrasts to neurotransmitter, the role of those calcium buffer proteins or neuropeptides are not elucidated yet. Nonetheless, they have been commonly used in research as they reliably enabled the identification of ensemble of neurons that exhibit same processing capabilities.

Based on large number of electrophysiological studies, it is known that those interneurons populations display stereotyped firing patterns and also specific innervation patterns (Klausberger and Somogyi, 2008). For example in the *Cornu Ammonis* 1 (CA1) region of the hippocampus, two interneurons populations, parvalbumin positive (PV^+) and cholecystokin positive (CCK^+) cells, included so-called basket cells which innervate the perisomatic region of excitatory pyramidal cells in the CA1. Although they share similar anatomical properties, they express distinct molecular markers and importantly they can be differentiated by their firing pattern. Indeed, upon stimulation PV^+ cells provide a strong transient inhibition by generating fast spikes whereas CCK^+ produces asynchronous spikes which in turn mediate a long-lasting inhibition on CA1 cells (Klausberger and Somogyi, 2008).

Combining anatomical, molecular and functional criteria to define cell types provide an objective identification scheme which allows to investigate the function of specific cell types within a neuronal circuit. Nonetheless, recent studies demonstrated that certain populations that were commonly viewed as a homogenous ensemble of neurons contain subpopulations which exhibit very distinct activity patterns. Indeed PV^+ interneurons included predominantly basket cells and axo-axonic cells. PV^+ interneurons provide either feedforward inhibition or feedback inhibition and critical for generation of network oscillations such as the theta and gamma oscillations as well as sharp waves ripples (Hu et al., 2014). In a recent study, it has been observed that population of PV^+ basket cells form two distinct networks namely low or high PV networks configurations (Donato et al., 2013). Those are defined by the level of parvalbumin they express. Interestingly, mice housed in enriched environment displayed a higher number of low PV^+ neurons and showed an enhanced structural plasticity. In contrast, fear conditioning induced an elevation of high PV^+ neurons, however without affecting structural plasticity (Donato et al., 2013). Given that PV^+

share the same morphology and processing capability, it raises the question of how how distinct PV^+ network can arise. Following study has revealed that the birth time of PV^+ basket cells plays a crucial role in the recruitment of those cells in various hippocampal-dependent learning tasks (Donato et al., 2015). Indeed timing of neurogenesis was found to give rise to PV^+ interneurons with distinct connectivity pattern and plasticity regulation.

To conclude, neuronal cells types can be defined by anatomical, molecular and functional properties. However, recent data revealed a more complex picture of neuronal diversity and suggests also to consider neurogenesis for defining cell types. During the formation of the neocortex, the corticogenesis, the expression of distinct transcription factors direct specification programs of neuronal progenitors to give rise to entirely different cell types. Therefore in the second part, I will discuss how the origin and the timing of birth of neurons can specify their identity and therefore can be considered as classification criteria.

The vast majority of interneurons are generated from the medial or caudal ganglionic eminences which are transient structures during brain development located outside of the neocortex in the ventricular zone of the telencephalon (Wonders and Anderson, 2006). Excitatory neurons are born in the neocortex, in the layers adjacent to the ventricle which are called ventricular zone (VZ) or subventricular zone (SVZ). The neocortex is composed of 6 horizontal cell layers which are generated in an inside-out fashion during corticogenesis (Molyneaux et al., 2007). Neurons that are first born contribute to the deep cortical layers while the one born later form the upper cortical layers. For a long time it has been though that the fate of neuronal progenitors in the VZ or SVZ become more restrictive as the development of the brain progress (Molyneaux et al., 2007). However recent studies reported that neuronal progenitors inherit specification program before their differentiation (Costa and Muller, 2014).

A large body of evidences demonstrated that each cortical layer contains very diverse subpopulations of neurons (Molyneaux et al., 2007; Harris and Mrsic-Flogel, 2013). Indeed each layer displays specific neuronal cell populations with distinct anatomy, gene expression programs, firing pattern or connectivity (Molyneaux et al., 2007; Harris and Mrsic-Flogel, 2013) . For example the transcription factor CTIP2 is

crucial during corticogenesis for the specification of a subpopulation called corticospinal motor neurons in layer V which projects to the spinal cord (Arlotta et al., 2005). Indeed, ablation of CTIP2 in mice impaired axonal projections of the corticospinal motor neurons to the spinal cord, demonstrating that cell-type specific gene expression programs regulate the specification of cortical subpopulations (Arlotta et al., 2005).

To sum up, neurogenesis provides supplementary information about the localization and connectivity of adult neurons. Moreover some transcription factors such as CTIP2 remains expressed in the adulthood and thus can be also used as a molecular marker to define the subpopulation in the layer V.

1.2.1. Molecular mechanisms to establish specific connectivity in neuronal circuits

Previous section described that the brain comprises of a large variety of neurons which are organized into highly precise neuronal circuits. The assembly of neuronal circuits relies on correct connections between neurons. How do neurons within this ocean of cells know who its matching partner is? In 1963 Sperry emit the chemoaffinity hypothesis which posits that a neuron can recognize its matching partner because both cells express the molecular identification tags that exhibit cytochemical affinities (Sperry, 1963).

Here, I will discuss the concept of self-recognition which enables neuronal cell to distinguish between the self from the non-self. This recognition is crucial to generate correct innervation patterns as it prevents self-crossing and promotes optimization of field covering (Zipursky and Grueber, 2013). I will also discuss the molecular mechanisms that determine the specificity of synapse formation at the cellular and subcellular levels. Moreover I will provide evidences of transsynaptic complexes which have been demonstrated to initiate the formation of synapses.

1.2.1.1. Molecular mechanisms for neuronal self-recognition

Proper development of neuronal circuits requires recognition mechanisms enabling neurons to discriminate themselves from other. This concept called self-recognition plays an essential role for neuronal processes to form proper innervation patterns (Zipursky and Grueber, 2013). Studies in flies and mammals have revealed that self-recognition is established by homophilic interactions between cell-adhesion molecules which result in repulsion of neurites of the same cell and segregation of sister branches (Zipursky and Grueber, 2013). Due to immense number and anatomical proximity of neuronal cells, a high molecular diversity is required to encode cell identity. Cell surface receptor families with high molecular diversity like Down syndrome cell adhesion molecule (Dscam) and Protocadherin (Pcdh) have been proposed to provide this function in the invertebrate and vertebrate nervous system respectively (Zipursky and Grueber, 2013). In this section I will discuss molecular mechanisms by which Dscam and Pcdh establish self-recognition in the nervous system and how much of molecular diversity is required for establishing self-recognition.

DSCAM 1 and *2* genes encode for surface receptors which were discovered in 1998 during a screen to identify gene responsible for Down syndrome in human (Yamakawa et al., 1998). Later, the paralogs of *DSCAM* genes in Drosophila were identified. Dscam are single-pass transmembrane proteins of the immunoglobulin (Ig) superfamily. The receptors are organized into an extracellular ectodomain displaying 10 Ig domains, 6 fibronectin type III repeats, a transmembrane domain and a C-terminal cytoplasmic tail (Schmucker et al., 2000). Unlike the human and mouse *Dscam 1* (Agarwala et al., 2001), alternative splicing regulation at *Dscam 1* gene is more extensive in Drosophila and generates 19'008 different ectodomains which can contain two different intracellular domains (Figure 1A)(Schmucker et al., 2000). The alternative splicing at Dscam 1 was found to be based on stochastic decisions (Neves et al., 2004; Miura et al., 2013). Thus, the extraordinary number of Dscam 1 molecules provides molecular basis for self-recognition.

Dscam 1 gained some attention when a mutant fly generated through mutagenesis was reported to present disorganized axons and impaired sister branches segregation in the mushroom body (Wang et al., 2002a). Following studies

have demonstrated that Dscam 1 also promote repulsion between sister dendrites (Hughes et al., 2007; Matthews et al., 2007; Soba et al., 2007; Zhu et al., 2006).

The molecular basis of self-recognition is provided by the homophilic nature of Dscam 1 interactions. In fact, Dscam 1 isoform displays strictly isoform-specific interactions (Wojtowicz et al., 2004). Thus it is believed that neurites of the same neuron express the identical set of isoforms on the cell surface and that upon contact the isoforms engage homophilic interactions which then trigger neurite repulsion.

Single neuron express only between 14 and 50 DSCAM mRNAs, which constitutes an infinitesimal part of Dscam1 repertoires (Neves et al., 2004). This raises the question of how important is Dscam1 diversity in establishing self-avoidance? Interestingly, the re-expression of a single isoform within in a *Dscam1* knock-out neuron is sufficient to restore self-avoidance (Hughes et al., 2007; Matthews et al., 2007; Soba et al., 2007). However at the global neuron population levels thousands of Dscam1 isoforms are required to establish proper neuronal wiring (Hattori et al., 2009; Chen et al., 2006).

As mentioned above, mammalian *DSCAM 1* gene is not subject to the same extensive alternative splicing regulation observed in the Drosophila (Agarwala et al., 2001). Instead, the Dscam1 functional mammalian counterpart is thought to be represented by the clustered Protocadherin (Pcdh) receptors family. Clustered Pcdh belong to cadherin superfamily. As the name suggests, clustered Pcdh are organized in three linked gene clusters namely α (alpha), β (beta) and γ (gamma) (Figure 1B) (Wu and Maniatis, 1999; Wu et al., 2001) . In mice *Pcdh-α* and *-γ* gene contain respectively 14 and 22 variables exons which encode the extracellular domain that comprise of EC1 to 6, a transmembrane domain and a portion of the cytoplasmic domain. Three constant exons then encode the common part of the cytosolic domain. Pcdh β is divergent from the Pcdh α and γ because it is composed only of 22 exon genes. The particularity of the Pcdh α and γ is that each variable exon possesses its own promoter (Tasic et al., 2002; Wang et al., 2002b).

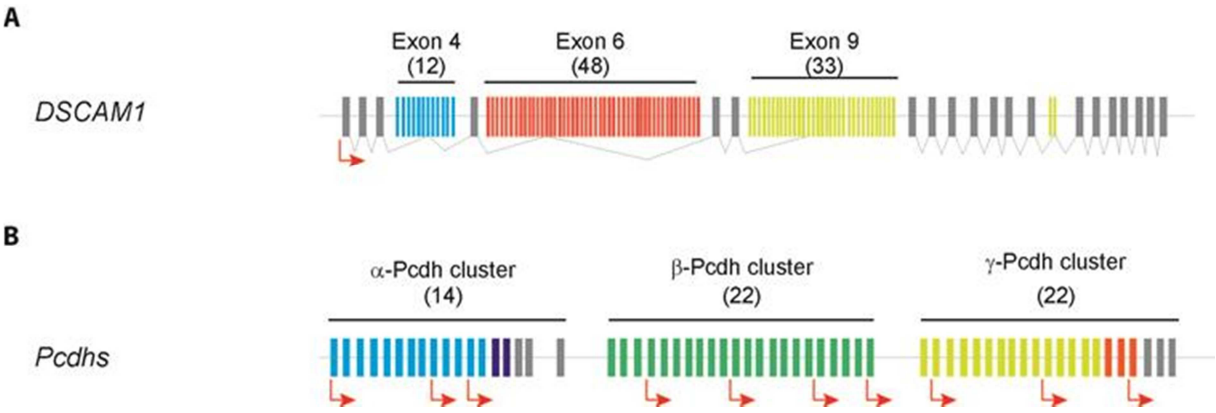

Figure 1- Genomic organization of DSCAM1 and protocadherins

Schematic depiction of Drosophila DSCAM1: alternative exon clusters 4, 6, 9 and 17 are colored. (A) Alternatively spliced segments 4,6 and 9 contain 12, 48 or 33 alternatively spliced exons. At each cluster mechanisms ensure that only one alternative exon is included into the mature mRNA. (B) Simplified model of the clustered protocadherin locus (Pcdh). Each of the 58 potential alpha-Pcdh, beta-Pcdh, and gamma-Pcdh transcripts is expressed from individual promoters preceding the variable exons (exons in blue, green and yellow, respectively; some selected promoters indicated as red arrows). Figure is adapted from (Schreiner et al., 2014c)

Single-cell reverse transcription PCR (RT-PCR) revealed that cerebellar Purkinje cells select the variable exon promoter stochastically and depending on which isoforms the promoter choice can be the same on both alleles or different on each allele (Esumi et al., 2005; Hirano et al., 2012; Kaneko et al., 2006).

The self-avoidance property of Pcdh has been revealed by the deletion of all 22 variable exons of Pcdh-γ gene in starbust amacrine cells (SAC) in the retina and in Purkinje cells in the cerebellum and cortical neurons (Lefebvre et al., 2012; Garrett et al., 2012). Retinal SAC cells form radially symmetric patterns. However in the *Pcdh-γ* knock-out SAC, the dendrites cross each other at higher frequency and also bundle together, which is very similar to the phenotype exhibited by the *Dscam 1* knock-out mushroom body (Wang et al., 2002a). Moreover Pcdh-γ establishes self-avoidance in a cell autonomous manner. Importantly those phenotypes can be rescued by expression of a single Pcdh isoform independently of its identity. In addition to the self-avoidance, studies have also reported that Pcdhs are involved in many neuronal development processes including neuronal survival, synapse formation, axonal targeting, dendritic arborization and self-recognition based of avoidance in dendrites (Chen and Maniatis, 2013).

Pcdh genes can generate in theory 58 potential different protein isoforms which is far below than *Dscam 1* gene (Zipursky and Grueber, 2013). In contrast to Dscam 1, Pcdhs form multimers (most presumably tetramers) which have been described to form transsynaptic complexes only when multimers at both sides of the membranes are identical (Rubinstein et al., 2015; Schreiner and Weiner, 2010; Thu et al., 2014). Indeed Pcdhs assemble as homologous or heterophilic multimers and neurites repulsion occurs only when all isoforms are identical. Pcdh form multimers in *cis*-interaction (same cell) with the EC6 where the molecular identity of the isoforms is not determining (promiscuous interactions). In the other hand Pcdh form multimers in *trans*-interaction (one cell with another) in a homophilic fashion with their EC1-EC4 domains (Schreiner and Weiner, 2010; Rubinstein et al., 2015). Thus in this configuration, there are potentially 521.855 possible tetramer combinations which in turn increases dramatically the recognition interfaces (Schreiner and Weiner, 2010). Therefore, through stochastic expression of distinct sets of Pcdh in each neurons and through homophilic transsynaptic multimers interactions, Pcdhs provide molecular substrate for neuronal identity and thereby a mean to recognize the self from the non-self in mammalian nervous system.

To conclude, self-recognition is crucial for accurate neuronal wiring and it is mediated by repulsive interaction between neuronal processes. Moreover, the molecular basis of self-recognition is provided by cell adhesion molecule families which produce highly diverse recognition interfaces either by extensive alternative splicing or by combinatorial expression and homophilic interactions of multimers.

1.2.1.2. Molecular mechanisms to specify synaptic connections

Neuronal wiring depends on correct matching of the pre- and postsynaptic partners. Although self-recognition enables neurons to distinguish between each other, it does not induce formation of synapses leading to the question of how specific synaptic connections are generated in the nervous system. On the one hand, neuronal activity can instruct synapses formation. This comprises of spontaneous or sensory-driven activity. Neuronal stimulation can promote the transcription of specific genes which in turn can induce synapses formation or change synaptic molecular composition (West

and Greenberg, 2011). On the other hand, neurons are “hard-wired”, in other words, there are genetically-encoded wiring programs to induce and specify synaptic connections (Yogev and Shen, 2014). In this work I will concentrate on molecular programs that are encoded in neuronal cell populations that give rises to highly specific synaptic connectivity.

Ramon y Cajal has recognized that neuronal wiring displays very specific connectivity patterns at different layers. Indeed the specificity is observed at the level of the choice of partners (cell-type specific) and of the contact site in a subcellular domain of a neuron. Here I will discuss molecular mechanisms by which neurons form synaptic contacts with matching partners and at the proper subcellular segments. In addition, I will provide examples of synaptic cell adhesion molecules that instruct the differentiation of synapses and that modulate synaptic transmission properties.

1.2.1.2.1. Cell-type specificity

For proper functioning of neuronal circuits, it is crucial to connect different neuronal cell populations in a specific logic. During synaptogenesis, by using intracellular calcium signaling it has been reported that neurons probe their environment and sample partners (Lohmann and Bonhoeffer, 2008). Indeed, upon initial contacts between dendrites and axons a transient calcium influx is generated. It was then observed that local calcium signal was stronger at synaptic sites which will be stabilized over a long time period. This study raises the question of the molecular mechanisms that allow neurons to engage synaptic interactions with the matching partner. Studies in the spinal cord have reported that transcription factors can control transcription programs for correct targeting of neuronal processes (Vrieseling and Arber, 2006). Here, I will provide evidences that cell-type specific interactions are mediated by adhesive or repulsive cellular responses triggered by cell-surface molecules.

In the cerebellum the formation of synapses between pontine neurons and granules cells is thought to be regulated by a combination of adhesive and repulsive cellular responses. During the development, pontine neurons make transient synapses with Purkinje cells before they form synapse with granule cells. Indeed, in

the second postnatal week, Purkinje cell-pontine neurons synapses are eliminated resulting in selective innervation with granules cells (Kalinovsky et al., 2011). The synapse elimination was showed to be dependent on BMP4 expression in the Purkinje cells (Kalinovsky et al., 2011). Using conditional knock-out in which BMP4 is selectively ablated in Purkinje cells, it was observed that Purkinje cell-pontine neurons synapses persisted in the mature brain, indicating that BMP4 provides repulsive signal to remove inappropriate synapses. On the other side, it was reported that positive signal involving Cadherin-7 could also contribute to the formation of synapses between pontine neurons and granules cells (Kuwako et al., 2014). Cadherin-7 is expressed by pontine neurons and granules cells. The knock-down of Cadherin-7 in pontine neurons increased the number of pontine neurons axons innervating Purkinje cells and this phenotype was rescued by expression of Cadherin-7 which is resistant to siRNA interference in pontine neurons. Thus, these studies highlight the complexity and possible cross-talk between different cellular pathways to direct cell-type specific innervation.

Another member of Cadherin has also been reported to be involved in formation of cell-type specific synapses in the hippocampus (Williams et al., 2011). Cadherin-9 is selectively expressed in the Dentate Gyrus (DG) and CA3 (Bekirov et al., 2002). DG mossy fibers form giant synapses only onto proximal dendrites of CA3 pyramidal neurons. Those pyramidal cells also receive inputs from other CA3 cells and from entorhinal cortex. The *in vivo* knock-down of Cadherin-9 in DG led to the alteration in mossy fibers size and density but left the other synapses formed by CA3 cells and entorhinal cortex intact. Moreover, mossy fibers buttons density was reduced (Williams et al., 2011). The fact that a substantial synapse number is still detected in the knock-out raises the question of how much does Cadherin-9 contribute specifically to the formation of the DG-CA3 synapses. The authors suggest that the loss of Cadherin-9 could be compensated by the other Cadherin members which are also expressed in the hippocampus.

Similar molecular mechanisms based on adhesive or repulsive properties to establish whole-cell are also reported in visual cortex or in fly nervous system (reviewed by Yogev and Shen, 2014)

Thus, cell-type specific synapses depend on the expression of molecules which elicit either adhesive or repulsive cellular response upon contact. As mossy fibers from the

DG form only synapses onto distal dendritic tree segments in the hippocampus, it strongly indicates that the process of selecting the correct cellular partner and the subsequent proper innervation targeting are closely linked to each other.

1.2.1.2.2. Subcellular synaptic specificity

Neurons have the possibility to form synapses at distinct subcellular compartments. These subdomains comprise of dendritic tree (proximal versus distal parts), perisomatic region or axon initial segment. Precise subcellular targeting is crucial because the position affects the response of the postsynaptic cell. Indeed, inhibitory synapses formed onto cell soma or at the initial segments provide distinct type of inhibition compared to those made onto distal dendrites. Perisomatic synapses can suppress the initiation of action potential whereas dendritic inhibition suppresses calcium-dependent potentials (Miles et al., 1996). Moreover the timing of these inhibitions differs. Perisomatic synapses provide strong transient inhibition at the onset of action potential series whereas distal dendritic synapses give rise to late but small persistent inhibition which depends on the rate of action potentials (Pouille and Scanziani, 2004).

Specific subcellular synapse formation implies the existence of mechanisms to guide directly axons to correct subcellular target domain. The best example to illustrate this, is provided by Ankyrin-G and Neurofascin 186 complex in the cerebellum (Ango et al., 2004). Cerebellar GABAergic basket cells interneurons form so-called pinceau synapses onto axon initial segment of Purkinje cells (Ango et al., 2004). After their migration in the molecular layer, basket cells send their axons to the axon initial segment of Purkinje cells. For this, basket cells axons follow a subcellular gradient established by cell adhesion molecule called Neurofascin 186. This gradient is generated through membrane protein Ankyrin-G which expression is restricted to axonal initiation segment of Purkinje cells. Indeed in normal mice, Ankyrin-G recruits somatic Neurofascin 186 to the axon initial segment and thereby creates a gradient. In Purkinje cell-specific Ankyrin-G knockout mice, Neurofascin 186 gradient is disrupted. This results in reduction of inhibitory pinceau synapses and in aberrant axon projections of basket interneurons. Therefore, Neurofascin 186 and Ankyrin-G

actively guide GABAergic basket cells axons to innervate specifically axon initial segments of Purkinje cells.

Thus by generating a subcellular gradient of cell adhesion molecules, axons can be targeted to appropriated subcellular segments, determining, where synapses are formed.

1.2.1.2.3. Initiation of synapses formation through synaptogenic complexes

The cell surface adhesion molecules described above lack the capability to induce the formation of synapses and therefore, additional molecular mechanisms are required for this. In this part, I will describe synaptogenic complexes that can operate at different synapses to promote the differentiation of excitatory and inhibitory synapses and synaptic molecule that can modulate release probability of synaptic vesicles and plasticity.

In the central nervous system most prominent example of transsynaptic complex capable to induce synapse formation is illustrated by the complex comprising of presynaptic Neurexins and postsynaptic Neuroligins (Dean et al., 2003; Scheiffele et al., 2000; Krueger et al., 2012). In co-culture assays, it has been demonstrated that Neuroligin promotes the formation of *de-novo* presynaptic structures (Scheiffele et al., 2000). Co-cultures assays enable to determine whether a molecule can induce synapse formation and thus they have been extremely useful for validating synaptogenic candidates. In those assays, non-neuronal cells are transfected with a putative synaptogenic molecule and then co-cultured with neuronal cells. If a molecule possesses synapse organizing capabilities, it will induce formation of synaptic structures on neuronal process that contact with the nonneuronal cell. This can be detected by the expression of synaptic markers specific for mature synapses. In the case of Neuroligin study, HEK293T cells were transfected with Neuroligin and then mixed with pontine explants. It was then demonstrated Neuroligin induced the differentiation of presynaptic structures of contacting axons (Scheiffele et al., 2000)s. By electron microscopy, it was then

confirmed that synaptic contacts consisted of functional presynaptic structures as vesicle clusters could be observed at the active zones in the axons.

In the case of Neurexins, their synapse organizing function was revealed by an alternative method (Dean et al., 2003). Concretely, hippocampal neurons were transfected with Neurexin 1 β tagged with vesicular stomatitis virus (VSV) epitopes. Anti-VSV antibodies that were previously multimerized with secondary antibodies were then added to the cultures. It was then observed that at Neurexin 1 β aggregates, synapsin which is a presynaptic protein of the vesicle release machinery had accumulated, demonstrating that Neurexin induce the formation of presynaptic structures. Additional experiments reported that Neurexin and Neuroligins can promote the synapse formation in a bi-directional manner (Graf et al., 2004; Chih et al., 2006).

How do Neurexin-Neuroligin complex assemble synaptic structures? Neuroligin triggers the differentiation of postsynaptic structures by its recruitment of postsynaptic scaffold protein PSD-95 but also of AMPA and NMDA (Barrow et al., 2009; Mondin et al., 2011; Heine et al., 2008) receptors. Studies have shown that Neurexin intracellular domain interact with CASK (Hata et al., 1996) and Mint (Biederer and Sudhof, 2000). It has then been proposed that this interaction provides the link between the vesicle release machinery and calcium signaling, which are both elements essential for presynaptic release of vesicle (Reissner et al., 2013).
A very interesting element about Neurexin-Neuroligin complex, is that they can induce the formation of *de novo* synapse which can be either excitatory or inhibitory (Chih et al., 2006). To differentiation into glutamatergic or GABAergic synapses is regulated by alternative splicing at Neurexin (Chih et al., 2006). The regulation of alternative splicing in Neurexin will be discussed in the next part.

Thus, Neurexin and Neuroligin transsynaptic complex provides a molecular mechanism by which synapses formation can be triggered but beside them, other cell surface molecules have been reported to induce the formation of synaptic structures (Missler et al., 2012; Woo et al., 2013). For example the protein tyrosine phosphatase receptors (PTP) family, which is expressed presynaptically, has been demonstrated to organize both excitatory and inhibitory synapses (Takahashi and Craig, 2013).

Indeed protein tyrosine phosphatase LAR (leukocytes common antigen-related) was reported to interact with NGL-3 (Netrin-G ligand-3) to promote the differentiation of excitatory synapses (Woo et al., 2009). Interestingly, co-cultures

assays demonstrated that NGL-3 can induce the formation of excitatory and inhibitory synapses on contacting axons whereas LAR promoted the clustering only of excitatory synaptic structures in contacting dendrites. To further investigate the synaptogenic activity, NGL-3 was either overexpressed or knocked-down in neuronal cultures. It resulted to an increase and decrease of synapse density respectively. Moreover in the knock-down cultures, neurons displayed a reduction of mEPSC frequency which supports the finding of reduction of synapses number. Thus, this study demonstrated that excitatory synapses can be induced by the transsynaptic LAR-NGL3 complex.

As previously mentioned, PTP family member can also induce the formation of inhibitory synaptic structures. Indeed PTPδ has been reported to promote formation of inhibitory synapses by interacting with Slitrk3 (Takahashi et al., 2012). Using co-culture assays, fibroblasts expressing Slitrk3 and PTPδ induced selectively the formation of inhibitory pre- and postsynaptic structures respectively. In the analysis of mice in which Slitrk3 was deleted, it was observed that the number of inhibitory synapses in the CA1 was reduced. Moreover electrophysiology recordings showed a decrease in inhibitory transmission. *Slitrk3* knock-out mice displayed an increase susceptibility to seizure, indicating that the observed reduction of inhibitory synapses has a large impact on excitatory and inhibitory balance in the brain.

Together, the formation of glutamatergic and GABAergic synapses can be triggered by different synaptic cell adhesion molecules. The experimental data have shown that their expression is sufficient to induce *de novo* synapses by recruiting either the vesicle release machinery or the respective postsynaptic core machinery. The abundance of synaptogenic proteins is puzzling. Most of the synaptogenic molecules that induce excitatory structures exhibit no selective expression across the brain, thus it remains to determine whether those different molecules have a synergic effect in the formation of synapses or whether they have additional functions at the synapses.

As the molecular identity of a presynapse is genetically-encoded and cannot be changed, the synaptic differentiation is most likely instructed and imposed by the presynapse. The diversity of synapses goes beyond excitatory and inhibitory. Currently, there is no evidence of molecules that could instruct this type of sub specification. Instead, a recent study has identified a cell adhesion molecule which is

capable to regulate the plasticity and the release probability properties (Sylwestrak and Ghosh, 2012). In the hippocampus CA1 pyramidal axons receive inputs from SOM and PV positive interneurons. On the one hand, the SOM positive OLM (*oriens lacunosum moleculare*) interneurons from the *stratum oriens* form facilitating synapses which have low release probability. On the other hand, PV positive interneurons produce depressing synapses which have a high probability release. Elfn1 (extracellular leucine-rich fibronectin containing 1 protein) is selectively expressed in the SOM positive OLM interneurons and is absent in PV cells. The ectopic expression of Elfn1 in PV cells converted PV synapses from depressing into facilitating. Those experiments show that postsynaptic Elfn1 regulate release probability.

To conclude, the formation of excitatory and inhibitory synapses can be triggered by different synaptic molecules which can recruit synaptic component necessary for synaptic transmission. As the *in vivo* analysis suggests, those molecules presumably act co-operatively.

1.3. Alternative splicing code for synaptic recognition?

During brain development, neurons from different cell-types assemble into circuits which exhibit highly precise synaptic innervations. This raises the question of how the nervous system achieves the coding of all parameters required for extremely specific synaptic connectivity. On the one hand, proteins coded by different genes can contribute to certain aspects of selective synaptic wiring. Nevertheless, the number of the genes in mammals remains limited. Interestingly additional mechanisms enable to expand dramatically protein diversity, in particular alternative splicing. As illustrated with the example of *Dscam*1 gene in fly, alternative splicing is a source for protein diversification and thus constitutes a potential mechanism to specify the multiple parameters for establishing accurate synaptic connectivity.

1.3.1. Alternative splicing

Alternative splicing permits to generate different transcripts isoforms according the combination of exons included in the final messenger RNA. Thus, alternative splicing is a key process controlling gene expression through regulation of transcripts abundance, transcripts localization and diversity of encoded protein isoforms (Black, 2003; Kelemen et al., 2013).

Alternative splicing is a common mechanism as 95% of human genes can be alternatively spliced (Pan et al., 2008; Wang et al., 2008). The direct consequence of alternative splicing is the tremendous expansion of protein diversity (Black, 2000). Alternative splicing can confer proteins isoforms distinct biological functions including enzymatic activity, interaction with proteins or DNA but it can also regulate subcellular localization (Kelemen et al., 2013). A recent study has reported that at a large scale, each protein isoform should be viewed as if it was encoded by separate gene rather as a minor protein variant because each isoform exhibits distinct interaction partners (Yang et al., 2016). Moreover alternative splicing can also regulate mRNA stability by targeting it to nonsense-mediated decay (NMD)(McGlincy and Smith, 2008; Kelemen et al., 2013).

Splicing is the mechanism that enables to excise introns and to ligate exons in the pre-messenger RNAs and is catalyzed by spliceosome machinery (Figure 2) (Black, 2003). Exons are defined by three elements. They contain a 5' and 3' splice site and a branching point which is followed by a polypyrimide tract (Black, 2003).

Alternative splicing arises through the competition of several splice sites. It leads then to the retention or the exclusion of cassette exon or intron. The most common mechanisms is to create a competition between several splice sites is to either promote or inhibit splice sites recognition by the spliceosome (Black, 2003). In consequence, it will promote the retention or the exclusion of the mRNA sequence. For example, proteins can be recruited at so-called exon splice enhancer sequences to facilitate the recognition of splice sites. The S/R (Serine/Arginine) protein family has been described to promote the recruitment of U1 snRNP at the 5' splice site and of U2AF complex to the 3' splice site (Tacke and Manley, 1999). Moreover, the accessibility of splice factors can be sterically hindered leading to the skipping of the element. For example polypyrimidne tract-binding protein binds to the polypyrimidine

tract which in turn blocks physically the access of U2AF complex to the 3' splice site (Spellman and Smith, 2006). Moreover, additional RNA-binding proteins regulate alternative splicing and the concentration or the activity of regulatory proteins can also affect alternative splicing choice (as reviewed by Chen and Manley, 2009).

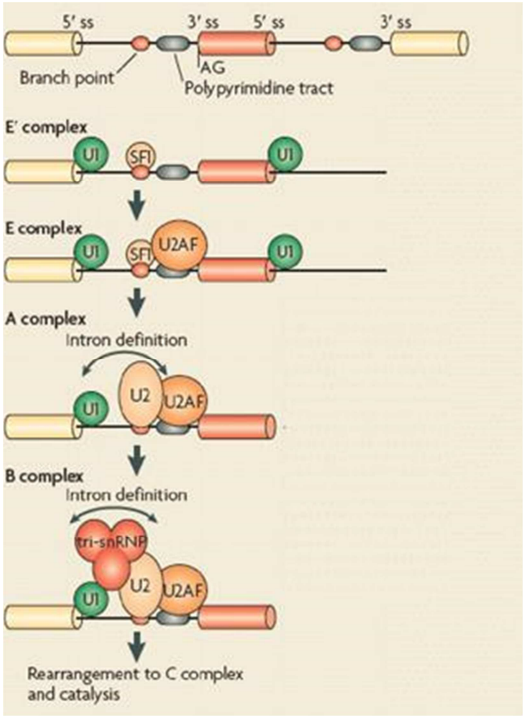

Figure 2-Spliceosome assembly

The assembly of the spliceosome occurs stepwise (Li et al., 2007) . It is initiated by the binding of U1 snRNP to the 5' splice site and then then splicing factor 1 at the branching point which then recruits U2AF factor to the polypyrimidine tract and on the 3' splice site. This forms the E-complex and does not require ATP. Then, the splicing factor 1 is replaced by U2 snRNP which is recruited by U2AF in an ATP-dependent manner to bind to branching point via RNA-RNA pairing leading to the A complex. This is followed addition of U4/6 and U5 to transit to the B complex. Finally spatial rearrangements and remodelling including the removal of U1 and U4 lead to the formation of the catalytic complex which can now proceed to the excision of introns in two transesterification steps. (Figure modified from Chen and Manley, 2009)

Beside to cassette exon retention or exclusion, alternative splicing comprises of additional events (Black, 2003). For example through usage of alternative promoters or polyA sites can switch the 5' or the 3' end of a transcript. Alternative splicing can use alternative 5' or 3' splice sites to generate a longer or shorter cassette exon. Retention or exclusion can occur independently from each cassette exons or it can occur in a mutually exclusive manner resulting in single exon retention at a time. Finally intron can be retained in the final mRNA and be later excised.

To conclude alternative splicing has the potential to increase considerably the molecular diversity of proteins. In the case of *Nrxn* genes, alternative splicing produces in theory more than 12'000 different isoforms (Tabuchi and Sudhof, 2002). Therefore its molecular diversity in combination with it synaptogenic activity make Neurexin an ideal candidates to specify certain aspects of synaptic connectivity.

1.3.2. Neurexin

Neurexins were first purified as receptors for the black widow spider toxin α-latrotoxin in 1990 (Petrenko et al., 1990). Later, Neurexins were cloned and the analysis of the genes gave rise to the hypothesis that Neurexin are receptors expressed at cell surface, presumably at the presynapses and importantly, that the genes contain several alternative spliced segments. Based on these findings, they emitted the speculation that through alternative splicing, Neurexins possess a remarkable and large molecular diversity which could function as cell surface recognition molecules.

1.3.2.1. Genomic and protein organisations

Neurexins are encoded by three genes (*Nrxn1, 2, 3*) *in* mammals (Figure 3A). Each gene contains two alternative promoters α and β which give rise to the long α and short β primary transcripts. As initially reported, *Nrxn* genes expression is regulated by alternative splicing. *Nrxn* genes contain up to six canonical alternative splice segments (AS1-6) which are localized in the extracellular domain (Tabuchi and Sudhof, 2002; Treutlein et al., 2014). If all theoretical permutations were possible there would be more than 12'000 different isoforms that could be generated (Tabuchi and Sudhof, 2002).

The extracellular domain of Neurexin α is organized into 6 laminin-neurexin-sex hormone binding globulin (LNS) domains with 3 epidermal growth factor-like domains interspersed (Ushkaryov et al., 1992). Neurexin β contains only 1 LSN domain which is the same as the Neurexin α LNS6 with the exception of an unique amino-terminal sequence in Neurexin β (Ushkaryov et al., 1992). Neurexins contain posttranscriptional modifications: they are *N* and *O*-glycosylated (Ushkaryov et al., 1994). The cytosolic domain contains a PDZ domain for intracellular trafficking, a potential endoplasmatic retention signal and a cytoskeleton integrating protein 4.1 (Fairless et al., 2008).

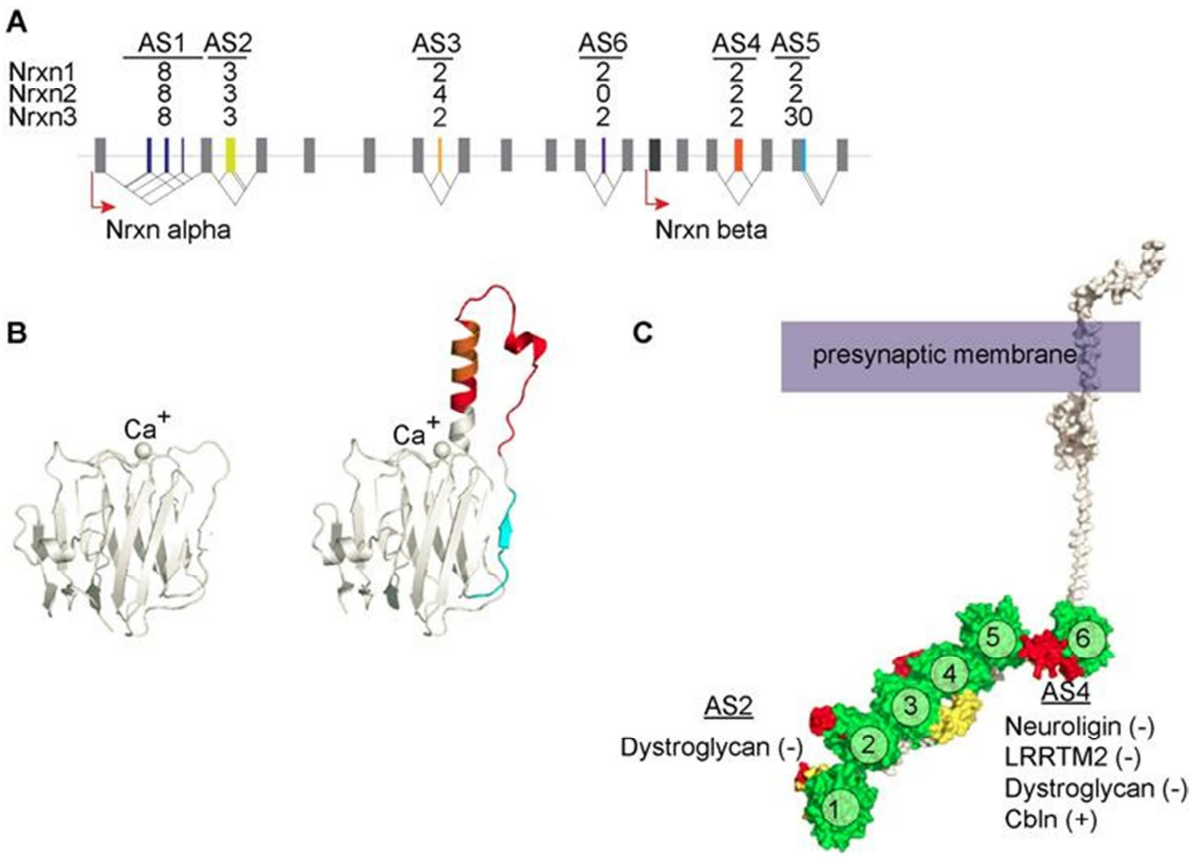

Figure 3- Alternative splicing is the source of Neurexin molecular diversity and regulates interactions with postsynaptic ligands.

(A) Alternative splicing regulation at *Nrxn* genes. There are up to 6 conserved alternatively spliced segments (AS1-6). Alternative exons are shown in color, constitutive exons in gray. Some segments consist of simple cassette exons, whereas others contain multiple alternative acceptor and7or donor splice sites (Schreiner et al., 2014a). **(B)**. Structure models representing LNS domain of Neurexin β with (right) or without (left) splice insert at AS4. Splice insert incorporation at AS4 (in orange/red) induces the formation of an α-helix (modified from (Reissner et al., 2013)). **(C)**. Structural model representing Neurexin α with list of isoform-specific postsynaptic ligands. The parentheses indicate the required presence (+) or absence (-) of the splice inserts at AS2 and AS4.LNS domains, green (numbered 1 to 6), EGF-like domains, yellow, alternative spliced segments AS2-4, red. (modified from (Reissner et al., 2013))

The elucidation of the structures of Neurexins α and β have shed more light in how alternative splicing regulates ligand binding (Chen et al., 2011; Miller et al., 2011). Neurexin α forms a L-shape with a long arm comprising of LNS2-5 plus EGF2

and a short arm with EGF3 and LSN6 domains. Each LNS domain forms a structure called β sheets sandwich which contains 11 sheets (β1-β11). Except for the LNS1, each LNS domain is thought to contain a Ca^+ binding site and each site is in close vicinity of an alternative splicing segment. The EGF1 and 2 domains build a small, compact and stable structure to link each LNS domain. In contrast, EGF3 constitutes a flexible hinge between LSN5 and 6 suggesting that LNS2-5 long arm can adopt different conformations. The alternative exon insertions at AS2 and 3 in the LNS2 and 4 respectively do not affect the long arm core structure and neither does the Ca^+ binding. In opposite, the insertion of splice insert at AS4 results in a dramatic rearrangement of the LNS6 module (Koehnke et al., 2008; Shen et al., 2008). Alternative exon at AS4 is localized in a loop region between two β sheets (β10 to β11) which spans over the entire β sheet sandwich (Koehnke et al., 2008; Shen et al., 2008). Upon exon insertion at AS4 which comprises of 30 amino acids, the loop region rearranges into an α-helix which orientates vertically to the LNS6 (Figure 3B) (Koehnke et al., 2008; Shen et al., 2008). The major consequence of this structure alteration is that the Ca^+ binding site is less exposed. Moreover using isothermal titration calorimetry to measure affinity for calcium, it was reported that LNS6 containing the alternative exon exhibits a higher affinity for Ca^+ (Shen et al., 2008). Taking this together, alternative splice shapes the structure of Neurexin and thereby facilitates or prevents the access to the epitopes.

1.3.2.2. Alternative splicing in *Nrxn* genes to specify synapses

At the *Nrxn* genes, alternative splicing drives the molecular diversity. A large body of evidence has demonstrated that the major function consequence of alternative splicing is to regulate the binding affinity of Neurexin with a large variety of postsynaptic ligands (as reviewed by Reisser and al., 2013). This in turn enables Neurexin to nucleate distinct synaptic complexes.

A number of Neurexin ligands bind in an isoform-independent manner. Those ligands comprise of $GABA_A$ receptors (Zhang et al., 2010), Calsyntenin (Pettem et al., 2013), Cask (Hata et al., 1996), synaptotagmin (O'Connor et al., 1993) Mint (Biederer and Sudhof, 2000) and Neurexophilin (Missler et al., 1998). Regarding the

rest of Neurexin ligands, their binding is regulated by alternative splicing, mostly at AS4 (Figure 3C). For example, Neuroligins bind preferentially to Neurexin containing the splice insert at AS4 (Nrxn AS4 (-))(Boucard et al., 2005; Chih et al., 2006). Neuroligin which are encoded by 4 genes (*NL1-4*) can also be alternatively spliced at two sites namely A and B (Ichtchenko et al., 1995). Moreover, Neuroligin 1 and 2 were found to promote the differentiation of excitatory and inhibitory synapses, respectively (Chih et al., 2005b). Affinity measurements by surface plasma resonance indicated that Neurexins α and β with or without the splice insert at AS4 bind to all Neuroligin isoforms, albeit with a wide range of affinity (Koehnke et al., 2010). Thus, the transsynaptic interaction of Neurexin and Neuroligin is regulated at the AS4. In addition to Neuroligin, Neurexin AS4 that lacks the splice insert also interacts with Leucin-rich repeat transmembrane protein 2 (LRRTM2) (de Wit et al., 2009; Ko et al., 2009) and dystroglycan (Sugita et al., 2001) (Figure 3C).

Other ligands have also been reported to bind with different Neurexin isoforms. For example, in the cerebellum, it was reported that Neurexin 1 that contains splice insert at AS4, Neurexin 1 AS4(+), together with Cbln1 and GlurD2 forms a trisynaptic complex to regulates the formation of synapses between granules cells and Purkinje cells (Uemura et al., 2010; Ito-Ishida et al., 2012a). Moreover, postsynaptic Dystroglycan interacts with Neurexin that lacks splice insert at AS2 and 4 (Sugita et al., 2001; Reissner et al., 2014) (Figure 3C). Thus, alternative splicing plays a crucial role by specifying the identity of Neurexin ligands.

The diversification of Neurexin by alternative splicing raises the question if presynaptic Neurexin isoforms can nucleate transsynaptic complexes with different postsynaptic ligands to induce the assembly of distinct functional synapses. Using co-cultures, it has been demonstrated that HEK293T cells expressing Neurexin 1 β AS4 (+) promoted the formation of excitatory and inhibitory postsynaptic structures on contacting dendrites (Chih et al., 2006). In contrast, Neurexin 1 β that lacks the splice insert at AS4 was selective for GABAergic postsynaptic complexes (Chih et al., 2006). In addition to Neurexin AS4 isoforms, Neurexin AS2 could potentially be involved in the assembly of inhibitory synapses. Indeed, Neurexin AS2 (-) specific ligand, Dystroglycan has been reported to co-localize with inhibitory postsynapses (Levi et al., 2002; Reissner et al., 2014). Thus, those data suggest that Neurexin

isoforms have a functional consequence for synapse specification therefore Neurexin diversity could provide a splice code for instructing different types of synapses.

In a recent study, in which the function of AS4 splice insert was investigated *in vivo*, it has brought into light, that beside its synaptogenic activity, Neurexin could regulate certain aspects of synaptic transmission (Aoto et al., 2013). In this study, mice expressing constitutively Neurexin 3 AS4 (+) isoform were generated by converting a weak splicing acceptor sequence into a canonical sequence. For the constitutive expression of Neurexin 3 AS4(-) isoform, loxP sites were flanking the alternative exon and upon Cre recombinase expression, the cassette exon was excised from genomic DNA sequence. The analysis of cultured neurons revealed that the splice site insert regulates the endocytosis of postsynaptic AMPA receptors. In fact, constitutive inclusion of Neurexin 3 AS4 (+) resulted in a selectively decrease in AMPA-mediated current. This phenotype was due to the higher internalization rate of AMPA receptors at the synapses. Moreover, constitutive Neurexin 3 AS4(+) expression decreased LRRTM2 level at the postsynapses. To analyze if splice insert at AS4 regulates plasticity *in vivo*, Cre recombinase was injected in the CA1 of mice which have splice insert floxed by loxP sites. By applying a protocol to elicit NMDA receptor-dependent long-term plasticity by stimulating in the CA1 region and recording in the subiculum, it has been found that constitutive expression of Neurexin 3 AS4 (+) transcripts in all neuronal cells in CA1 led to the abolishment of this type of plasticity. Surprisingly this phenotype could be rescued by any *Nrxn* transcripts that lack the splice insert.

To conclude, the data from *in vitro* and *in vivo* data demonstrated that alternative splicing at Neurexin is crucial for synapses specification and for synaptic transmission.

1.3.2.3. Neurexin diversity regulates synapses formation and synaptic transmission *in vivo*

As a large body on studies, mostly performed *in vitro* system, have highlight that diversity of Neurexin is involved in the formation of synapses but also in the regulation of the synaptic transmission. This part is dedicated to *in vivo* studies in

which single or several *Nrxn* genes were deleted in order to investigate the function of Neurexin diversity in synapse formation and synaptic transmission in mouse brain.

To address the question of whether Neurexin diversity is important in the brain, a Neurexin α-triple knock-out mouse was generated (Missler et al., 2003). Electron microscopy analysis in the brain stem of the triple knock-out showed no altered ultrastructures of presumably excitatory and inhibitory synapses. However a selective decrease in inhibitory synapses density was observed. Analysis of the synaptic transmission detected a decrease both in mEPSC and mIPSC frequency in the mutant mice. Additional recordings pointed at defects at the presynapses as the synaptic probability release of inhibitory neurons and short-term plasticity were severely altered in the triple knock-out. By applying different blockers of Ca+ channels, it was determined that N- and P/Q-type Ca+ channels were defective and therefore were the cause of the impaired presynaptic transmission. Rescue experiments by genetically re-expressing a single Neurexin α could reduce the defect in synaptic transmission. Because the re-expression of a single Neurexin β did not ameliorate synaptic defec,t it has been hypothesized that the extracellular domain of Neurexin is involved in regulation of Ca^{+}-mediated currents (Missler et al., 2003; Zhang et al., 2005). Thus, the analysis of the *Nrxn α*-triple knock-out indicates that Neurexins α regulate the number of synapses and are involved in presynaptic Ca^{+} channel signaling to regulate synaptic transmission.

The function of Neurexin β diversity has been addressed in several single KO mutant mice. For example, analysis conditional dominant-negative mutant of Neurexin 1 β in the adult mouse brain has revealed a reduction of mEPSC and mIPSC (Rabaneda et al., 2014). Moreover Neurexin 1 β isoforms were shown to regulate endocannabinoid pathway (Anderson et al., 2015). This pathway regulates synaptic strength by suppressing neurotransmitter release in a retrograde signaling of lipid molecules from the postsynaptic cell to the presynaptic cell that express cannabinoid receptors (Castillo et al., 2012). Using conditional Neurexin 1 β knock-out hippocampal neurons in cultures, it was found that ablation of Neurexin 1 β increases 2-AG synthesis in the knock-out neuron which is the endogenous agonist of cannabinoid receptor CB_1. In consequence, due to the increased stimulation of presynaptic CB_1 receptors, mEPSC frequency was elevated. To validate that Neurexin 1 β isoforms also regulates

endocannabinoid signaling *in vivo*, CA1 pyramidal afferent of Neurexin 1 β knock-out cells were stimulated and synaptic response in the subiculum was recorded. The subiculum receives CA1 axon inputs and consists of regular and fast burst-firing pyramidal neurons. Upon stimulation in CA1, it was observed that burst-firing pyramidal neurons exhibited a decreased in neurotransmitter release and a blocking in long-term potentiation. These results indicate that Neurexin 1 β in CA1 controls the tonic activation of endocannabinoid pathway *in vivo*.

.

In a recent study, it has been reported that diversity of Neurexin 3 α and β was differentially implemented in two distinct neuronal circuits (Aoto et al., 2015). To generate a Neurexin 3 α and β knock-out, the strategy consisted to delete the common exon (exon 18) by inserting flanking loxP sites. Upon delivery of Cre enzyme, the recombination would result in a frame shift in the downstream sequence and thus gives rise to a translated protein without membrane anchoring which should be non-functional. The analysis in the hippocampus of the Neurexin 3 α/β knock-out is reminiscent of the previous study where Neurexin3 AS4(+) is constrictively expressed (Aoto et al., 2013). Indeed reduced AMPA-mediated transmission and increased internalization of AMPA receptors were detected. Surprisingly, the re-expression of Neurexin 3 AS4 (-) was sufficient to rescue the loss of all Neurexin 3 α/β isoforms. Unexpectedly, the analysis of synaptic transmission in the olfactory bulb revealed that Neurexin 3 α/β isoforms might be involved in distinct synaptic functions in the olfactory system. Indeed, in olfactory neuronal cultures AMPA-mediated current was unchanged. In contrast, it was found that mIPSC and of evoked IPSC amplitude were decreased in the knock-out cultures. Vesicles release probability was also decreased in the knock-out neurons. Recues experiments have indicated that re-expression of Neurexin 3 that contains the splice insert at AS4 is able to rescue synaptic defects and that intracellular domain of Neurexin also matters for synaptic transmission in olfactory bulb. This study indicates different function of Neurexin 3 α and β in distinct neuronal circuits.

Together, functional analysis of Neurexin in the mouse brain highlight its contribution for establishing synapses during development but also for regulating synaptic transmission in the adult brain. Recent studies indicate that Neurexin AS4 isoforms

regulate synaptic functions. Nonetheless, endogenous Neurexin mRNAs repertoires across different neuronal populations have not been investigated yet.

1.3.3. Expression Neurexin isoforms in the mouse brain

Genome-wide analysis of human gene expression has revealed that alternative splicing produces protein isoforms which are expressed in a tissue-specific manner (Pan et al., 2008; Wang et al., 2008). Spatial regulation is critical for controlling the function of genes. In Neurexin, the isoforms repertoire in the brain remains an open question. Indeed, what are the combinatorial exon usages of Neurexins in the brain? Are Neurexin isoforms expressed stochastically or selectively in neuronal cell populations? What are the mechanisms that regulate spatial regulation of Neurexin?

Due to this extraordinary molecular diversity, it has been technically difficult to assess the real diversity of Neurexin *in vivo*. Indeed, sequencing methods such as Illumina yield to very small reads (100-150 nt) which is insufficient to obtain information about combinatorial exon usage. However the recent development of new sequencing methods provides new tools to tackle this question. One of these methods called PacBio single molecule real-time sequencing (PacBio SR sequencing) has the capability to sequence very long DNA molecules, up to 30 kb in a single read (English et al., 2012; Eid et al., 2009). Thus, a recent study has been using this sequencing method to address the question of the real diversity of Neurexin *in vivo* (Treutlein et al., 2014). In this study, the sequencing Neurexin 1-2-3 β isoform repertoires showed that all predicted Neurexin β variants were expressed. However, due to the insufficient sequencing depth, the sequencing results for Neurexins α are difficult to interpret. Through their analysis, an additional alternative splice site (AS6) was identified which is only present in the *Nrxn 1* and *3* genes. Thus, this method can be applied for short transcripts β transcripts, however, for the longer α transcripts, which are the major source of isoform diversity, the question whether the entire molecular diversity is present *in vivo* remains to be tested.

Several studies have support that alternative splicing at *Nrxn* genes is not based on stochastic processes. Analysis of *Nrxn1-2-3* α and β primary transcripts by *in situ hybridization* (ISH) showed that both primary transcripts are expressed in the

brain in an overlapping manner (Ullrich et al., 1995). The expression patterns suggest that Neurexins are expressed by diverse neuronal populations. Moreover, PCR amplification of samples from different brain regions revealed that the incorporation of splice insert at different splice segments was differentially regulated across brain areas (Iijima et al., 2011; Ehrmann et al., 2013). In addition, a recent study has determined the expression profiles of single neurons from different neuronal cell populations and compared to each other (Fuccillo et al., 2015). For this, the cytoplasmic content of different cell types was analyzed using a high throughput microfluidic chip called Fluidigm which allows to run a high number of quantitative PCR (qPCR) reactions simultaneously using very small amount of material. Paired-wise comparison indicated that neurons from the same population are more similar to neurons from divergent origins. For example it was found that CCK and PV interneurons, which both innervate the same target cell population presented different relative abundance of *Nrxn1 AS4(+)* transcripts. Taken together, these findings strongly suggest that expression of Neurexin isoforms is regulated in a cell-type specific manner. Nonetheless, the Fluidigm is a powerfull method to test a large range of genes by qPCR, it provides only relative abundance values, thus, the real ratio of isoforms that lacks or that contains a splice insert at a specific splice segment between different neuronal populations remains to be determined.

The existence of cell-type specific Neurexin repertoires leads to the question of the regulation mechanisms. Most of RNA binding proteins regulating alternative splicing are expressed ubiquitously in the brain (Kelemen et al., 2013). However a number of studies have identified STAR (signal transduction activator of RNA) RNA binding family as regulator of Neurexin alternative splicing (Iijima et al., 2011; Ehrmann et al., 2013). STAR are composed of three members called SAM68, SLM1 and SLM2. While SAM68 is expressed ubiquitously in the brain, SLM1 and SLM2 have been reported to exhibit restricted and non –overlapping expression in distinct neuronal populations (Iijima et al., 2011; Ehrmann et al., 2013). For example in the hippocampus, DG granules cells express SLM1 while CA1 and CA3 pyramidal neurons are positive for SLM2. In addition, inhibitory interneurons of the *stratum radiatum* and *stratum lacunosum moleculare* were predominantly positive for SLM1 and not for SLM2 (Iijima et al., 2014).

Using mini-gene splice reporters it was demonstrated that all STAR members promotes the exclusion of splice insert at AS4 in all three *Nrxns* in a dosage-

dependent fashion (Ehrmann et al., 2013; Iijima et al., 2014). Moreover, genetic ablation of SAM68, SLM1 or SLM2 also results in a reduction of *Nrxn1 AS4(-)* transcripts in the brain (Iijima et al., 2014; Traunmuller et al., 2014; Iijima et al., 2011). Thus, STAR RNA binding family provides a regulation mechanism to regulate spatial expression of Neurexins.

To conclude, alternative exon incorporation rates is differentially regulated in the brain, which result from cell-type specific gene expression programs. Nonetheless it remains to explore the real diversity of Neurexin α in vivo and to investigate Neurexin isoform ratios across different neuronal populations.

1.4. Dissertation project

Studies have demonstrated that alternative splicing is the source of diversity in *Nrxn* genes (Tabuchi and Sudhof, 2002). Moreover, alternative splicing regulates interaction of Neurexin with a large variety of postsynaptic ligands and thereby promotes the assembly of functionally distinct postsynaptic complexes (Reissner et al., 2013).

Spatial logic of Neurexin expression has been addressed by several studies and showed that Neurexin isoforms are selectively expressed across the brain (Iijima et al., 2011; Ullrich et al., 1995; Fuccillo et al., 2015). However several questions remain unsolved. For example the splicing activity within a population *in situ* has not been determined. In addition, the real alternative cassette exon incorporation rate across different neuronal cell populations has not been assessed. Finally, it is unknown whether cell-type specific repertoires contribute to neuronal functions.

To explore the logic and the functional consequences of Neurexin molecular diversity in the brain, the aims of my project consist of:

1. Monitoring alternative splicing activity at the single-cell level with bichromatic reporters in the brain

2. Profiling endogenous Neurexin repertoires in different cell population with Ribotag transgenic mice

3. Testing the function of specific variants by generating conditional knock-out mice lacking the isoforms

2. Results

2.1. Preface

This chapter presents results data on the profiling of Neurexin isoforms repertoire across neuronal populations and of functional investigation of cell-type specific isoforms in the mouse brain. This chapter is divided into two sections. The first presents works on PacBio SR sequencing and on splice reporters. PacBio SR sequencing was collaboration with Dr. Dietmar Schreiner, a post-doc in our lab and the study is now published. I contributed to the PacBio study by validating the alignment results by quantitative PCR. Dietmar has initially designed the splice reporter strategy. When I joined the lab, I proceeded to their validation and to their implementation *in vivo*. In the second section which is about cell-type specific Neurexin isoform repertoires *in vivo*, I carried out most of the experiments, with the exception of two. The dual labelling by immunostaining and *in situ hybridization* was performed by Dietmar and Caroline Bornmann, a technician in our lab. The analysis of PV and SML2 immunolabelling in CA1 in hippocampus was done by Lisa Traunmüller, a PhD student in our lab.

2.2. Mapping Neurexin isoform repertoire in the brain

2.2.1. Introduction

Nrxn1-3 genes retain the extraordinary capability to undergo extensive alternative splicing at multiple segments which has the potential to generate a remarkable molecular diversity (Ushkaryov et al., 1992). Using PCR amplification, it was demonstrated that alternative exon choice at single site presents regional differences across the brain (Iijima et al., 2011; Fuccillo et al., 2015). However, the fundamental questions regarding the molecular diversity of neurexins remain. First, what is the combinatorial usage of alternative splicing sites *in vivo*? Are multiple alternative exons at different alternatively spliced exons indeed extensively combined to generate thousands of isoforms or is the diversity dominated by more limited combinations? Second, what is the spatial logic of Neurexin isoform expression? Are specific isoforms enriched in specific cell types or do cells stochastically chose certain isoforms?

The reason why it was not possible to investigate the actual repertoire of Neurexin isoforms is that no technologies could sequence single long mRNA transcripts, an approach that is essential to assess combinatorial use of alternative splice insertions. Recently the development of a third generation sequencing method called PacBio single molecule real-time (SR) sequencing offers the possibility to sequence single long (>10kb) cDNAs. Therefore, this method is well suited for deciphering combinatorial alternative splicing in Neurexins and their molecular diversity (English et al., 2012; Eid et al., 2009) (Figure 4 A). This chapter describes the application of PacBio Sequencing to the assessement of neurexin diversity in the mosue brain. In the second part of this chapter, I will describe a novel approach to investigate selective alternative splicing choices at the single cell level using bi-chromatic splicing reporters and their application in the mouse brain

2.2.2. Interrogation of combinatorial alternative splicing events by PacBio SR Sequencing

For examining the potential contribution of Neurexin diversity to neuronal wiring specificity it is essential to dissect the actual number of Neurexin isoforms that are generated under physiological conditions. Based on the described genomic information, 574 Neurexin 1 α, 384 Neurexin 2 α and 5760 Neurexin 3 α transcripts are predicted to arise by combinatorial use of alternative exons at 5 alternatively spliced segments. Considering these potential isoform numbers, the minimal sequencing depth required to detect such isoforms is 3000-4000 reads for Neurexin 1 and 2 and 40'00 for Neurexin 3 (at least if all isoforms were expressed at the same level). However it is more likely that in biological samples the distribution of isoforms is unequal. Thus, likely, a higher sequencing coverage is required. 100'000 for α Neurexin 1 and 2 and 150'000 for α Neurexin 3, independent full-length cDNAs were isolated and separately submitted for PacBio sequencing. The number of postfiltered reads required for minimum sequencing depths was reached (Table 1).

To map the reads, the sequences were aligned to the *in silico* transcriptome, i.e. an exhaustive combination of known alternative splice insertions in the transripts resulting from the three Neurexin genes. We used two mapping algorithms: BLASR (the native Pacbio aligner) and BLAST. There were two issues with BLASR mapping algorithm. First, BLASR could not always distinguish candidate transcripts. Second, to validate the exon incorporation rate a systematic experimental validation was carried out and the results showed high correlation with the BLAST but not with BLASR (Figure 4B-C). For these reasons, the sequences alignments were done with the BLAST-based algorithm.

The mapping results showed that Neurexin 1 and 2 use almost all combinations possible of alternative exons (Figure 4D). Surprisingly, Neurexin 3 α sequencing alignments identified lower transcripts numbers than predicted (Figure 4 D). Because of the high number of reads, this is unlikely to be due to insufficient sequencing depth. Instead when looking closer at the exon choice, it was observed that at AS3 and AS5 exon permutations occurred in a stereotyped fashion (Figure 5), thus, greatly restricting the actual number of exon permutations detected in endogenous transcripts

Interestingly, our mapping approaches identified a novel alternatively spliced segment, which we called AS6 (Figure 5). Furthermore a novel alternative donor site was discovered at AS3 (Figure 5). The presence of these novel alternatively spliced segments elevates the potential diversity of Neurexin 3 transcripts to 11,520 isoforms. However, the selective/stereotyped splicing decisions at AS3 and AS5 reduced the actual diversity, with 645 isoforms detected in the adult brain.

Thus, when combined with validated mapping algorithms, PacBio RS sequencing technology can be applied for dissecting isoform diversity of gene families undergoing complex alternative splicing. Our analysis revealed the existence of a new alternative splicing segment and alternative donor site. Importantly it was showed that Neurexin 1 α and 2 α use almost all combinations possible of alternative exons whereas Neurexin 3 α displayed a restricted stereotyped exon usage which reduced considerably its diversity. However with more than 1000 isoforms expressed in the adult mouse brain, *Nrxn* genes have clearly the potential to specify certain aspects of specific neuronal wiring.

To investigate whether the molecular diversity correlates with cellular diversity in different brain regions, the Neurexin 1 α repertoires of the whole brain, cortex, cerebellum and cerebellar granule cells were sequenced. Those samples range from the most highest to a lower cellular complexity and therefore represent suited systems to determine if molecular diversity is linked to cellular identity. The libraries of Neurexin 1 α in those samples were prepared exactly as previously described. The mapping results revealed that Neurexin 1 α repertoire changes across the samples (Figure 6A). Moreover the relative abundance of the most abundant isoforms was different in each sample (Figure 6C). Indeed in the less complex granule cells cultures, the most abundant isoform account for 23 % for the total repertoire while this was only 6 % in the cortex. This means there is a strong enrichment of specific isoforms in a purified cell population (Figure 6D). In sum, our results demonstrate the existence of cell-type specific Neurexin repertoires in the mouse brain.

2.2.2.1. Conclusions

To conclude, this study demonstrated that PacBio SRsequencing method is a powerful tool that finally answered the question of the real diversity Neurexin in the

brain. The results also provided evidences of the link between the molecular diversity and the cellular identity. Although granule cell cultures are considered as a homogenous cell preparation, the absolute number of Neurexin variants detected remained substantial. This could be caused either by the fact that each individual granule cell expresses a large number of isoforms or because granule cells cultures are less homogenous than expected and therefore individual or groups of granules cells expressed distinct sets of Neurexin isoforms. Given that the PacBio SR sequencing method requires large amount of input material, it reaches its limitation and does not enable to test these hypotheses. Indeed a different method is required which allows extracting the information of exon usage at the single-cell level and preferentially *in situ*, in an unperturbed environment.

A recent study has also investigated Neurexin isoform expression by profiling single-cell Nrxn mRNAs (Fuccillo et al., 2015). Cytoplasmic content of electrophysiologically-defined cells was aspirated with a patch pipette. By quantitative PCR, the authors performed pairwise comparisons of Neurexin alternative splice insertions across different neuronal cell types. The results showed that neurons from the same cell type exhibit more similar alternative splicing choices than cells from other neuronal populations. Thus these data further strengthen the PacBio sequencing as it demonstrates that insert incorporation rate varies between neurons cell populations. By comparing the variation of gene expression level of several housekeeping genes it was observed that neurons from the same cell type present differences that can reach the factor of 100. This raises the questions whether those variations arise from cellular heterogeneity or whether they are due to technical issues of the method.

	Nrxn1β	*Nrxn2β*	*Nrxn3β*	Total
Subreads *				**648,549**
Mean subread length *				**1091.97**
Full-length subreads *	**114,842**	**124,006**	**100,632**	**339,480**
BLAST unique alignments	**44,884**	**43,376**	**36,452**	**36,452**
Full-length CCS reads	**14,112**	**17,112**	**13,122**	**44,346**

(*) - post filter

Table 1 - Summary of libraries and SMRT cell sequencing runs obtained for a total Neurexin 1,2,3 library.

Primary transcripts for *Nrxn1,2,3 alpha* and *beta* were amplified from adult mouse cortex, mixed in equimolar amounts, and subjected to PacBio sequencing and mapping. Right column shows total read and alignment counts and average read lengths (*), respectively. Under these conditions, coverage of full-length alpha transcripts was very low (<2,500 reads) only *Nrxn-β* transcripts were analyzed.

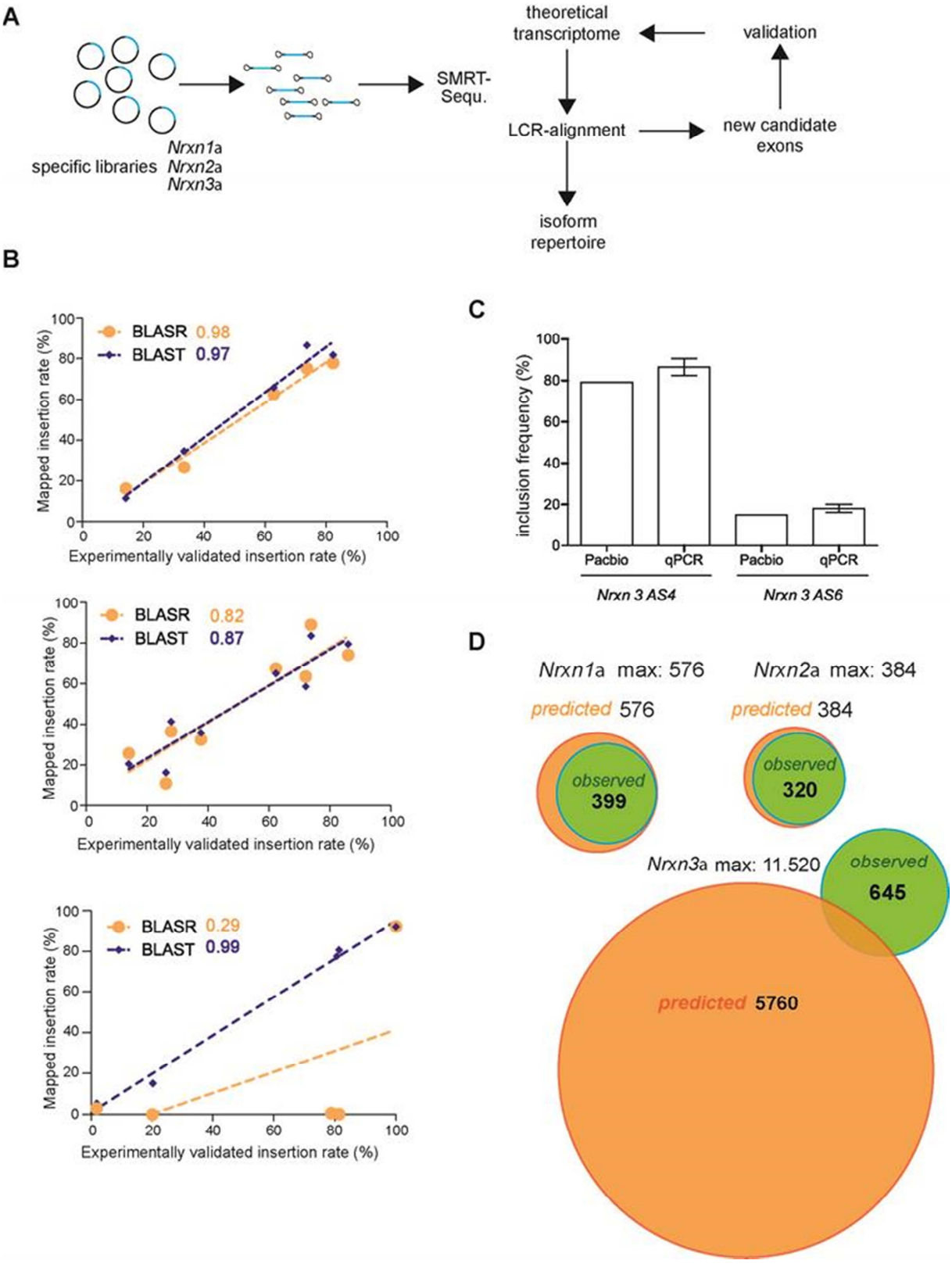

Figure 4- Deep single molecule sequencing of *Nrxn* α transcripts

(A) Experimental workflow: cDNA for Nrxn α was amplified from plasmid-based libraries, ligated to SMRTBell adapters, and subjected to SMRT sequencing (SMRT-Sequ.). Full-length continuous long for identification of novel splice events, followed by experimental validation. **(B)** Validation of BLAST- and BLASR-based mapping results for Nrxn1 α -2α -3α. Inclusion frequencies extracted from the PacBio sequencing data were compared to those

calculated from semi-qPCR using primer pairs flanking each of the alternatively spliced segments (AS1–AS6). Alternative exon insertions were considered en block, i.e., distinguishing only the presence or absence of alternative exons, as some alternative exon variations can not easily be distinguished. **(C)** Validation of PacBio-derived incorporation rates for novel alternative splice insertions at Nrxn1 α AS6 and Nrxn3 α AS6 by quantitative, real-time PCR. **(D**) Depiction of predicted and observed variant numbers. Green circles: detected transcripts. Orange circles: transcripts predicted based on the existing data.The maximal isoform numbers (max) were calculated based on exhaustive combinatorial use of all alternative splice insertions.

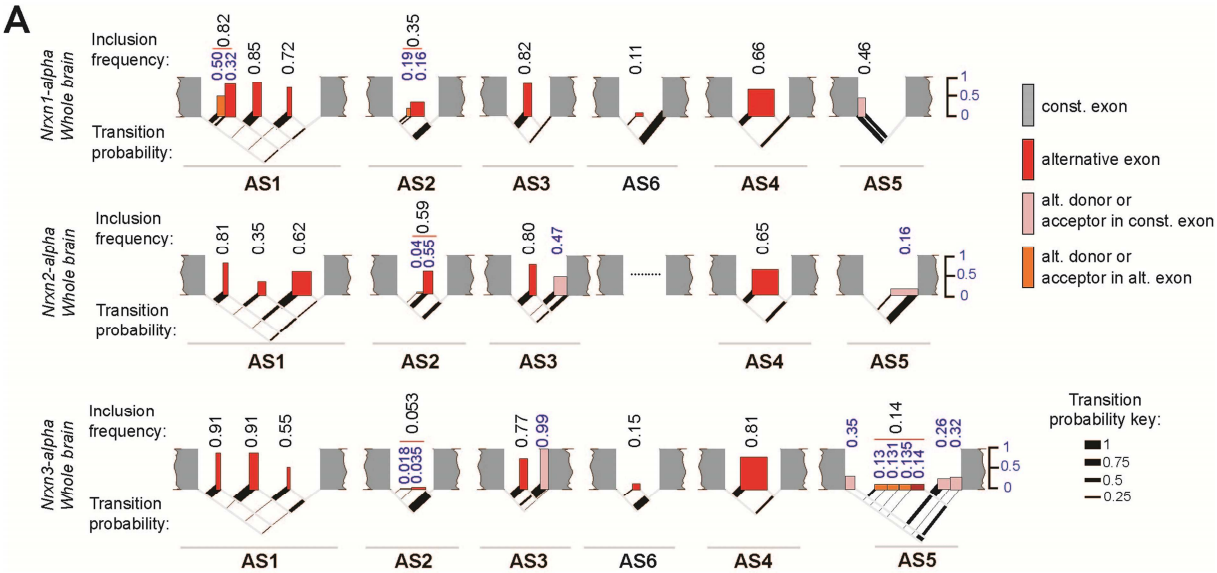

Figure 5- Spliceograms of *Nrxn α* transcripts

The inclusion frequencies of alternative exons and usage of alternative donor/acceptor sites are indicated by the height of the rectangles and by the numbers above them. The transition probabilities are indicated by the thickness of the lines according to the key shown on the right. const., constitutive; alt., alternative.

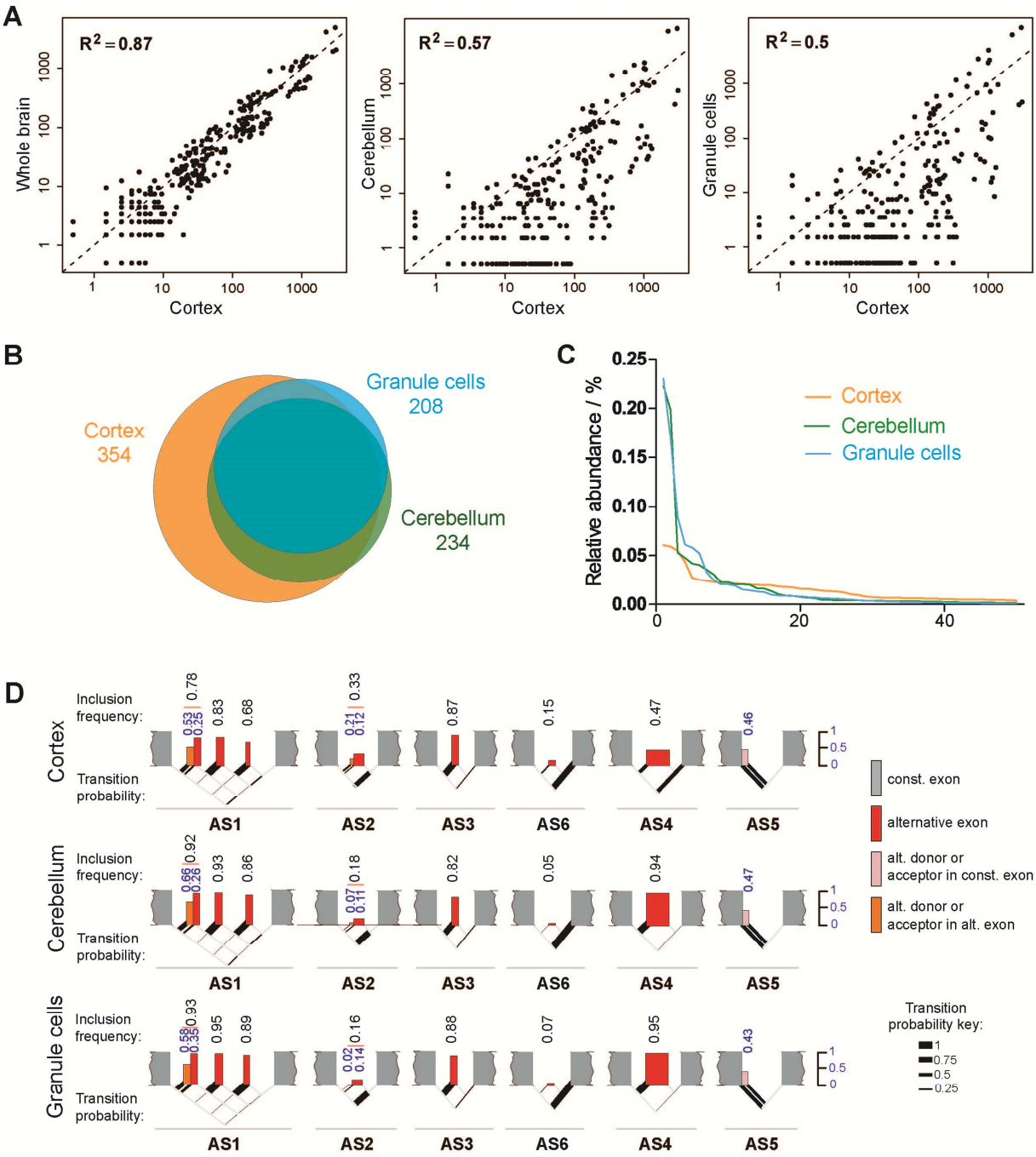

Figure 6- Comparison of Nrxn 1 α relative abundance in different brain regions and purified cells

(A). Correlation analysis of log-transformed sequence counts for Nrxn1a transcripts detected in different brain regions. A baseline value of 0.5 was added to the sequencing count of each isoform detected only in one sample. **(B)** Comparison of Nrxn1a variants detected in postnatal day 35 mouse cortex, cerebellum, or purified cultured granule cells (5 days *in vitro*). Proportional Venn diagrams demonstrating total number of identified variants. Overlapping and nonoverlapping areas demonstrate common and unique variants, respectively. **(C)** Relative representation of 50 top ranked variants plotted for cortex (orange), cerebellum (green), and cerebellar granule cells (blue).**(D)**. Spliceograms for Nrxn 1 transcripts detected in different brain areas. The average frequencies of alternative (alt.) exon inclusions (red) are symbolized by the height of rectangles and are indicated with numbers above. Transition probabilities are indicated by the thickness of the connecting lines. const., constitutive.

2.2.3. Single-cell read-out for alternative splicing regulation *in situ*

While the experiments described above provide strong evidence for a cell-type specific alternative splicing regulation of Neurexins they do not allow for interrogation of splicing regulation in single cells or to examine modification of alternative splicing regulation over time. In the following study we addressed the question of alternative splicing regulation at the single-cell level by bichromatic reporters.

2.2.3.1. Design of bichromatic splice reporters

To visualize alternative splicing activity at the single-cell level we designed a minigene reporter encoding for mCherry and GFP (Figure 7 A). The concept is to link the exon usage choice with the expression level of one or both fluorescent proteins. To do this, the minigene was inserted between the fluorescent proteins and encodes for the two flanking constitutive exons, the two intronic sequences and the alternative cassette exon. An additional single nucleotide was inserted in the alternative exon. As consequence, when the alternative exon is incorporated in the final mRNA, a frame shift is generated in the GFP coding sequence, resulting in the expression and the detection of red signal only in the cell. In contrast, upon cassette exon exclusion the cell expresses both mCherry and GFP fluorescent proteins. To facilitate the fluorescent level quantification by microscopy, both fluorescent proteins were fused to nuclear localization signal (NLS) to concentrate the signal within the nucleus. Thus, this design allows to monitor alternative splicing choice by quantifying mCherry and GFP fluorescent level in every cell.

There are two problems with this splice reporter approach. First the frame shift generates a premature stop codon in the downstream constitutive exon. To avoid any imbalance in the molar ratio of splicing variants because one isoform could be target of nonsense-mediated decay, the coding sequence downstream of the premature stop codon was removed from the exon. Second, the minigene itself could act as a negative regulator of protein stability as it could be considered as a junk protein sequence and therefore prone to degradation. Therefore the minigene was flanked by two self-cleaving 2A peptide signals to separate the mCherry and GFP proteins from the translated minigene protein.

2.2.3.2. Implementation of splice reporters for *Nrxn* genes

We focused on alternative splicing activity at the AS2 and AS4 of the *Nrxn1-3* genes because it was demonstrated that retention or the exclusion of those cassette exons can promote the formation of different class of synapses and also regulate biochemical interactions with a large number of different postsynaptic partners (Reissner et al., 2013). At the AS4 the alternative exon contains 90 bp and at the AS2 the alternative exon contains 45 bp with two alternative donor sites (a and b) separated by 15 bp (Figure 7C). At the AS2, the additional single nucleotide was inserted being upstream of the donor site a, thus the splicing reporter for this site does not distinguish between selection of the donor site a or b.

2.2.3.3. Validation of splice reporters in heterologous cell cultures

To test if the fluorescent microscopy data correspond to the cellular alternative splicing activity, mRNAs and protein levels were analyzed. To quantify the visual read-out, we calculated the ratio of intensity signal of GFP over mCherry.

At the AS2 the HEK293T splicing machinery displays similar activity towards all three *Nrxn* genes (Figure 8). The cassette exon was preferentially excluded from transcripts. Analysis of total RNA from transfected HEK293T cells show the presence of an unique band which corresponds to the isoform lacking the cassette exon (Figure 8B). Moreover both fluorescent signals were detected which also fits with the expected outcome (Figure 8B). The PCR products were all validated by sequencing. By contrast, we observed a differential alternative splicing activity toward AS4 in the three *Nrxn* genes which could be detected in the fluorescent quantifications (Figure 8C-D). While the cassette exon in *Nrxn 1* and *3* was preferentially excluded, *Nrxn 2* presented a mixture of both isoforms.

Given that red signal is detected in both alternative splicing events the relative amount of skipping isoform requires a benchmark for normalization. For this purpose, the intronic sequences from the minigene were removed (Figure 7B). In this configuration the skipping benchmark reporter- that corresponds to situation in which cells produce only isoform without splice insert, generates a transcript yielding mCherry and GFP molecules in an equimolar fashion. Using this normalization

method we concluded that 74% of total *Nrxn2 AS4* isoforms are lacking the alternative exon while this percentage is reduced to 16% in *Nrxn3 AS4* (Figure 8H).

Finally, the GFP/mCherry ratio quantification provides information about the distribution of the splicing activity among the cells. In the case of AS4, splicing machinery of HEK293T cells exhibits are broader cell-to-cell variation in *Nrxn2* gene compared to *Nrxn1* and *3* (Figure 8G).

Together, these results validated that the dual-color based quantification from our advanced bichromatic splicing reporters activity matches with processing at the RNA level and also at the protein level. Moreover, our data show that single-cell resolution can be achieved and thereby assessing splicing activity heterogeneity within a sample.

To test if splicing reporters recapitulate the regulation of endogenous *Nrxns* mRNAs, we co-transfected the RNA binding protein SAM68 expression vector which promotes exon skipping at AS4 (Figure 9) (Iijima et al., 2011). We observed that the presence of SAM68 in the cells shifted the alternative splicing activity toward exon skipping. The fluorescent microscopy data were further confirmed by total RNA and protein levels. To conclude, these results demonstrated that the Neurexin splice reporters contain regulatory elements to reproduce same regulation as endogenous *Nrxns* mRNAs.

2.2.3.4. Application of splice reporters to explore *Nrxn* splicing regulation *in vivo*

To assess the alternative splicing activity within a neuronal cell population we delivered the splice reporters in cortical neurons by *in utero electroporation* (Saito and Nakatsuji, 2001; Tabata and Nakajima, 2001). Because the cortical layers are generated sequentially during development (Molyneaux et al., 2007), by electroporating the neuronal precursor cells in the subventricular zone at embryonic stage 14.5 (E.14.5), we predominantly target excitatory pyramidal neurons of layers II-III (Figure 10A). Those neurons receive mainly intracortical inputs which differ from the pyramidal neurons of layer IV which receive mainly inputs from the thalamus (Harris and Mrsic-Flogel, 2013).

First, our analysis did not detect any subgroup within cortical layers II-III that displays a different preference in exon usage. The analysis of all splice reporters indicates that alternative splicing processing could be different for AS2 and AS4 at the three *Nrxn* genes (Figure 10B). For example, the analysis of processing at AS2 between Nrxn1 and Nrxn2 shows that splice insert incorporation is differentially regulated (Figure 10C-D). Moreover, the clustering analysis suggests that the cell-to-cell variation at Nrxn1 is larger than at Nrxn 2 (Figure 10D).

To compare the alternative splicing activity in the cortical neurons on layers II-III with the neurons from all 6 layers, we extracted the mRNAs from electroporated brain areas and used two primer sets recognizing specifically *Nrxn* mRNA from the splice reporter and endogenous Nrxn mRNAs (Figure 10E). This analysis revealed that exon usage is different in cortical neurons of layers II-III compared to the neurons of all layers (Figure 10F). This further supports the existence of cell-type specific alternative splicing regulation of the *Nrxn* genes.

2.2.3.5. Conclusions

In summary, we presented here an assay using bichromatic reporter to detect splicing event at the single-resolution. Those reporters could also be used to monitor effects of activity in the processing of alternative splicing in vivo but also the expression pattern during development.

Development of advanced bichromatic splice reporters

Several works have reported the use of mono-or bichromatic reporters to monitor single-cell splicing events. For example splice reporters were used to profile isoforms expression in mixed cell populations across differents tissues (Kuroyanagi et al., 2013; Kuroyanagi et al., 2006; Ohno et al., 2008; Takeuchi et al., 2010; Miura et al., 2013; Orengo et al., 2006) or to investigate regulation mechanisms (Takeuchi et al., 2010; Kuroyanagi et al., 2006; Kuroyanagi et al., 2013; Newman et al., 2006). Moreover splicing reporters were combined with benchmark normalizers for relative

quantification of isoform ratio to follow the cell-to-cell variability in alternative splicing activity within a population (Gurskaya et al., 2012).

Our splice reporters present some common features with those described by Gurskaya et al., 2012 . Nevertheless, to explore alternative splicing activity of *Nrxns* genes in the mouse brain *in situ*, we have included additional features. To optimize the signal readout for quantification we added three modifications which were 1) removal of premature stop codon in splicing reporter transcript to escape non-sense mediated decay, 2) insertion of nuclear localization signal to concentrate fluorescence signal in the nucleus and thus preventing the diffusion of signal in distal neuronal processes and finally 3) insertion of self-cleaving 2A peptide to increase protein stability. After validating our splicing reporters in heterologous cells we could successfully apply this method *in vivo*. Therefore our work showed that our reporter assay can be used to monitor and quantify alternative splicing activity at the single-cell level in a complex tissue such the brain. Furthermore this assay can be combined with the usage of markers to identify cells.

Cell-type and gene-specific regulations of alternative splicing in *Nrxn* genes

The comparison of alternative splicing activity between nonneuronal and neuronal cells highlights the presence of neuron-specific regulatory mechanisms. Our results showed that exon usage at both alternative spliced segments differs between the cell populations. Indeed alternative splicing pattern at AS4 presents opposite exon usage preferences between the two cell populations. In addition we also observed that the processing at AS2 and AS4 differs between the three Neurexins.

There are RNA-binding proteins that facilitate or inhibit incorporation of alternative exons (Chen and Manley, 2009). Through their selective expression in brain, this provides a mechanism to achieve specific isoforms expression in neuronal tissue. For example, RNA-binding proteins SLM1 and SLM2 regulate processing at AS4 of Neurexin 1 and are selectively expressed in the brain (Iijima et al., 2014).

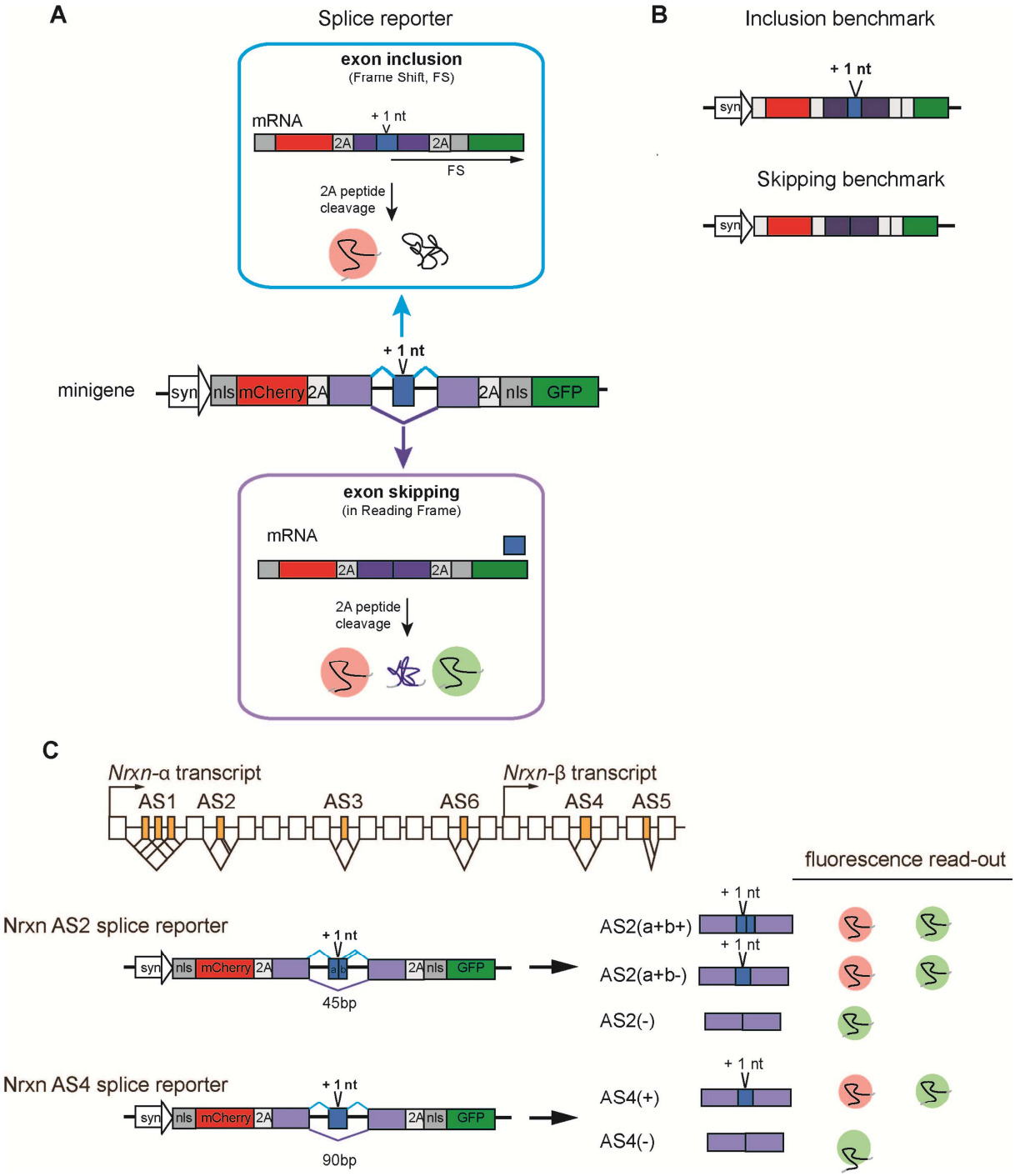

Figure 7 - Design of splice reporters

(A) The minigene contains constitutive exons (in violet) which flank the alternative cassette exon (in blue). In addition, the minigene contains intronic sequences. A single nucleotide was introduced in the splice insert which causes a frame shift upon its inclusion in the final transcript. Therefore changes in the alternative splicing choice are connected to changes in the reading-frame that can be detected at the protein level. mCherry and GFP sequences are fused to a nuclear localization signal (nls) to concentrate fluorescence signal in the nucleus and to a self-cleavage 2A peptide to increase protein stability. **(B)**. Design of benchmarks reporters to normalize green and red fluorescence ratio. **(C)**. Upper part represents genomic structures of *Nrxn* based on *Nrxn 1 α* with the canonical alternative splice segments (AS1-6) in orange. Lower part illustrates the expected fluorescence read-out of splice reporters for Nrxn AS2 and AS4.

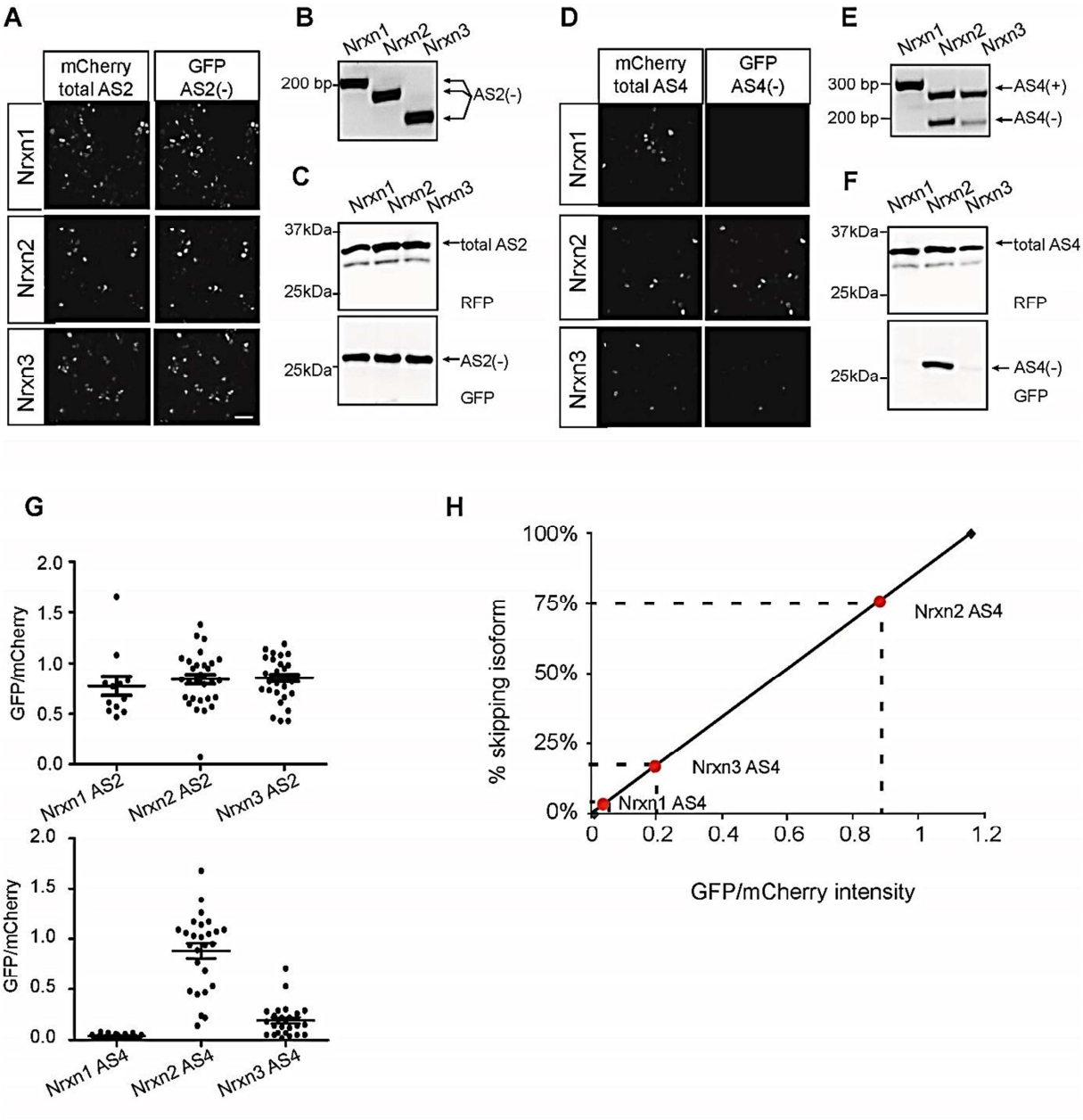

Figure 8- Alternative splicing activity processing at AS2 and AS4 of Nrxn in heterologous cells

Splicing reporters for AS2 and AS4 were transfected in HEK 293T cells.
(A-C) Alternative splicing activity processing activity at AS2 of *Nrxn1-3.* **(A)**. Representative images of HEK293T cells transfected with respective splice reporters for AS2. **(B)**. Analysis of total RNA of *Nrxn1-2-3 AS2* by RT-PCR. **(C).** Analysis of total protein levels of Neurexin 1-2-3 AS2 splice reporters. **(D-F)**. Alternative splicing activity processing activity at AS4 of *Nrxn1-3*. **(D)**. Representative images of HEK293T cells transfected with respective splice reporters for AS4. **(E)**. Analysis of total RNA of *Nrxn1-2-3 AS4* by RT-PCR. **(F)**. Analysis of total protein levels of Neurexin1-2-3 AS4 splice reporters. **(G)**. Fluorescence-based single-cells GFP/mCherry quantification of respective splice reporters expressed in HEK293T cells. **(H)**. Calculated GFP/mCherry ratios for splice reporters Neurexin 1-2-3 AS4 were normalized to the GFP/mCherry ratio displayed by skipping benchmark reporter to obtain the relative amount of skipping isoform. Scale bar represents 20 um

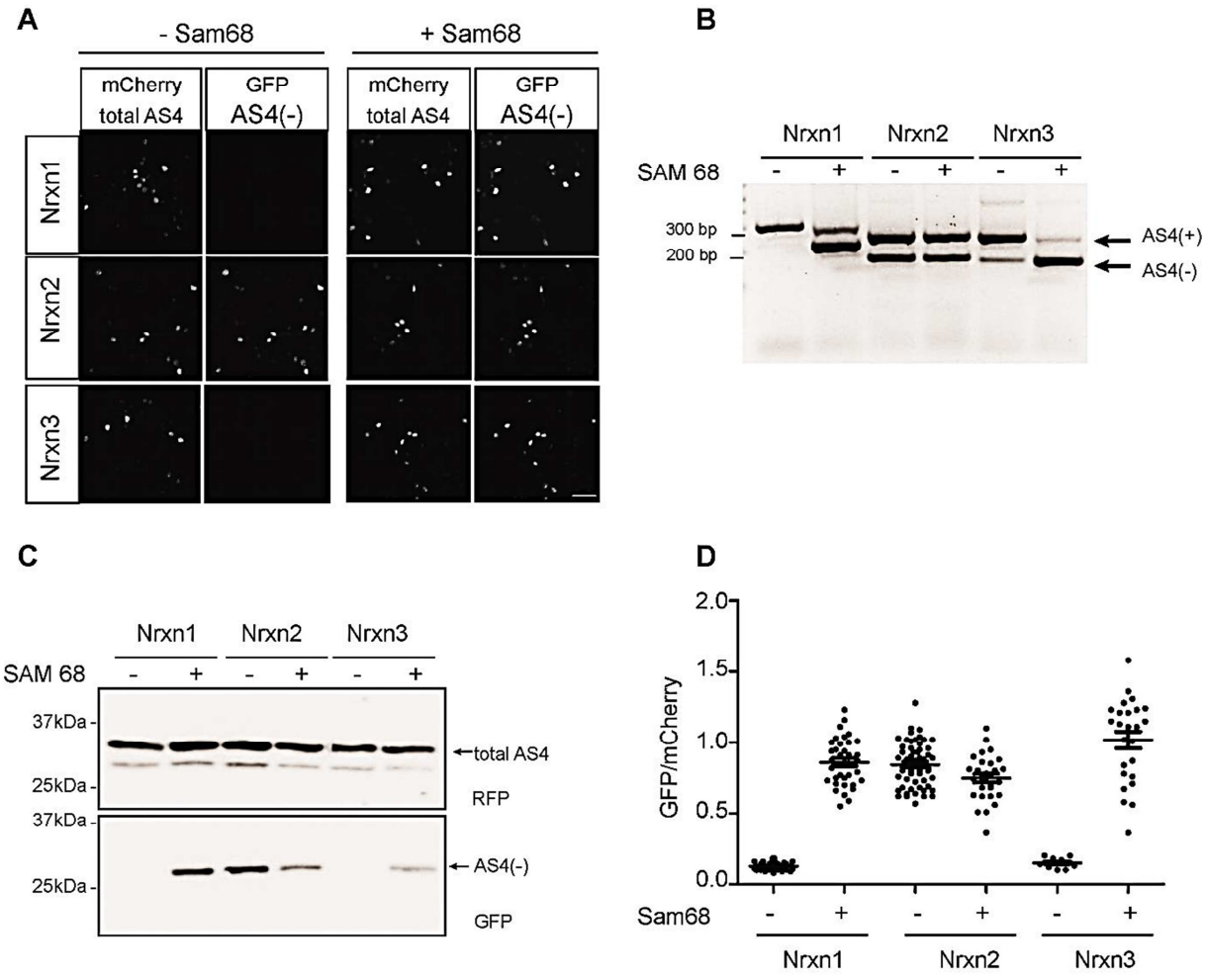

Figure 9-Splice reporters exhibit similar regulation as endogenous *Nrxn* by SAM68

Splice reporters for AS4 of Nrxn 1-2-3 were co-transfected with RNA-binding protein SAM68 in HEK298T cells.
(A).Representative images of HEK293T cells transfected with respective splice reporters for AS4 in the presence or in the absence of SAM68. **(B-D).** total RNA, protein and fluorescence-based single-cell quantifications demonstrate that the presence of SAM68 induces alternative exon skipping at AS4.

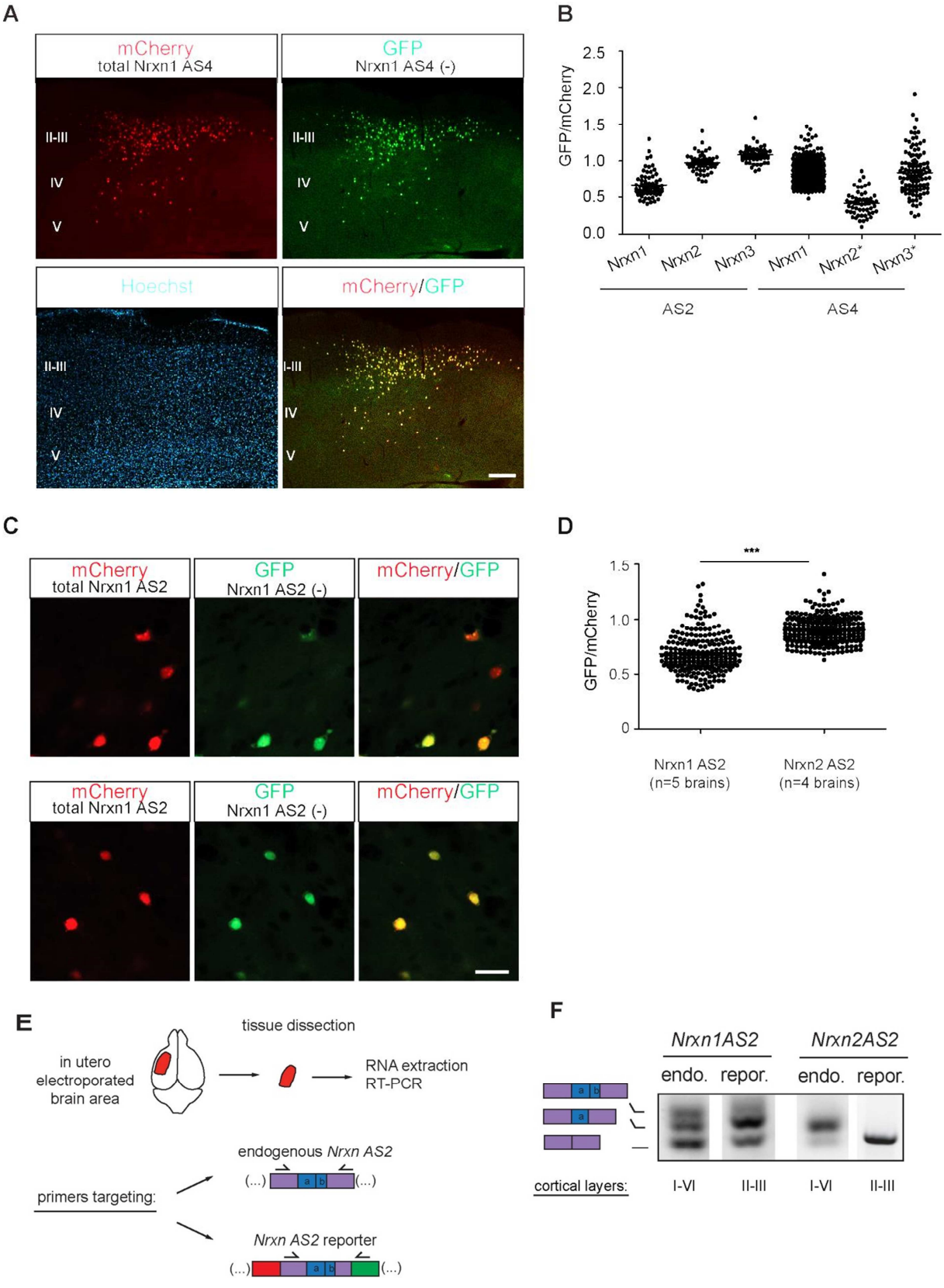
A
mCherry
total Nrxn1 AS4
GFP
Nrxn1 AS4 (-)
Hoechst
mCherry/GFP
II-III
IV
V
B
GFP/mCherry
2.5
2.0
1.5
1.0
0.5
0.0
Nrxn1
Nrxn2
Nrxn3
Nrxn1
Nrxn2*
Nrxn3*
AS2
AS4
C
mCherry
total Nrxn1 AS2
GFP
Nrxn1 AS2 (-)
mCherry/GFP
D
***
GFP/mCherry
1.5
1.0
0.5
0
Nrxn1 AS2
(n=5 brains)
Nrxn2 AS2
(n=4 brains)
E
tissue dissection
in utero
electroporated
brain area
RNA extraction
RT-PCR
primers targeting:
endogenous Nrxn AS2
(...)
a
b
(...)
Nrxn AS2 reporter
F
Nrxn1AS2
Nrxn2AS2
endo.
repor.
endo.
repor.
cortical layers:
I-VI
II-III
I-VI
II-III

Figure 10- Analysis of alternative splicing processing in cortical neurons of layers II-III

Splice reporters were delivered in cortical neurons of layers II-III by *in utero electroporation* at E14.5 and electroporated animals were analyzed at P21-22.
(A). mCherry and GFP fluorescence expression in cortical neurons of layers II-III electroporated with Nrxn1 AS4 splice reporter. II-III, IV and V represent layer 2-3, 4, and 5. Scale bar represents 200 um. **(B)**. Summary of fluorescence-based single-cell quantification of GFP/mCherry ratio of cortical neurons of layers II-III respective splice reporters. *n=1* animal per splice reporter, splice reporters marked with asterisks were in addition labelled with immunofluorescence.**(C)**. Fluorescence expression of cortical neurons of layers II-III electroporated with Nrxn1 and 2 AS2 splice reporter. Scale bar represents 25 um. **(D)**. Fluorescence-based single-cell quantification of GFP/mCherry ratio for Nrxn1 and 2 splice reporters. *n*= 5 and 4 brains for Nrxn 1 and 2 AS2 splice reporters respectively, unpaired t-test, *p<0.0001* . **(E)**. Experimental protocol to compare mRNA expression of endogenous versus exogenous (from splice reporters) in the cortex. The electroporated brain area was dissected at P21-22 by following the red fluorescence. Because the downstream flanking constitutive exon is truncated in the splice reporter, specific primers for endogenous and for splice reporters could be designed. **(F)**. Analysis by RT-PCR to compare the *Nrxn 1* and *2 AS2* expression in cortical neurons II-II versus all cortical layers. end.= endogenous, repor.=reporter

2.3. Cell-type specific Nrxn expression of Nrxn isoform

2.3.1. Selective expression and functions of Neurexin isoforms in Parvalbumin positive interneurons in the mouse hippocampus (manuscript in preparation).

Summary

Synaptic specificity is a hallmark of neuronal circuits and a key factor for their appropriate function. Synaptic properties are thought to be encoded by cell type-specific transcriptional and post-transcriptional programs that shape composition of synaptic recognition complexes. However, the nature of such programs is only beginning to emerge. We here demonstrate that transcripts encoding the synaptic adhesion molecules neurexin-1,2,3 undergo highly differential, cell type-specific alternative splicing in pyramidal cells and parvalbumin-positive interneurons (PV-cells) in the mouse hippocampus. Cell type-specific alternative splicing depends on differential expression of the RNA-binding protein Slm2 and coincides with selective co-expression of a splice isoform-specific neurexin ligand in PV-cells. We generated conditional ablation of *Nrxn* alternative splice insertion selectively in PV-cells and investigate whether synaptic properties were altered. This work identifies cell type-specific alternative splicing as a critical mechanism to control Neurexin function in hippocampal interneurons.

Introduction

Specific synaptic connectivity and function are essential for the appropriate operation of neuronal circuits. A large degree of this structural and functional specificity is thought to be

genetically encoded. For example, synaptic partners express matching pairs of adhesive factors or afferents are repelled from inappropriate targets through chemorepulsive signaling molecules (Sanes and Yamagata, 2009; Shen and Scheiffele, 2010). Gene families encoding large numbers of isoforms generated through multiple genes, alternative promoters, and extensive alternative splicing hold the potential to generate recognition tags for specific trans-synaptic interactions (Zipursky and Sanes, 2010; Schreiner et al., 2014c; Takahashi and Craig, 2013; Reissner et al., 2013). However, given the difficulty of mapping and selectively manipulating the endogenous isoform repertoires it is poorly understood whether splice isoforms indeed contribute to specific synaptic properties. Neurexins (*Nrxn1,2,3*) represent one such gene family of highly diversified synaptic adhesion molecules. Through the use of alternative promoters (alpha and beta) and alternative splicing at up to six alternatively spliced segments (AS1-6) more than 1,300 transcripts are generated that are expressed in the mature mouse nervous system (Schreiner et al., 2014b; Schreiner et al., 2015; Treutlein et al., 2014). Isoform diversity scales with the cellular complexity of brain regions and purified cells are strongly enriched for a targeted set of specific isoforms, demonstrating that at least some neurexin isoforms are expressed in a cell type-specific manner (Schreiner et al., 2014b). Finally, pairwise comparisons of transcripts isolated from single cells suggest that single cells within one cell type might exhibit more similar splicing patterns than cells from divergent origins (Fuccillo et al., 2015). However, the actual alternative exon incorporation rates across cell types and the functional contribution of cell type-specific isoform repertoires have not been examined.

Importantly, individual splice insertions in the neurexin proteins control biochemical interaction with an array of synaptic ligands (Reissner et al., 2013). Based on ectopic expression experiments it has been postulated that neurexin isoforms might contribute to an alternative splice code for selective synaptic interactions and differ in their tethering at neuronal synapses (Boucard et al., 2005; Chih et al., 2006; Futai et al., 2013; Aoto et al., 2015; Fu and Huang, 2010; Graf et al., 2006). However, interpretation of such findings is

complicated by the fact that the manipulations involved overexpression of isoforms in cells where endogenous isoform repertoires were unknown. In the human population mutations in *Nrxn1*,*2*, and *3* are associated with neurodevelopmental disorders such as autism and schizophrenia (Kim et al., 2008; Yan et al., 2008; Kirov et al., 2009; Rujescu et al., 2009; Gauthier et al., 2011; Vaags et al., 2012). Global deletion of the majority of Nrxn transcripts in mice or global restriction of the *Nrxn3* alternative splicing at AS4 disrupts function and plasticity of glutamatergic synapses (Aoto et al., 2013; Etherton et al., 2009). Global deletion also modifies GABAergic transmission. However, function of neurexin isoforms in interneurons has not been examined with targeted approaches. Thus, the consequences of a selective disruption of the neurexin splicing pattern in interneurons (or any cell type) where the endogenous alternative splicing signature is known have not been assessed.

In this study we uncover cell type-specific alternative splicing of neurexins in fast-spiking GABAergic interneurons expressing the calcium binding protein parvalbumin (PV-cells). We demonstrate that *Nrxn3* alpha transcripts are highly expressed in PV-cells and exhibit differential incorporation of alternative exons as compared to pyramidal cells of the hippocampus. This alternative splicing switch depends on cell type-specific expression of RNA-binding proteins and coincides with the cell type specific expression of a neurexin splice isoform-specific ligand.

Results

Neurexin alpha mRNAs are highly expressed in pyramidal cells and parvalbumin-positive interneurons of the mouse hippocampus

To begin to assess the functional relevance of neurexin isoforms in interneuron populations of mice we first examined expression of the primary neurexin transcripts by *in situ hybridization*. Similar to what has been reported for rat hippocampus

(Ullrich et al., 1995) we find significant expression of *Nrxn1, 2* and *3* alpha transcripts in *cornus ammonis* (CA) pyramidal cells as well as presumptive interneurons (Figure S1). To specifically interrogate *Nrxn* transcripts in genetically defined cell populations we tagged ribosomes in CA pyramidal cells and parvalbumin-positive interneurons, a population of GABAergic, fast-spiking cells that encompasses chandelier and basket cells (Hu et al., 2014). We used a conditional HA-tagged Rpl22 allele (Sanz et al., 2009) crossed with a CamK2^{cre} (Tsien et al., 1996) and PV^{cre} drivers (Hippenmeyer et al., 2005), respectively (see Figure 1 and Figure S2 for the selectivity of HA-Rpl22 expression in the resulting CamK2^{Ribo} and PV^{Ribo} mice). We then performed RiboTrap purifications (Heiman et al., 2014) of polysome-associated mRNAs from adolescent (P24-P28) CamK2^{Ribo} or PV^{Ribo} mice. The enrichment of mRNAs from the respective cell populations in RiboTrap purifications was confirmed by quantitative real-time PCR. Thus, CamK2^{Ribo} preparations showed enrichment of the CA1-specific marker wsf1 (consistent with high cre-activity in the CA1 area, see Figure 1 and Figure S2) and de-enrichment of interneuron and astrocyte markers. By contrast, PV^{Ribo} preparations were highly enriched in interneuron markers and mRNAs specifically expressed in fast-spiking baskets cells (*PV, ErbB4*). *Nrxn1,2,3* mRNAs were recovered in CamK2^{Ribo} and PV^{Ribo} cell-derived transcript preparations. Notably, amongst all neurexin transcripts *Nrxn3* alpha was most highly enriched in the PV-cell population. PV-cell expression of *Nrxn3* was further confirmed by dual labeling with *in situ hybridization* using *Nrxn3 α* probes and immunostaining labeling using antitbody against RFP in in mice where PV-cells were genetically labelled with red fluorescent protein (PV^{cre}:Ai9)expression (Figure 1D).

An interneuron-specific program of neurexin alternative splicing, RNA binding proteins and splice-isoform specific ligand.

To quantitatively probe alternative exon incorporation rates in the neurexin transcripts we used radioactive PCR amplification with flanking primers and limited amplification cycle numbers. Importantly, this flanking primer method is not plagued by problems of differential PCR primer efficiencies that are encountered in real-time PCR. We uncovered similar usage of alternative exons at AS2, 3 and 6 (except for *Nrxn2* AS2) across all preparations but remarkably divergent alternative exon incorporation rates at AS4 (Figure 2 and Figure S3). While in CamK2^{Ribo} cells AS4 was largely skipped there was a high level of alternative exon inclusion in PV^{Ribo} cells. Thus, highly selective, cell type-specific alternative exon incorporation rates of neurexin mRNAs generate divergent *Nrxn* splice isoform repertoires in glutamatergic CA pyramidal cells and PV interneurons.

Neurexin alternative splicing at AS4 is regulated by the STAR-family of RNA-binding proteins, in particular the protein Slm2 which regulates skipping of the alternative exon (Iijima et al., 2014; Iijima et al., 2011). Thus, we tested whether the cell type-specific alternative splicing at AS4 may be a consequence of differential expression of Slm2 in pyramidal and PV-cells. We observed high expression of Slm2 protein in pyramidal cells (as previously reported (Stoss et al., 2004)). By contrast, there is no significant expression of Slm2 in the vast majority of PV-positive cells in the CA1 region of the hippocampus (Figure 2C). We further explored differential expression of STAR family RNA binding proteins by quantitative PCR on polysome-associated transcripts from Camk2^{Ribo} and PV^{ribo} mice (Figure 2D). Given that global ablation of Slm2 results in a significant loss of the skipped (AS4-) neurexin isoforms (Traunmuller et al., 2014; Ehrmann et al., 2013) this strongly suggests that differential

expression of Slm2 in pyramidal versus PV-cells is indeed responsible for the cell type-specific alternative splicing of neurexins in the hippocampus.

Neurexin AS4+ isoforms bind to a class of extracellular ligands called Cblns (Ito-Ishida et al., 2012b; Uemura et al., 2010). Notably, we detected strong enrichment of Cbln4-encoding transcripts in the PV-positive cell population whereas Cbln2 was strongly de-enriched (Figure 2E). Thus, pyramidal neurons in the hippocampus express high levels of Slm2 which drives production of AS4- splice isoforms, and there are low levels of Cblns2 and 4. By contrast, PV-cells lack STAR-family RNA-binding proteins, consequently exhibit high levels of alternative exon inclusion at AS4, and the cells co-express the AS4+ specific ligand Cbln4. Thus, there are distinct Neurexin-related molecular programs encompassing the expression of RNA-binding proteins, alternative splicing regulation, and co-expression of splice-isoform-specific ligands that distinguish pyramidal cells from PV-positive interneurons in the mouse hippocampus.

Conclusions

In this study we have identified cell-type Neurexin isoform repertoires between two fundamentally different neuronal populations which are the excitatory Camk2 positive CA1 pyramidal cells and the PV positive interneurons in the mouse hippocampus. Moreover we report that cell-type specific expression of isoforms is determined by genetically encoded gene expression program. First we demonstrated that *Nrxn* α transcripts are highly expressed in CA1 pyramidale neurons and in PV positive interneurons. Second, we show that alternative exon incorporation rate is highly divergent at alternative splice segment 4 (AS4) between both population. This opposite regulation is due to differential expression of RNA binding protein SLM2

which drives the expression of *Nrxn* transcripts lacking the alternative splice insert at AS4 in CA1 pyramidal neurons. Moreover we also observed a correlation of isoform-specific ligand Cbln4 in PV interneurons.

Cell-type specific alternative splicing machinery instructs the neurexin isoform code

A major finding of this study is the strong differential alternative splicing regulation of neurexin transcripts in pyramidal cells and parvalbumin-positive interneurons. Previous work provided evidence for cell type-specific repertoires of full-length neurexin transcripts (Schreiner et al., 2014b) and pairwise comparison of alternative exon amplifications between single cells (Fuccillo et al., 2015). However, none of these studies uncovered links between splicing machinery, alternative exon incorporation rates, cell type-specific function of endogenous isoforms.

Our observation that AS4 insertion-containing *Nrxn3* mRNAs are predominant in PV-cells and abundant in the entire hippocampus was surprising as it had been previously suggested that these *Nrxn3* AS4+ isoforms make up only 10% of *Nrxn3* in the mouse hippocampus (Aoto et al., 2013). We note that the estimates of exon incorporation provided by Aoto et al rely on extrapolation from several different PCR assays which can result in the mis-interpretation of isoform contents due to differential primer efficiencies. We and others observed significantly higher abundance of AS4+ isoforms in the hippocampus using radioactive PCR assays or semi-quantitative PCR, as well as mass-spectrometric assays that probe *Nrxn3* AS4+ variants on the protein level (Figure 2 and (Schreiner et al., 2015; Traunmuller et al., 2014; Ehrmann et al., 2013)). Thus, we conclude that these variants are indeed

significantly expressed, at least in the mouse strains used in our studies.

The highly selective alternative splicing choices in the neurexin pre-mRNAs suggest that they result from neuronal cell-type specific expression of alternative splicing factors. The high, preferential expression of *Nrxn1,2,3* AS4- (skipped) variants in pyramidal cells discovered here correlates with the high expression of Slm2 protein in pyramidal cells and the near complete loss of these variants in Slm2 knock-out mice (Traunmuller et al., 2014; Ehrmann et al., 2013). Moreover, we demonstrate here that Slm2 is absent from the majority of PV-positive interneurons, and that these cells correspondingly generate high levels of AS4+ neurexin isoforms. Finally, we demonstrate that this selective expression of AS4+ variants coincides with PV-cell enrichment of Cbln4, an AS4+ specific neurexin ligand. Thus, a cell type-specific gene expression program emerges that regulates neurexin isoform content and function in neurons.

Functional consequences of cell type-specific splicing regulation

A differential function of neurexin AS4 splice variants at glutamatergic and GABAergic synapses had been previously hypothesized based on cellular in vitro assays. Thus, cultured hippocampal neurons preferentially develop GABAergic postsynaptic specializations when brought into contact with non-neuronal cells expressing neurexin-1 beta AS4+ isoforms (Chih et al., 2006; Graf et al., 2006). By contrast, glutamatergic and GABAergic synapses are formed in response to AS4- variants. These findings provided a first insight into potential synapse-specific activities of neurexin splice variants. The data presented here demonstrate that endogenous neurexin isoforms expressed in pyramidal and PV-cells differ

dramatically in their alternative splicing regulation at AS4.

In the mouse cerebellum, Neurexin-Cbln1 interactions have been demonstrated to be essential for the formation and stability of parallel fiber synapses (Ito-Ishida et al., 2012b; Uemura et al., 2010). Similar to the cerebellar neurons, PV-cells express a Cbln family protein (Cbln4). Immnolabeling experiment showed that Cbln4 is expressed on the dendrites and in the perisomatic region of CA1 pyramidal cells, suggesting that Cbln4 is associated with inhibitory synapses (Chacon et al., 2015). Cbln4 is secreted protein (Iijima et al., 2007) .Using binding assays, we found that Cbln4 binds with Neurexin 1 α and β AS4 + (Dietmar Schreiner, unpublished data) confirming previous studies (Yasumura et al., 2012). In contrast Cbln4 interaction with Neurexin 3 α and β AS4 + is very low (Dietmar Schreiner, unpublished data). In cerebellum, the postsynaptic ligands of Cbln1 is GlurD2 (Uemura et al., 2010). Nonetheless, GlurD2 is not expressed in the hippocampus, instead, Cbln4 has been reported to interact with DCC in the hippocampus (Wei et al., 2012). Thus, Neurexin 1 AS4+ could form a complex with Cbln4 and DCC in the hippocampus.

.

Figure 1

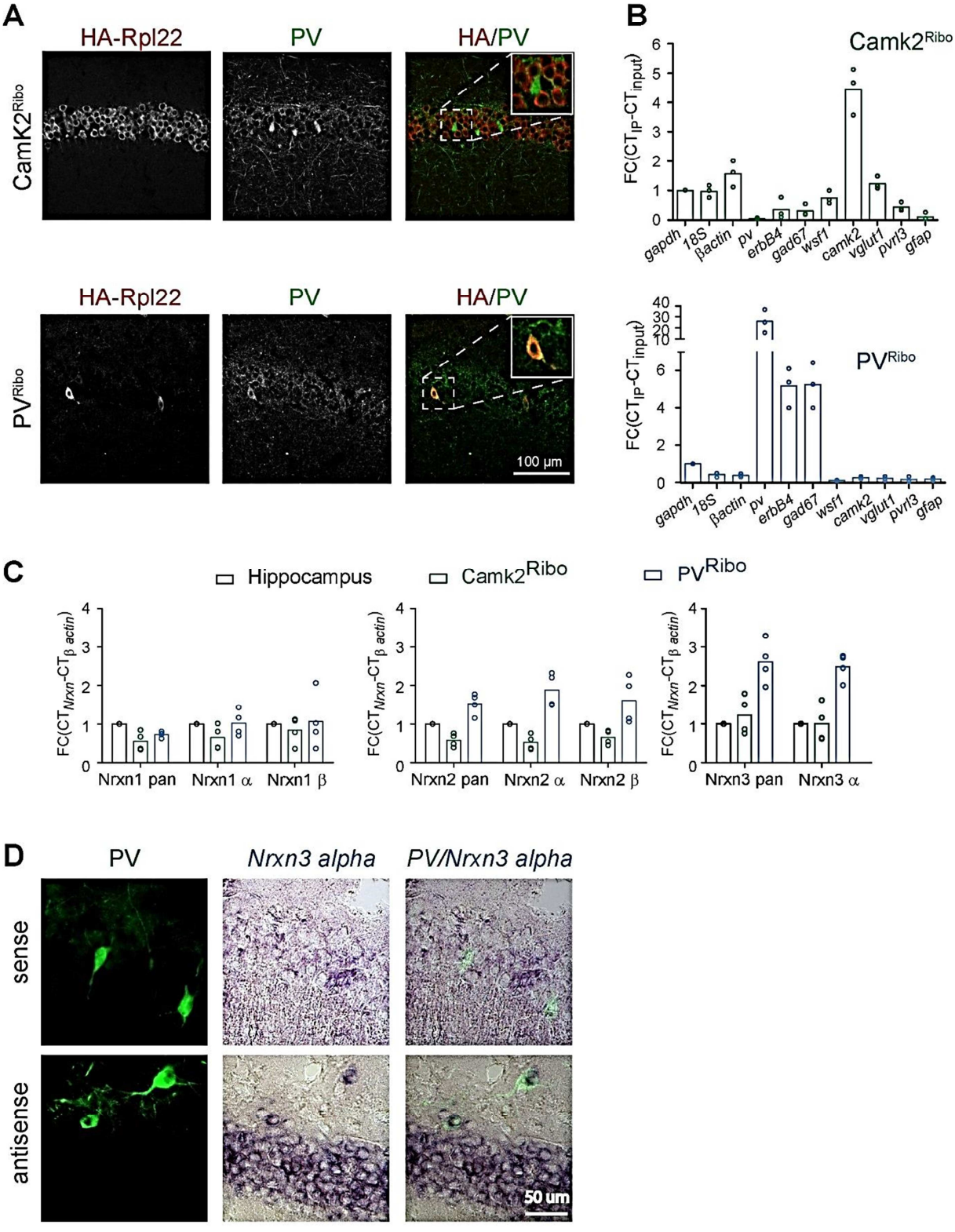
A
HA-Rpl22
PV
HA/PV
CamK2Ribo
PVRibo
100 µm
B
Camk2Ribo
PVRibo
FC(CTIP-CTinput)
gapdh
18S
βactin
pv
erbB4
gad67
wsf1
camk2
vglut1
pvrl3
gfap
C
Hippocampus
Camk2Ribo
PVRibo
FC(CTNrxn-CTβ actin)
Nrxn1 pan
Nrxn1 α
Nrxn1 β
Nrxn2 pan
Nrxn2 α
Nrxn2 β
Nrxn3 pan
Nrxn3 α
D
PV
Nrxn3 alpha
PV/Nrxn3 alpha
sense
antisense
50 um

Figure 1: Neurexin transcripts are expressed in parvalbumin-positive interneurons

(A). Conditional expression of Rpl22HA in pyramidal cells ($CamK2^{Ribo}$) and fast-spiking interneurons (PV^{Ribo}) in mouse hippocampus (P28). Immunereactivity for epitope-tagged Rpl22 (anti-HA, red in merge), anti-parvalbumin (green in merge) is shown. Inset in merge shows an enlargement of the boxed area.
(B). Purification of cell type-specific polysome-associated transcripts by RiboTrap affinity purification. Transcript levels were assessed by real-time qPCR for general markers of glutamatergic neurons (vGlut1, CamK2), markers of CA1 pyramidal cells (wsf1), CA3 (pvrl3), general GABAergic markers (gad67, erbb4), and parvalbumin (pv). Enrichment in the immunoisolate was calculate relative to the input and was normalized to vglut1 and gad67 for the $Camk2^{Ribo}$ and PV^{Ribo} purifications, respectively.
(C). Expression of *Nrxn1,2,3* transcripts in PV and Camk2 cells was examined by real-time qPCR. Transcript levels in each preparation were normalized to the level of beta-actin transcripts and enrichment in the immunoisolate was calculated relative to the input levels in total hippocampus.
(D). Expression of *Nrxn3* α in PV-cells in CA1 (postnatal day 21) revealed by dual labeling with *in situ hybridization* using *Nrxn3 α* probes and immunostaining using antibody against RFP in mice where PV-cells are genetically marked by cre-dependent expression of red fluorescent protein (PV^{cre}::$A9^{Tom}$)

Figure S1

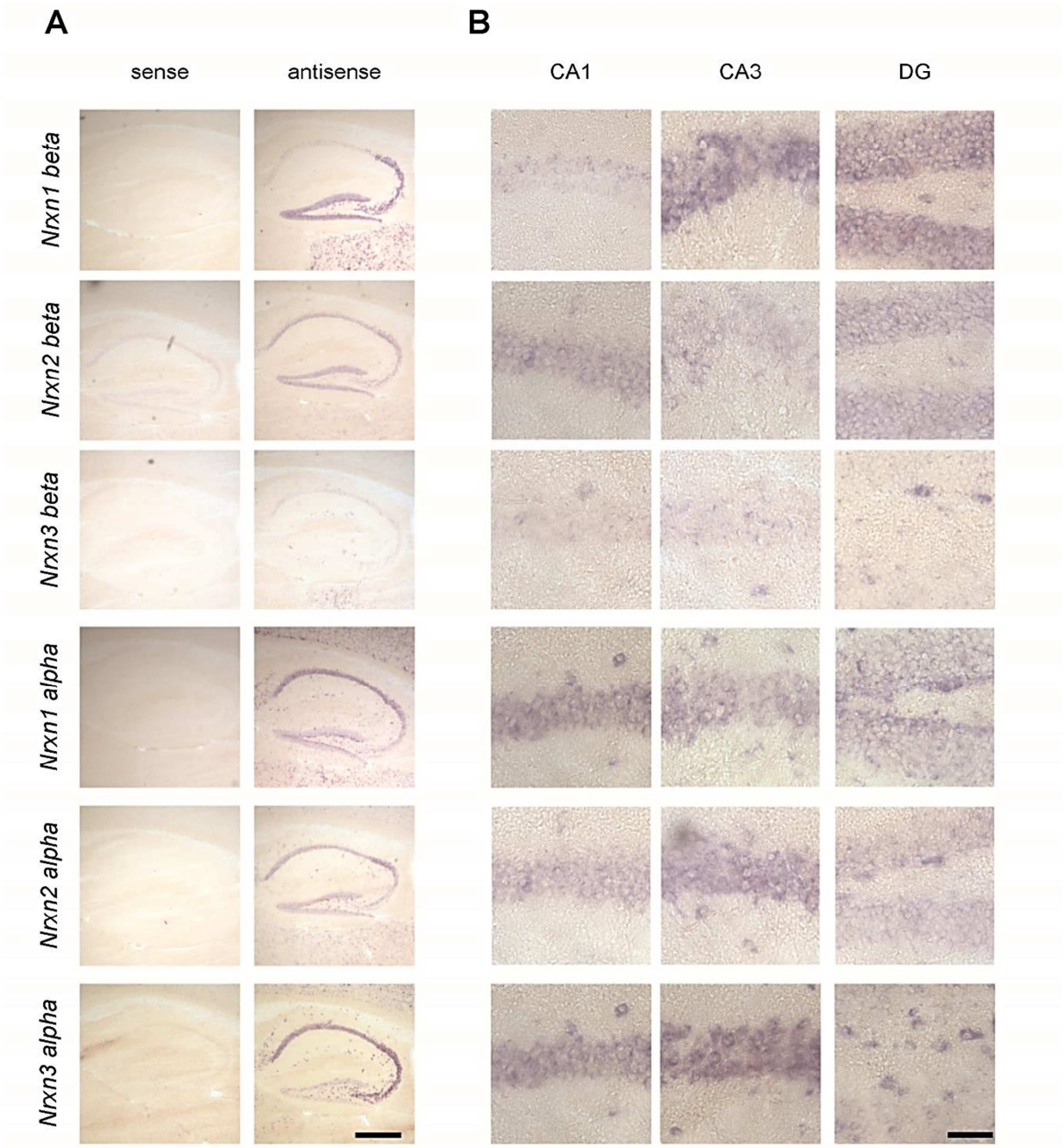

Figure S1. Detection of primary *Nrxn* transcripts by *in situ hybridization*.
Relative to Figure 1

(A). In situ hybridization on mouse hippocampal tissue with probes specific for Nrxn1alpha and Nrxn3alpha transcript. Panels show overview images at low magnification and enlarged fields of area CA1 and CA3. Scale bar in 4x panels is 200 µm and 50 µm in 40x panels.
(B). In situ hybridization on PVcre::stopTom mouse tissue. Parvalbumin-positive interneurons are marked with anti-RFP antibodies and HRP-reaction. Transcripts for Nrxn1alpha and Nrxn3 alpha are shown in blue.

Figure S2

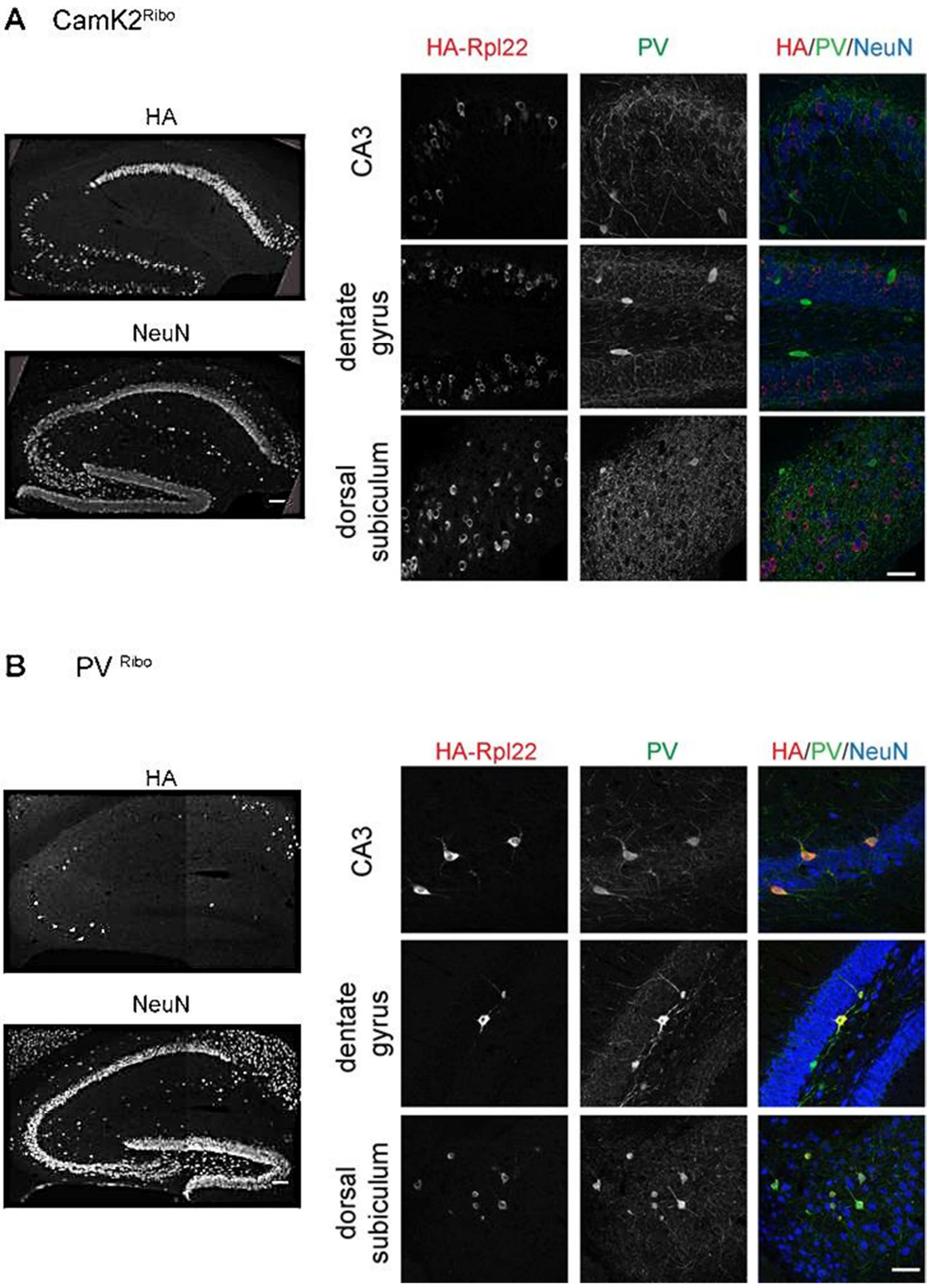
A CamK2Ribo
HA
NeuN
HA-Rpl22
PV
HA/PV/NeuN
CA3
dentate gyrus
dorsal subiculum
B PV Ribo
HA
NeuN
HA-Rpl22
PV
HA/PV/NeuN
CA3
dentate gyrus
dorsal subiculum

Figure S2. Conditional Rpl22 expression in mouse hippocampus.
Relative to Figure 1

(A). HA-tagged Rpl22, conditionally expressed in Rpl22HA::CamK2a^{cre} (CamK2^{Ribo}) or **(B)** Rpl22HA::PV^{cre} (PV^{Ribo}) mice, was detected with anti-HA antibodies (red). Parvalbumin-expressing cells are marked with anti-PV antibodies (green) and hippocampal architecture is revealed with anti-NeuN antibodies (blue; mouse hippocampus, age P25, area CA3, DG is dentate gyrus, sub is dorsal subiculum). Note that CamK2a^{cre}-dependent recombination of the RPL22HA allele in CA3 and dentate gyrus is sparse. Scale bar of the low magnification images is 100 µm and of the large magnification is 50 µm.

Figure 2

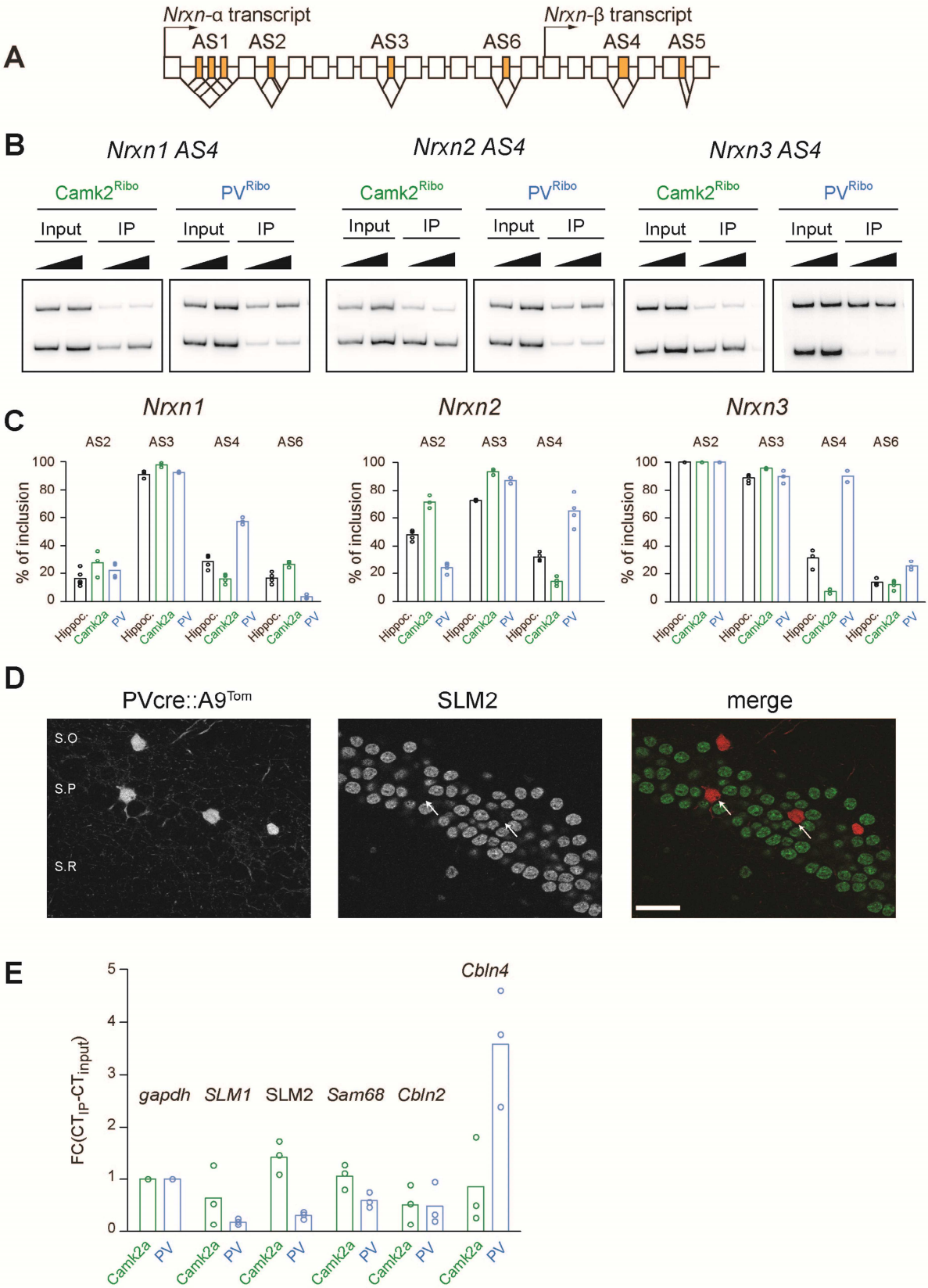
A
Nrxn-α transcript
Nrxn-β transcript
AS1 AS2 AS3 AS6 AS4 AS5
B
Nrxn1 AS4
Nrxn2 AS4
Nrxn3 AS4
Camk2Ribo
PVRibo
Input IP
C
Nrxn1
Nrxn2
Nrxn3
AS2 AS3 AS4 AS6
% of inclusion
Hippoc. Camk2a PV
D
PVcre::A9Tom
SLM2
merge
S.O
S.P
S.R
E
Cbln4
gapdh SLM1 SLM2 Sam68 Cbln2
FC(CTIP-CTinput)
Camk2a PV

Figure 2: Cell-type-specific alternative splicing

(A). Schematic illustrating genomic structure of the Nrxn gene (example based on mouse Nrxn1). Alternatively spliced segments are numbered (AS1-6) and alternative exons are highlighted in orange. Constitutive exons appear as white boxes.
(B).Analysis of alternative splicing pattern in total hippocampus, $Camk2^{Ribo}$ and PV^{Ribo} preparations. In the upper panel, radioactive PCR amplifications for *Nrxn1,2,3* AS4. For each sample two PCR reactions were run in such configuration that in the second reaction the double amount of cDNA was used. In lower panel alternative exon insertion rates at alternatively spliced segments 2,3,4, and 6 in *Nrxn1,2,3* transcripts for total hippocampus, $Camk2^{Ribo}$ and PV^{Ribo} preparations. The insertion rates were measured by radioactive PCR with limiting cycle numbers and were quantified for assays conducted on 3 independent Ribotrap purifications. Raw data for the radioactive PCR amplifications are shown in Figure S3.
(C). Expression of Slm2 in PV-cells in mouse hippocampus (postnatal day25) was examined using mice in PV^{cre}::$A9^{Tom}$ mice. Dual immunohistochemistry on vibratome sections reveal high Slm2 expression in hippocampal pyramidal cells but no detectable expression in PV-cells in and adjacent to the *stratum pyramidale*.
(D). STAR protein and Cbln mRNA expression by Ribotrap

Figure S3

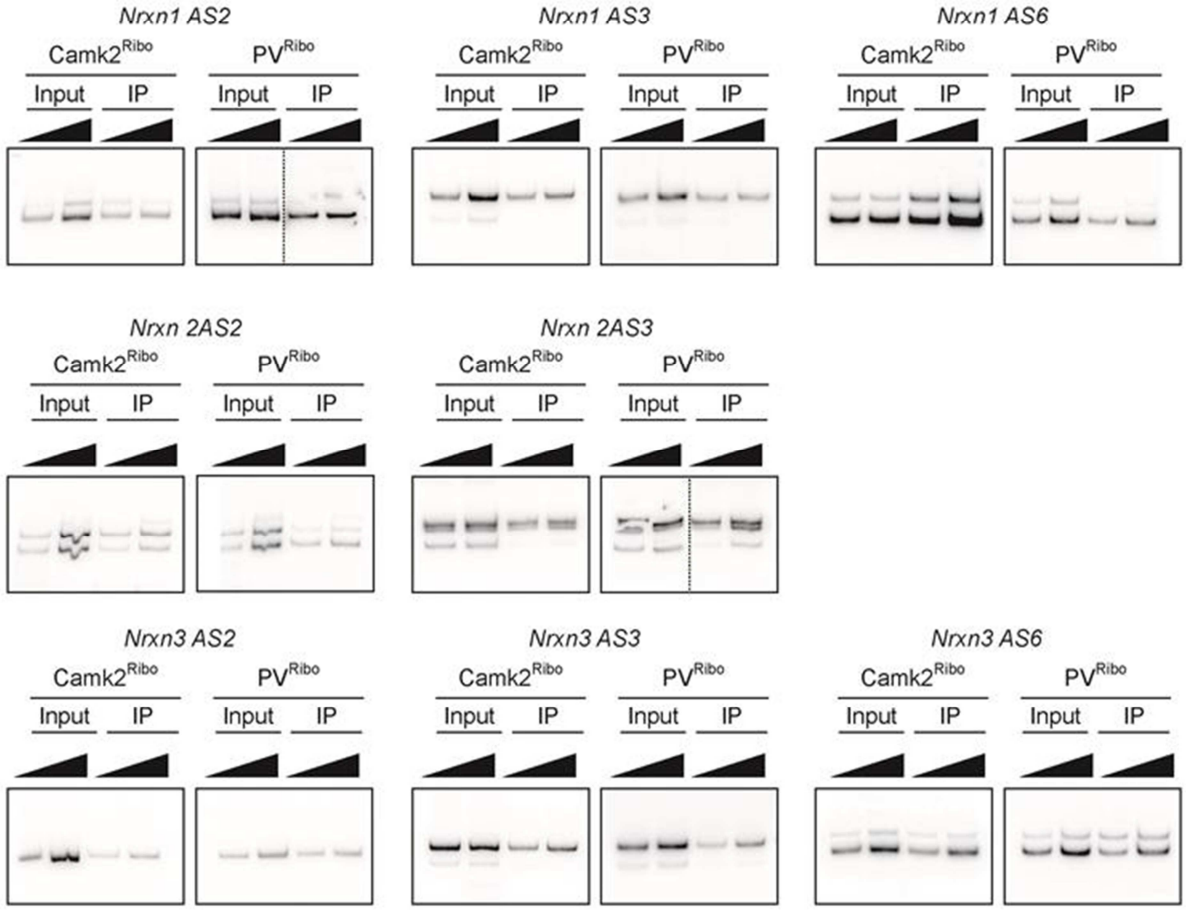

Figure S3. Examples of assessment of alternative exon incorporation rates by radioactive RT-PCR.
Relative to Figure 2

Alternative exon incorporation rates was determined by radioactive RT-PCR.
For each sample two PCR reactions were run in such configuration that in the second reaction the double amount of cDNA was used. In lower panel alternative exon insertion rates at alternatively spliced segments 2,3,4, and 6 in *Nrxn1,2,3* transcripts for total hippocampus, $Camk2^{Ribo}$ and PV^{Ribo} preparations. The insertion rates were measured by radioactive PCR with limiting cycle numbers and were quantified for assays conducted on 3 independent Ribotrap purifications.

2.3.2. *In vivo* analysis of deletion of *Nrxn AS4(+)* isoforms in PV interneurons in the hippocampus

In this following section I will present the characterization of the Nrxn3 ex21Δ and Nrxn1/3 ex21Δ Parvalbumin conditional knock-out mice. The data comprises of morphological and behavioral analysis. To have a complete *in vivo* study to submit a manuscript electrophysiological recordings are currently carried out by several collaborators.

2.3.2.1. Conditional deletion of *Nrxn AS4(+) isoforms* in PV does not alter synaptic density and vesicle distribution

To assess whether the molecular program identified here is functionally relevant we generated a *Nrxn1* and *3* splice isoform-specific conditional single knock-out in which alleles where exon 21 (which encodes the alternative insertion at AS4) is flanked by loxP sites (Figure 12A). Upon germline ablation of exon 21 we observed a complete loss of exon 21-containing *Nrxn1* and *3* transcripts (Figure 11B).

We conditionally ablated exon 21 in *Nrxn3* in PV positive cells using PV^{cre} mice (*Nrxn3 ex21Δ*^{PV}). To determine if *Nrxn1* and *3 AS4+* isoforms are redundant, we generate a double knock-out mouse line in which both *Nrxn1* and *3* alleles are flanked with loxP sites and then crossed it with PV^{cre} mouse line (*Nrxn1/3 ex21Δ*^{PV}). Conditional mutant mice were born at Mendelian ratios and the mutant mice were viable and fertile (Figure 11C). Overall, hippocampal anatomy and density of parvalbumin-immunoreactive cells was unchanged, indicating that the mutation did not result in early developmental defects (Figure 14B). We then explored whether incorporation of exon 21 at AS4 is specifically required for controlling PV neuron synapse formation. We examined the density of perisomatic synapses in the *stratum pyraidale* by immunostaining with anti-synaptotagmin-2 antibodies which selectively mark terminals of PV-positive basket cells (Sommeijer and Levelt, 2012) and with anti-Neuroligin2 antibodies which label postsynaptic GABAergic sites (Varoqueaux et al., 2004a; Graf et al., 2004; Chih et al., 2005a) (Figure 12A). We observed no significant change in the number of Syt2- or NL2-positive structures in the *stratum*

pyramidale in both single and double conditional knock-out mice, indicating that synapse density is not significantly altered (Figure 12B). We further explored if the deletion of AS4 specific isoforms impairs the distribution of synaptic vesicles by electron microscopy. Perisomatic PV-termini were identified based on their location and ultrastructural characteristics (Takacs et al., 2015)(Figure 12C). Analysis of vesicle distribution showed no significant changes (Figure 12D). Moreover, the average number of vesicles and active zone length were not affected by the loss of *Nrxn AS4(+)* isoforms (Figure 13C). Taking our immunolabelling analysis and our ultrastructural quantifications together, they show that Nrxn1 and 3 AS4(+) isoforms are not regulating synapse density nor vesicle recruitment.

2.3.2.2. Impaired recognition memory in *Nrxn1/3 ex21Δ^{PV}*

Cognitive impairment and learning memory have been associated with PV dysfunctions of the hippocampus (Wonders and Anderson, 2006; Bannerman et al., 2014). Therefore we test double-knock out mice *Nrxn1/3 ex21Δ^{PV}* in different tasks that assess those parameters. PV defects can be associated with anxiety (Wohr et al., 2015). To test this, we placed mice in open arena and recorded their explorative behavior. The center of an arena is anxiogenic and therefore mice tend to avoid this area. Therefore the time spent in the center of an arena is a measure of the anxiety. Moreover, anxiety can be also tested in an elevated plus maze apparatus which contains two open and closed arms. Open arms are also anxiogenic, thus mice are expected to spend more time in closed arms. The results showed that double knock-out mice do not avoid open space, indicating the absence of anxiety (Figure 13A). Measurements of the distance travelled and the velocity showed that double knock-out mice were not hyperactive.

PV interneurons has been shown be involved with recognition memory (Fuchs et al., 2007; Barnes et al., 2015). Thus test if *Nxnn 1* and *3 AS4(+)* isoforms s involved in the formation of this type of memory, we performed a novel object recognition task (Figure 14C). We observed that *Nrxn1/3 ex21Δ^{PV}* conditional knock-out failed to remember the familiar object. Indeed they could not discriminate between the familiar and the novel object. These results demonstrated that the PV-

specific regulation of alternative splicing at AS4 of *Nrxn1* and *3* plays a crucial role in the regulation of short-term memory formation.

2.3.3. Conclusions

The *in vivo* investigations demonstrated that selective ablation of alternative exon 21 in PV positive interneurons does not display major morphology alterations but results in an impaired short-term memory formation. First we show that PV termini and postsynaptic inhibitory perisomatic synapses are unchanged in the *stratum pyramidale* in CA1. Second we report that genetic conditional deletion of alternative exon 21 of *Nrxn1* and *3* genes in PV interneurons results defect in learning. Indeed, in novel object recognition task, mutant mice failed to remember the familiar object they have previously encountered within a short interval.

Inhibitory perisomatic synapses density is unchanged

Co-cultures experiments have reported that expression of Neurexin 1 β AS4(+) drives the differentiation of inhibitory synapses on contacting dendrites (Chih et al., 2006; Graf et al., 2004). Using same co-culture assays we have found that, similarly to Neurexin 1 β AS4(+), Neurexin 3 α AS4(+) expression induces the differentiation of inhibitory structures (Dietmar Schreiner, unpublished). Therefore, the unchanged synaptic density result was unexpected.

The unaltered synaptic density was also confirmed by electrophysiology recordings. Indeed measurements of inhibitory currents in the CA1 region of the hippocampus indicated that the frequency and the amplitude of mIPSC was unaltered (Dr. Andrea Gomez and Dr. Le Xiao, unpublished data).

A possible reason for this could be due to a timing issue. Synaptogenesis happens in the two first postnatal weeks. Endogenous PV promoter is activated late in the second postnatal week. Thus, allele recombination at exon 21 occurs after the peak of synaptogenesis. It means that during the most duration of synapse formation, the endogenous correct splice isoform was expressed.

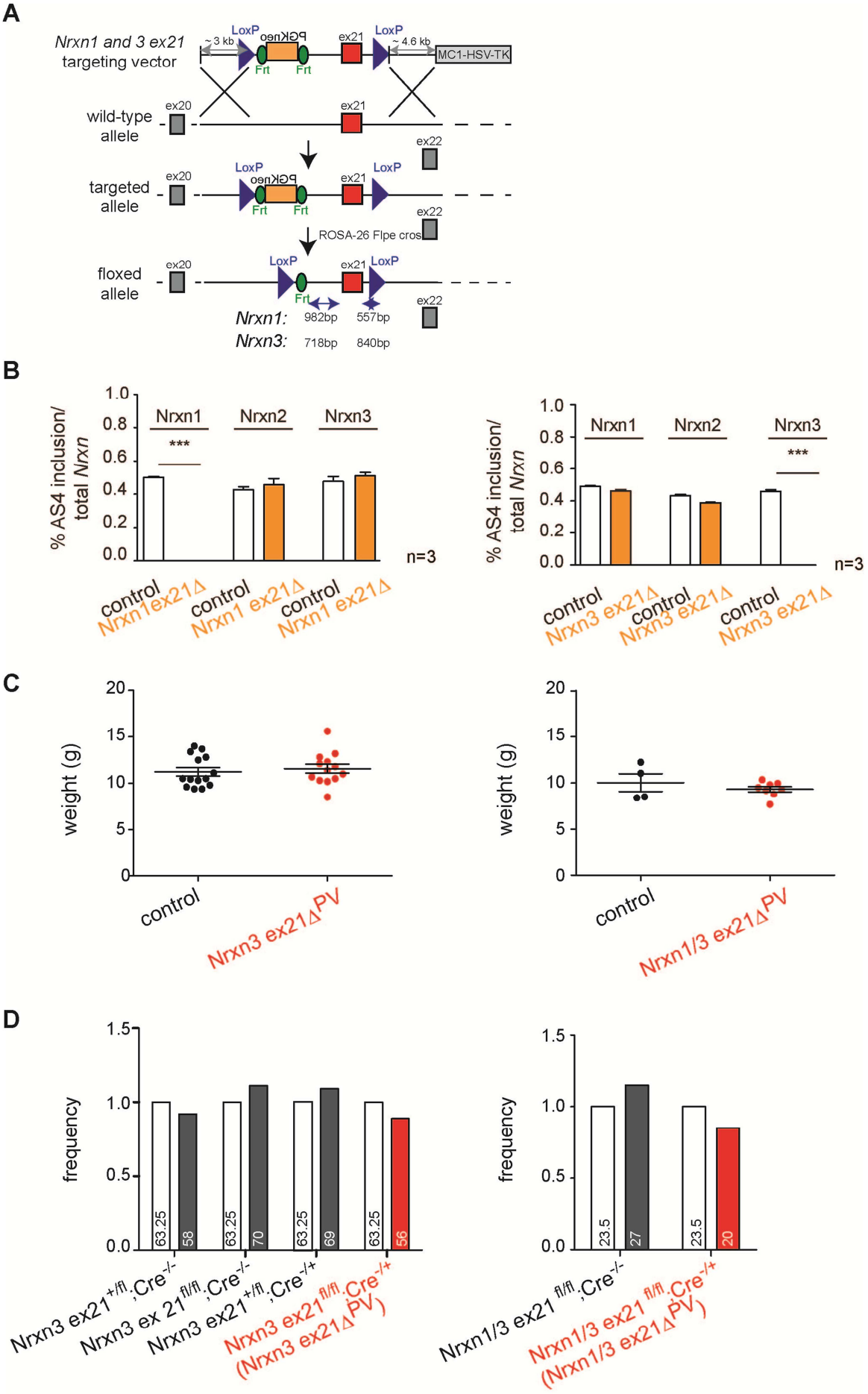
A
Nrxn1 and 3 ex21
targeting vector
~3 kb
LoxP
PGKneo
Frt
Frt
ex21
LoxP
~4.6 kb
MC1-HSV-TK
wild-type
allele
ex20
ex21
ex22
targeted
allele
ROSA-26 Flpe cros
floxed
allele
Nrxn1: 982bp 557bp
Nrxn3: 718bp 840bp
B
% AS4 inclusion/
total Nrxn
Nrxn1
Nrxn2
Nrxn3
***
n=3
control
Nrxn1ex21Δ
Nrxn1 ex21Δ
Nrxn3 ex21Δ
C
weight (g)
control
Nrxn3 ex21ΔPV
Nrxn1/3 ex21ΔPV
D
frequency
63.25
58
70
69
56
23.5
27
20
Nrxn3 ex21+/fl;Cre-/-
Nrxn3 ex 21fl/fl;Cre-/-
Nrxn3 ex21+/fl;Cre-/+
Nrxn3 ex21fl/fl;Cre-/+
(Nrxn3 ex21ΔPV)
Nrxn1/3 ex21fl/fl;Cre-/-
Nrxn1/3 ex21fl/fl;Cre-/+
(Nrxn1/3 ex21ΔPV)

Figure 11- Genetic ablation of exon 21 in *Nrxn 1* and *3* AS4 in mice

(A). Targeting strategy for conditional ablation of *Nrxn1* and *3 AS4 (+)* isoform (*Nrxn1*^{ex21} and *Nrxn3*^{ex21}). In the conditional allele *Nrxn1* and *3* exon 21 is flanked by loxP sites inserted 982 bp and 718 bp upstream and 557 bp and 840 bp downstream of the alternative exon, respectively. The targeting vector contained a Frt-site flanked neomycin resistance gene driven by the phosphoglycerate kinase 1 promoter (PGKneo). **(B)**. Analysis of *Nrxn1,2* and *3 AS4* mRNA in control and in *Nrxn1 ex21 Δ* and *Nrxn1 ex21 Δ* global knock-out. (unpaired t-test, $p<0.00001$) **(C).** Weight and genotype frequency in *Nrxn3 ex21 Δ*^{PV} and *Nrxn1/3 ex21 Δ*^{PV} conditional knock-out. The weight of mice at P25 is similar in control littermates and in the single and double conditional knock-out. **(D)**. *Nrxn3 ex21 Δ*^{PV} (n=253 mice) and *Nrxn1/3 ex21 Δ*^{PV} (n=47 mice) conditional knock-out mice are born in the expected mendelian ratios. fl=floxed

Figure 4

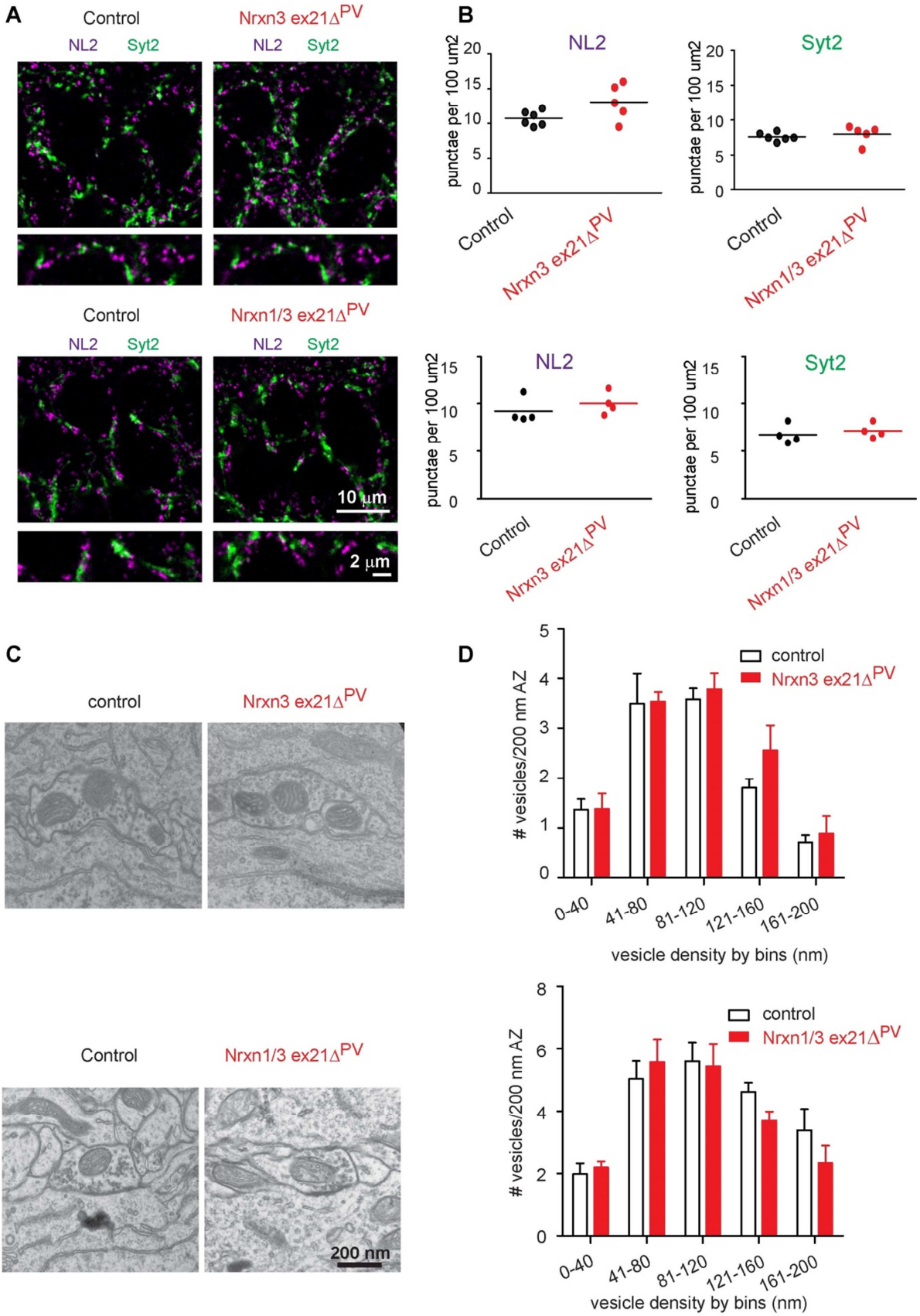
A
Control
Nrxn3 ex21Δ^PV
NL2
Syt2
Control
Nrxn1/3 ex21Δ^PV
10 μm
2 μm
B
NL2
Syt2
punctae per 100 um2
Control
Nrxn3 ex21Δ^PV
Nrxn1/3 ex21Δ^PV
C
control
Nrxn3 ex21Δ^PV
Nrxn1/3 ex21Δ^PV
200 nm
D
control
vesicles/200 nm AZ
0-40
41-80
81-120
121-160
161-200
vesicle density by bins (nm)

Figure 12- Synaptic density and vesicle distribution are not altered in *Nrxn3 ex21Δ^{PV}* and *Nrxn1/3 ex21Δ^{PV}*

(A).The density of perisomatic GABAergic synapses in hippocampus CA1 in control and in *Nrxn3 ex21Δ^{PV}* and *Nrxn1/3 ex21Δ^{pv}* mice aged between P24-P26 was examined by immunohistochemistry with anti-Synaptotagmin-2 (Syt2) and anti-Neuroligin 2 (NL2) antibodies. Syt2 immuno-reactivity is specific for presynaptic terminals of PV-cell synapses whereas NL2 is a common postsynaptic marker for most GABAergic synapses. Thus, only a fraction of NL2 puncta is apposed to Syt2-positive terminals. **(B)**. The density of Syt2 and NL2 puncta per 100 µm^2 of cell body area was quantified. Single dots in the graph represent the mean values of respective synapse marker of an animal. **(C)**. PV positive perisomatic termini were identified by the presence of large mitochondria in the synapses apposed on the membrane of the soma and by their round morphology. **(D).** Average number of vesicles located in 40 nm bins with increasing distance from the active zone normalized to 200 nm active zone length (mean ± SEM).

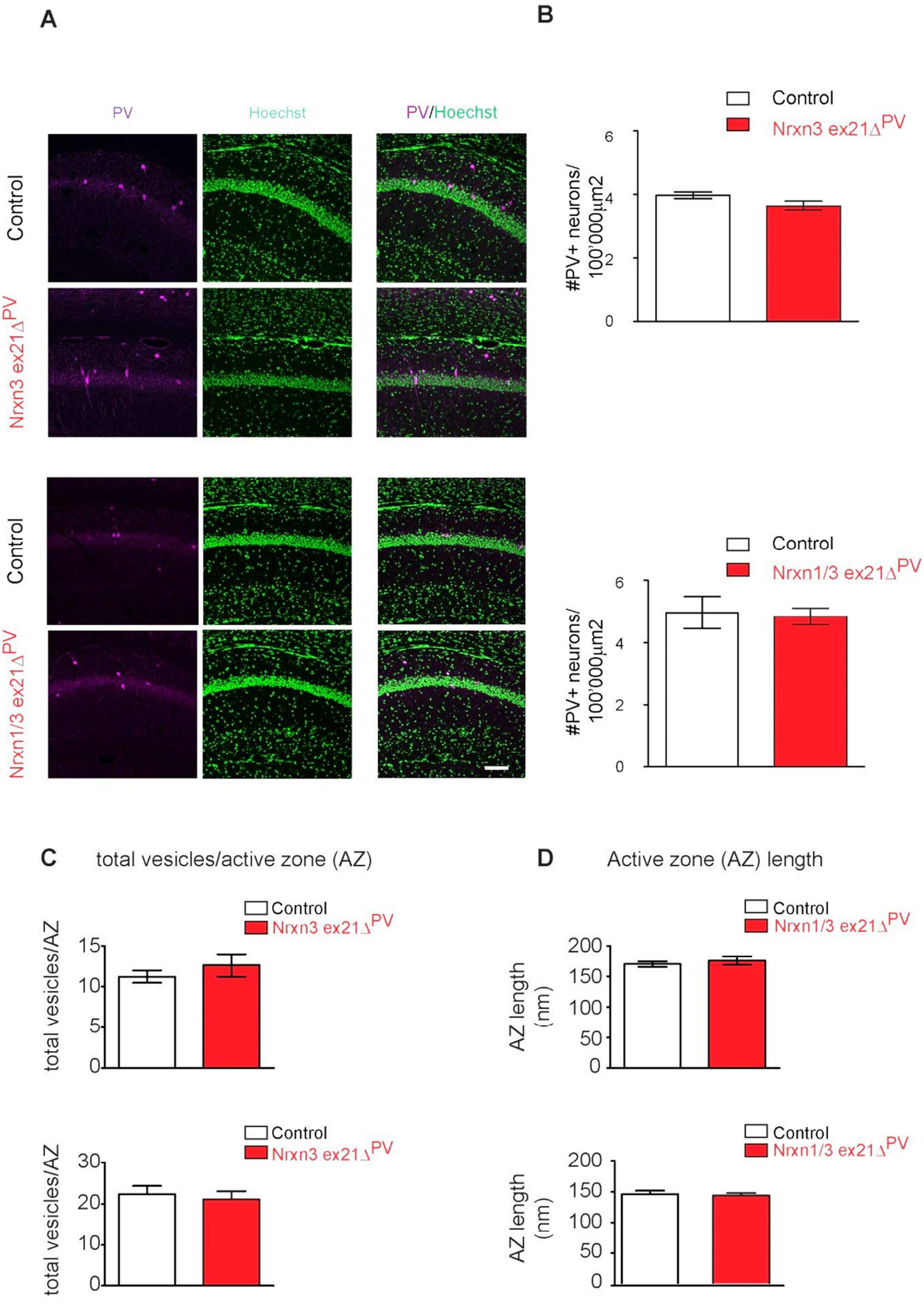
A
PV
Hoechst
PV/Hoechst
Control
Nrxn3 ex21Δ^PV
Control
Nrxn1/3 ex21Δ^PV
B
Control
Nrxn3 ex21Δ^PV
#PV+ neurons/ 100'000µm2
0
2
4
6
Control
Nrxn1/3 ex21Δ^PV
#PV+ neurons/ 100'000µm2
0
2
4
6
C
total vesicles/active zone (AZ)
Control
Nrxn3 ex21Δ^PV
total vesicles/AZ
0
5
10
15
Control
Nrxn3 ex21Δ^PV
total vesicles/AZ
0
10
20
30
D
Active zone (AZ) length
Control
Nrxn1/3 ex21Δ^PV
AZ length (nm)
0
50
100
150
200
Control
Nrxn1/3 ex21Δ^PV
AZ length (nm)
0
50
100
150
200

Figure 13 Quantification of PV cell number and of ultrastructural synaptic properties
Relative to Figure 12

(A). Immunolabelling of PV interneurons in the CA1 region of hippocampus. PV interneurons were identified using anti-PV antibody in magenta and Hoechst was used to label cell nuclei in green nuclear.Scale bar represents 100 um **(B)**. The quantifications of PV cell density in CA1 per 100'000 um^2 was analyzed in animals at P24-P26. (For *Nrxn3 ex21Δ^{PV}*, *n=3* for each genotype. For *Nrxn1/3 ex21Δ^{PV}* , *n=4* for each genotype mean ± SEM).**(C).** Average total vesicle numbers per active zone and average of active zone length analyzed (for *Nrxn3 ex21Δ^{PV}*: 146 control and 127 knock-out synapses. For *Nrxn1/3 ex21Δ^{PV}*: and 90 control and 76 knock-out synapses. For each mutant mice line 4 control and 4 knock-out were analyzed, mean ± SEM).

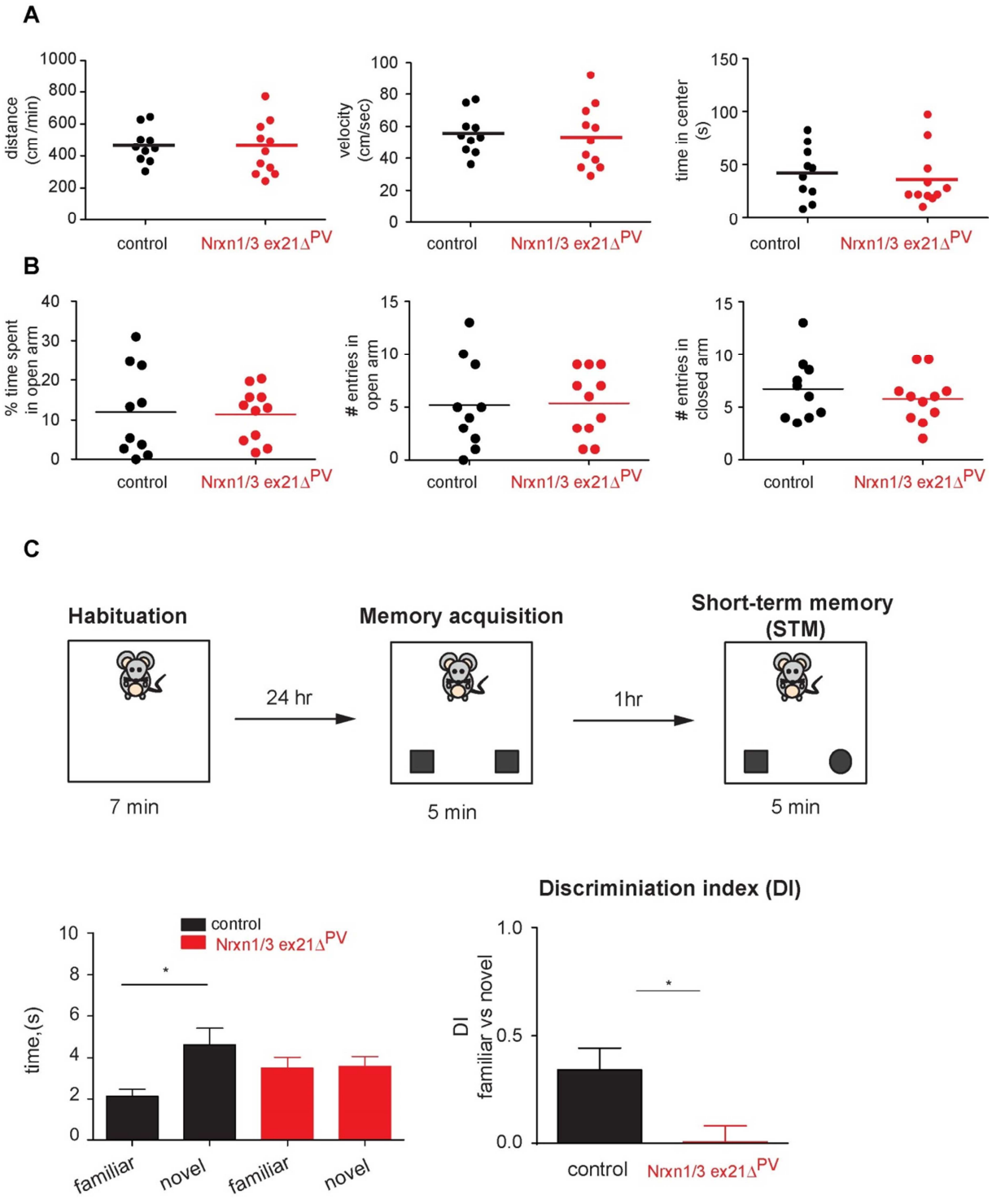
A
distance (cm /min)
1000
800
600
400
200
0
control
Nrxn1/3 ex21ΔPV
velocity (cm/sec)
100
80
60
40
20
0
control
Nrxn1/3 ex21ΔPV
time in center (s)
150
100
50
0
control
Nrxn1/3 ex21ΔPV
B
% time spent in open arm
40
30
20
10
0
control
Nrxn1/3 ex21ΔPV
entries in open arm
15
10
5
0
control
Nrxn1/3 ex21ΔPV
entries in closed arm
15
10
5
0
control
Nrxn1/3 ex21ΔPV
C
Habituation
Memory acquisition
Short-term memory (STM)
24 hr
1hr
7 min
5 min
5 min
control
Nrxn1/3 ex21ΔPV
time,(s)
10
8
6
4
2
0
*
familiar
novel
familiar
novel
Discriminiation index (DI)
DI familiar vs novel
1.0
0.5
0.0
*
control
Nrxn1/3 ex21ΔPV

Figure 14 –Short-term memory is impaired in *Nrxn1/3 ex21Δ^{pv}*

(A) Open field. Mice were allowed to explore a square arena (50 cm x 50 cm x 25 cm) for 7 min. *Nrxn1/3 ex21Δ^{PV}* exhibit no sign of anxiety and are not hyperactive. **(B)**. Elevated plus mazed. *Nrxn1/3 ex21Δ^{PV}* and control mice spend similar time in the open arm. **(C).** Upper panel describes the experimental protocol. **(D).** Novel object recognition task. In the right lower panel the discrimination index was calculated using following formula : ($time_{novel\ object}$- $time_{familiar\ object}$)/($time_{novel\ object}$+$time_{familiar\ object}$)*Nrxn1/3 ex21Δ^{PV}* spend similar time between the familiar and novel object. The discrimination index shows that *Nrxn1/3 ex21Δ^{PV}* failed to discriminate the familiar versus the novel object. (unpaired t-test, $p < 0.05$, control n= 8 mice, *Nrxn1/3 ex21Δ^{PV}* n=11 mice). mean ± SEM

More detailed information about behavioral testing is described in the material and methods part.

3. Discussion

3.1. Conditional deletion of *Nrxn1* and *3* AS4 + isoforms in PV interneurons impairs short-term memory formation

Novel object recognition task is a widely used behavior test to measure recognition memory (Ennaceur and Delacour, 1988). This test relies on natural propensity of rodents to explore novel objects. It is currently under debate to what extend does the hippocampus contribute to recognition memory (Antunes and Biala, 2012). Indeed, recognition memory has been shown to be dependent on interactions between hippocampus with perirhinal cortex, entorhinal cortex and medial prefrontal cortex. In rats, it is believed that the recognition of individual objects is mediated by perirhinal cortex and medial temporal lobe whereas the spatial coding recruits the hippocampus (Warburton and Brown, 2015). Therefore we cannot exclude that recognition memory also involved cortical PV interneurons.

Using Ribotag, we purified mRNA from PV positive interneurons of the cortex. The analysis of alternative splicing expression indicates that both cortical and hippocampal share the same preference for incorporation of exon 21 at AS4 (unpublished data). This finding suggests that splice insert insertion at AS4 is a common feature of in PV positive interneurons in the neocortex and that they share similar functional modality.

We have observed that double knock-out presented impaired short-term memory in novel object recognition task suggesting that circuits underlying that particular behavior are altered. This reveals the surprising finding that modification of alternative splicing regulation in two genes in a specific neuronal population leads to circuit alterations which results in a change of a behavior.

3.2. Can alternative splicing regulation at AS4 affect the PV output synapses?

Our behavior analysis indicated that selective genetic deletion of *Nrxn 1 and 3 AS4 +* isoforms in PV interneurons impairs memory formation. This raises the question of

what the alterations in PV interneurons are, that lead to the observed defective memory formation.

We first analyzed the synapse numbers using immunohistochemistry. Synapses density was assessed by using antibodies against SYT2 and Neuroligin 2 to label PV terminals and postsynaptic inhibitory synapses, respectively. SYT-2 is a synaptic vesicle membranes which is involved in fast Ca^{+} release of neurotransmitters and has been demonstrated to reliably identify PV axons (Sommeijer and Levelt, 2012; Wu et al., 2014). Neuroligin 2 is expressed at inhibitory synapses and is involved for PV synaptic transmission (Varoqueaux et al., 2004b; Gibson et al., 2009). Neuroligin 2 deletion results in a loss of perisomatic synapses in the hippocampus (Poulopoulos et al., 2009). Therefore, changes in Neuroligin 2 could be directly linked to loss of postsynaptic complexes apposed to PV terminals. Our quantification did not exhibit any differences in synaptic density in any of our knock-out mice. Based on our anatomical analysis, impaired short-term memory formation is not due to altered synapses numbers.

Next, we examined the synaptic vesicle distribution by electron microscopy imaging. Because CA1 pyramidal cells receive perisomatic inhibitions from PV and CCK interneurons, we need identification criteria to distinguish between two types of synapses. Based on a recent a study which has assessed the morphological differences between PV and CCK perisomatic synapses in the hippocampus, we considered as PV synapses those that form small and macular synapses which is in contrast to CCK synapses which are large and irregular (Takacs et al., 2015). Moreover PV termini display large mitochrondria. We found that distribution pattern of vesicles from the active zones was unchanged. This finding was further supported by mIPSC recording (Dr. Andrea Gomez and Dr. Le Xiao, unpublished). Indeed mIPSC events are mediated by spontaneous fusion of vesicle, and therefore, if a change in vesicle distribution were identified in the ultrastructural analysis, this would have been also reflected in the change of mIPSC frequency. Therefore, the impaired short-term memory formation is not due to altered distribution of synaptic vesicles.

In addition, the decay times measured in mIPSC recording which depend on the expression of receptors at postsynaptic sites were also unchanged. This suggests that molecular composition of gross GABAergic postsynaptic receptors is unaltered in the mutant mice. Since PV interneurons are not the only source of

GABAergic inputs onto CA1 neurons, a more precise evaluation of PV-CA1 transmission is required.

What additional synaptic parameters could account for the impaired short-term memory formation? Another possible mechanism could involve Ca^+ signaling at presynapses. Indeed, presynaptic vesicle release is triggered by local increase of Ca^+ at active zones which are close to calcium channels (Schneggenburger and Neher, 2005). Both Ca^+ channel composition and/or position could modify the transmitter release. Ca^+ influx can be regulated by the expression of different type of Ca^+ channels. For example in the PV interneurons, P/Q-type Ca^+ channels are predominantly expressed and were shown to trigger fast Ca^+ influx compared to the N-type Ca^+ channel (Hefft and Jonas, 2005). P/Q-type Ca^+ channels were also demonstrated to be essential for the short-term plasticity in PV interneurons. Indeed, by evoking 50 Hz burst of 10 action potentials, short-term depression was elicited at PV synapses. Bath application of ω-agatoxin blocked the short-term depression (Hefft and Jonas, 2005). Moreover deletion of subunits of P/Q-type Ca+ channels in PV^+ results in onset of epilepsy (Rossignol et al., 2013). Together, P/Q-type Ca^+ channels are essential for synapse function at PV synapses

Supporting this Ca^+ signaling hypothesis, the analysis of the *Nrxn α*-triple global knock-out has also reported an impaired presynaptic P/Q- but also N-type Ca^+ calcium channels (Missler et al., 2003). Interestingly, the phenotype could be rescued by the re-expresssion of Neurexin 1 α but not β proteins, suggesting that their extracellular domains interact with distinct ligands which in turn affect the presynaptic Ca^+ signaling. In the *Nrxn α*-triple global knock-out the total protein levels all types Ca^+ channels remain unchanged (Missler et al., 2003). Thus it is possible that Neurexins regulate indirectly the position of Ca^+ channels in the presynaptic terminals. Indeed, P/Q-type Ca^+ channels were found to be located very closely to the Ca^+ release sites (Wu et al., 1999). There are no evidence that Neurexin interact directly with P/Q Ca^+ channel. Instead the interaction could be mediated through Mint and Cask which have been reported to interact with Neurexin but also with P/Q-type Ca^+ channels (Spafford and Zamponi, 2003; Hata et al., 1996; Biederer and Sudhof, 2000).

How altered PV synaptic properties could result in impaired memory formation? Hippocampal PV basket interneurons form perisomatic synapses which provide strong inhibition that can suppress the generation of action potential in CA1

pyramidal cells. In addition to perisomatic inhibition, PV interneurons in the hippocampus are responsible for the generation of gamma oscillations (30-90 Hz) (Buzsaki and Wang, 2012). Indeed, the inhibition of PV interneurons suppresses oscillations in gamma bands (Sohal et al., 2009). Moreover manipulation of PV interneurons was reported to also impair recognition memory (Fuchs et al., 2007).

3.3. Does Neurexin 2 AS4 + isoform compensate for the loss of Neurexin 1 and 3 AS4+ isoforms?

Radio-labelled RT-PCR reactions showed that 60% of Neurexin 2 AS4 isoforms contained splice insert in PV positive interneurons. Therefore it is possible that Neurexin 2 AS4(+) variant compensates for the loss of Nrxn 1 and Nrxn 3 AS4(+) in the double knock-out mice. Recent studies have reported that Neurexin isoforms have redundant functions (Aoto et al., 2013). Indeed, hippocampal neurons in cultures that expressed constitutively Neurexin 3 AS4(+) showed decreased AMPA-mediated current. Expression of Neurexin 1 or 2 AS4(–) in those cultures was sufficient to rescue this phenotype, suggesting that Neurexin 1, 2 and 3 AS4(–) isoforms possess similar functions regarding the regulation of AMPA receptor trafficking. For these reasons, it is possible that Neurexin 2 AS4(+) has functions which are redundant with Neurexin 1 and 3 AS4(+) and therefore, compensates for the loss of AS4(+) isoforms in the *Nrxn1/3 ex21* Δ^{PV} double knock-out mice.

We did not assessed if in double knock-out the total protein level and the splice ratio of Neurexin 2 AS4 isoforms changed in PV interneurons. Instead have indirect evidences that the splicing ratio and the global protein levels remain the same in the knock-out mice. Using semi-quantitative RT-PCR, we found that the alternative splicing at AS4 of Neurexin 2 was not changed in mice in which exon 21 of *Nrxn1* and *3* genes was deleted globally in mice. Moreover using mass spectrometry, it was found that the global protein levels of Neurexin 1 and 2 in *Nrxn3 ex21 Δ* global knock-out were unchanged (Dr. Dietmar Schreiner, unpublished data). Thus, these data strongly suggest that Neurexin 2 AS4(+) isoforms level are not changed upon deletion of Neurexin 1 or 3 AS4(+) isoforms. Even though the Neurexin 2 AS4 was not upregulated in double knock-out, its presence could well compensate at least parts of the functions of Neurexin 1 and 3 AS4.

Preliminary data on novel object recognition tasks performed on single knock-out *Nrxn3 ex21* Δ^{PV} showed that mutant mice have a preserved short-term memory function (data not shown). This indicates that the deletion of a single gene is not sufficient to perturb short-term memory formation. Thus, for this particular type of memory, the occurrence of the phenotype requires dual deletion of AS4 in both Nrxn1 and 3.

Together, those data point at redundant functions of Neurexin AS4(+) isoforms and therefore, it is likely that in a triple knock-out, in which the Neurexin 2 AS4(+) isoform is also deleted, that more profound phenotypes might be revealed, e.g, the deficits in synapse number and ultrastructure. Indeed, in a previous study, it has been demonstrated that the severity of synaptic transmission correlated with the number of *Nrxn* α genes deleted (Missler et al., 2003).

3.4. Future experiments

The missing part of the study relies in the identification of functional alterations at PV positive interneurons following the deletion of *Nrxn1* and *3 AS4 (+)*. Therefore, the major goal in future experiments consists to uncover synaptic alteration(s).

3.4.1. Electrophysiogy recordings

The mIPSC recording in CA1 have demonstrated unchanged frequency, amplitude and kinetic. mIPSCs measurements represent the general activity state of the circuit and but do not assess the synaptic properties between the PV interneurons and the postsynaptic pyramidal neurons. Therefore to assess synaptic transmission properties at PV terminals, simultaneously whole-cell recordings of a PV neurons and principle neurons is necessary and currently performed by Dr. Le Xiao. In the paired-recording, action potentials are evoked in the PV neurons in current-clamp mode, and the IPSCs are recorded from the postsynaptic principle neurons. This will enable to assess several basic biophysical and transmitter release properties of pre- and post- synaptic neurons. For example, we would investigate if there are changes in the passive and active membrane properties of the presynaptic PV neurons in double

knock-out. We could also study the strength, reliability and kinetics of PV-generated IPSCs and compare the control with the knock-out. Moreover it is also possible to investigate presynaptic plasticity by applying high frequency stimulation in PV interneurons. Thus, if presynaptic Ca^{+} channel signaling was in fact perturbed, it would be revealed by changed short-term plasticity.

Parvalbumin interneurons generate gamma oscillations have been shown to be involved in the formation of recognition memory (Fuchs et al., 2007). Indeed, imprecise spike timing of fast-spiking PV interneurons can alter gamma oscillations. For this reason we would like to investigate if the *Nrxn1/3 ex21Δ^{PV}* mice also display perturbed gamma oscillations. This type of experiment is currently performed by Dr. Tania Burkat Rinaldi.

3.1.1. PacBio SR sequencing

We have demonstrated that mRNAs purification by using transgenic Ribotag in genetically-encoded neuronal populations was successful to generate cell-type specific endogenous profiles of Neurexin isoforms. We first have assessed the alternative exon incorporation rate at each alternative splice segment independently to each other. The results indicated that most of the alternative spliced segments, with the exception of AS4, were similarly regulated between Camk2 pyramidal cells in CA1 and PV interneurons. The previous study using PacBio RS sequencing revealed that purified cells expressed a targeted set of Neurexin isoforms. Thus as a next step, we could combine both methods to investigate the combinatorial usages in Camk2 pyramidal cells in CA1 and in hippocampal PV interneurons. To do this, we would pool cell-type purified mRNAs to prepare libraries before submission for sequencing. Indeed, PacBio RS sequencing requires a certain amount of starting material. In addition to the combinatorial exon usage information, the sequencing results will also enable to determine the relative abundance of each isoform within a population. Indeed, such finding would further strength that each neuronal population has its “signature” set of Neurexin isoforms.

4. Material and Methods

4.1. Expression vectors

The Nrxn splicing reporters were generated by placing mCherry upstream of the minigene in a pEGFP-N1 plasmid. The minigene consists of the alternative exon, the flanking constitutive exons and the flanking introns. Because the flanking introns exhibit large size, they were internally truncated leaving intact 500 bp of the intronic sequence up-and downstream of alternative exon. Similarly the up- and downstream intronic sequences of the flanking constitutive exons were shortened to 500 bp. As consequence the length of the intronic sequences between constitutive and alternative exons was 1000 bp. With the exception of Nrxn 1 AS2 splicing reporter where the intronic sequence between alternative exon and downstream constitutive exon was left intact because it was 1062 bp long. Each fluorescent protein was fused to a nuclear localization signal (upstream of mCherry ATG ACT GCT CCA AAG AAG AAG CGT AAG ACT GCT CCA AAG AAG AAG CGT AAG GGA GGT GGA AGT GGT GGA GGT GGA AGG and upstream of GFP ATG ACT GCT CCA AAG AAG AAG CGC AAG ACT GCT CCA AAG AAG AAG CGC AAG GGA GGT GGA AGT GGT GGA GGT GGA AGG) and a 2a signal self-cleavage peptide (GGC AGT GGA GAG GGC AGA GGA AGT CTG CTC ACA TGC GGA GAC GTC GAG GAG AAT CCT GGC CCA) was flanking the minigene. A single nucleotide was inserted into the alternative exon and only the mRNA lacking the alternative exon has GFP sequence in frame. Given that AS2 has two donor sites the theoretical number of mRNA is three but only upon the exclusion of the whole cassette exon GFP sequence is out-of-frame. Both other mRNAs containing cassette exon using one or the other donor sites generates mRNA where GFP reading frame is kept. Due to the introduction of a single nucleotide in the cassette exon which causes a frame shift, the downstream constitutive exon was checked for any premature stop codon. The sequence following the downstream sequence of the premature stop codon was removed leaving the downstream constitutive exon partially truncated. Transcription of splice reporters was controlled by neuron-specific Synapsin promoter.

4.2. Antibodies

Home-made guinea pig anti-RFP was used to detect mCherry at a dilution of 1:5000. For protein detection by western blot home-made rabbit anti-GFP was used at the

dilution of 1:200. For immunohistochemistry commercially available mouse anti-GFP (Invitrogen) was used at the dilution of 1:500. The following commercially available antibodies were used: mouse anti-NeuN (1:1000, MAB377, chemicon), Synaptotagmin-2 (1:500, znp-1, Zebrafish International Resource), Neuroligin-2 (1:500, Santa Cruz), anti-HA(1:200, 3F10, Roche) , anti-parvalbumin(1:5000, PVG214, Swant)

4.3. Cell cultures, Cell lysis and detection of proteins by Western Blot

Cells were lysed with Laemmli buffer (200mM DTT, 100mM Tris-HCl pH6.8, 2% SDS, 40% glycerol, 0.05% bromophenol blue) and were analyzed by immunoblotting with the primary antibodies for 24 hr at 4°C. For visualization, horseradish peroxidase (HRP)-conjugated secondary antibody and the enhanced chemoluminescent detection (Pierce) were used, signals were acquired using an image analyzer (LAS-3000; Fujifilm).

4.4. RNA extraction from cell cultures and mouse tissues

For splice reporter analysis human embryonic kidney 293T cells were cultured in Dulbecco's modified Eagle's medium (Invitrogen) supplemented with 10% fetal calf serum, L-glutamine (2 mM), penicillin, and streptomycin and grown in 5% CO2 at 37°C. For splicing reporter assays, cells were transfected using Fugene 6 reagent (Roche Applied Science) with expression vectors encoding the splice reporter with or without Sam68 protein. RNA and protein samples were harvested 24–36 hr post-transfection. Total RNA was isolated using Trizol reagent (Invitrogen), followed by removal of contaminating DNA using Turbo DNA-free (RNase-free DNase; Ambion). For purified mRNAs from Ribotrap, RNA was isolated using RNeasy micro plus kit (Quiagen). RNA was reverse transcribed using random hexamers and ImProm II Reverse Transcriptase (Promega).
Semi-quantitative PCR were performed with 2xFirepol MasterMix (Solis BioDyne).
DNA Oligonucleotides to amplify Neurexin transcripts with semi-quantitative PCR

*Nrxn1 AS2*_F	5'- TGG GAT CAG GGG CCT TTG AAG CA-3'
*Nrxn1 AS2*_R	5'- GAA GGT CGG CTG TGC TGG GG -3'

*Nrxn2 AS2*_F	5'- GCA CGA CGT CCG GGT TAC CC-3'
*Nrxn2 AS2*_R	5'- GGT CGG CTG TGT TGG GGC TG -3
*Nrxn3 AS2*_F	5'- TCC GGG GCC TTT GAG GCC AT-3'
*Nrxn3 AS2*_R	5'- GCG GTA CTT GGG CTT CCA CCA-3'
*Nrxn1 AS4*_F	5'- CTG GCC AGT TAT CGA ACG CT -3'
*Nrxn1 AS4*_R	5'- GCG ATG TTG GCA TCG TTC TC -3'
*Nrxn2 AS4*_F	5'- CAA CGA GAG GTA CCC GGC -3'
*Nrxn2 AS4*_R	5'- TAC TAG CCG TAG GTG GCC TT -3
*Nrxn3 AS4*_F	5'- CCA GGA ATG GGG GAA ATG CT -3'
*Nrxn3 AS4*_R	5'- TTG TCC TTT CCT CCG ATG GC -3'

DNA Oligonucleotides to amplify Neurexin splice reporters transcripts with semi-quantitative PCR

*Nrxn1 AS2 reporter*_F	5'- TGG GAT CAG GGG CCT TTG AAG CA-3'
*Nrxn1 AS2 reporter*_R	5'- AGC TTG CCG TAG GTG GCA TC-3'
*Nrxn2 AS2 reporter*_F	5'- GCA CGA CGT CCG GGT TAC CC-3'
*Nrxn2 AS2 reporter*_R	5'- AGC TTG CCG TAG GTG GCA TC -3

4.5. In utero electroporation

In utero electroporation was performed using a Sonidel CUY21SC Electroporator and CUY650P7 electrodes using the method established by Tabata and Nakajima(Tabata and Nakajima, 2001). Electroporation was performed at E14-14.5 and animals were sacrificed at P21-22 for analysis.

4.6. Immunohistology on brain mice

Animals were transcardially perfused with fixative (4% paraformaldehyde/15% picric acid in 100 mM phosphate buffer, pH 7.2). For splice reporters study tissues were sectioned at 50 µm in PBS on a vibratome (VT1000S, Leica) and floating sections were immunostained following standard procedures. For analysis of *Nrxn* knock-out mice brains were postfixed at 4°C overnight, cryoprotected in 30% sucrose in phosphate-buffered saline (PBS) and frozen. For assessing HA expression in Camk2Ribo and PVRibo mice, sections were cut at 40 µm with a cryostat, collected in PBS. Floating sections were immunostained following standard procedure using rat anti-HA (Roche), goat anti-PV (Swant) and mouse anti-NeuN (Chemicon). For quantitative analysis of NL2, Vgat and Syt2 punctae, sections were cut at 35 um and collected in PBS. Prior the staining a pepsin retrieval treatment was carried out, as

described (Panzanelli et al., 2011). Briefly, sections were incubated in prewarmed 0.1M PB at 37°C for 10min and then in 0.15mg/mL pepsin (Dako) dissolved in 0.2M HCl for 10 min.

4.7. Image acquisition and analysis

For splice reporter study images were acquired on a LSM 5 confocal microscope (Zeiss) and on a LIS-spinning disk confocal system and images were analyzed with Metamorph (Molecular device). The threshold intensity was set using the channel 561 nm. A region of interest was selected on the fluorescence signal intensity and then transferred on the channel 491nm. The average intensity of both channels was then recorded.

For synapse quantification in Nrxn KO images were acquired at room temperature on an upright LSM700 confocal microscope (Zeiss) using 63x Apochromat objectives and controlled by Zen 2010 software. Images for assessing the Rpl22-HA expression were acquired at room temperature on an inverted LSM500 confocal microscope (Zeiss) using 10x and 20 x objectives. The image acquisition and analysis were done blinded with respect to the genotype of the animals.

Images were assembled using Adobe Photoshop and Illustrator Software. For synaptic markers quantification, three to four brain sections on which four to six confocal plans in the CA1 per section were acquired. Using Fiji software soma area were manually drawned to measure the area. Synaptotagmin-2 punctae and peri-somatic Neuroligin 2 punctae were counted manually in separated channels and normalized to 100 um2. For each genotype (WT: n=6 animals; cKO : n=5 animals), the average synapses punctae for each animal was calculated. Statistical analysis were done with Prism software (Graphpad software)

4.8. Statistical analysis

Statistical analysis were done with Prism software (Graphpad software).

4.9. Ribotag translating polysomes affinity purification

For Ribotag purifications the procedure of Sanz and colleagues for affinity-purification of polysomes (Sanz et al., 2009) was modified as follows. Brain of mice between P24 to P28 were dissected ice-cold PBS and the hippocampus of one animal was lysed in 500 uL of supplemented homogenate buffer containing 100mM KCl, 50mM Tris pH 7.4, 12mM MgCl2, 100ug/mL Cycloheximide (Sigma), 1mg/mL Heparin (Sigma),1x cOmplete mini, EDTA-free protease inhibitor cocktail (Roche), 200 units/mL RNasin© plus inhibitor (Promega) and 1mM DTT (Sigma). The lysate was centrifuged at 2'000xg for 10 minutes. Igepal-CA380 was then added to the supernatant to a final concentration of 1%. After 5 minutes incubation on ice, the lysate was centrifuged at 12'000xg for 10 minutes. Anti-HA magnetic beads (Pierce) were added to the supernatant in following concentrations : 50uL/mL and 30 uL/mL of beads for Camk2Ribo and PVRibo samples respectively. The incubation was performed at 4°C for 4 hours. The beads were washed 4 times in washing buffer containing 300mM KCl, 1% Igepal-CA380, 50mM Tris pH7,4, 12mM MgCl2, 100ug/mL Cycloheximide (Sigma) and 1mM DTT(Sigma). The beads were eluted in 350uL of RLT plus buffer (Qiagen)

4.10. Quantitative PCR analysis and primers

Quantitative PCR was performed on a StepOnePlus qPCR system (Applied Biosystems). To assess Nrxn expression level gene expression assays were used with TaqMan Fast Universal Master Mix (Applied Biosystems) and comparative CT method. The mRNA levels were normalized to that of β-actin mRNA. To determine the enrichment fold of mRNA purification DNA oligonucleotides were used in FastStart Universal SYBR Green Master (Rox) (Roche) and comparative CT method.

Commercially available gene expression assays for *Gapdh, Nrxn1,2,3* were from Applied Biosystems:

Gapdh	Mm99999915g1
Nrxn1	Mm00660298_m1
Nrxn2	Mm01236851_m1
Nrxn3 alpha	Mm00553213_m1

Custom gene expression assays were from TIB Molbio

Nrxn1 alpha F	5’- CAG CAC AAC CTG CCA AGA -3’
Nrxn1 alpha F	5’- GTC CCA GGG TCA TTG CAG A-3’
Probe	FAM-TGG GCC ACT GAA GGA AGT CAT GCT-BBQ
Nrxn1 beta F	5’- CCT GGC CCT GAT CTG GAT AGT -3’
Nrxn1 betaF	5‘- TTG TCC CAG CGT GTC CG-3’
Probe	FAM-CTG AAT GAT GCT TGC TGC TGC CA-BBQ
Nrxn2 alpha F	5'- CAC CAC CTG CAC CGA AGA G -3’
Nrxn2 alpha F	5’- CCG GAG GCA CTG TCC ACT -3’
Probe	FAM-CCC CCT TCC CGA AGA TGT ATG TGG TC-BBQ
Nrxn2 beta F	5'- GTG CCC ATC GCC ATC AA -3’
Nrxn2 betaF	5- GAG GCC ATG TAT AGG TGA TGA GC -3’
Probe	FAM-CCC CCT TCC CGA AGA TGT ATG TGG TC-BBQ
Nrxn3 alpha F	5'- CTG TGA CTG CTC CAT GAC ATC ATA TT -3’
Nrxn3 alpha F	5’- CAG AGC GTG TGC TGG GTC T-3’
Probe	FAM-CGC TTT TCC CAA AGA TGT ATG TTG CAC CA-BBQ
Nrxn3 beta F	5’-AAG CAC CAC TCT GTG CCT ATT TCT –3’
Nrxn3 betaF	5’- CCA GGG GCG CTG TCA AT–3’
Probe	FAM-CGC TTT TCC CAA AGA TGT ATG TTG CAC CA-BBQ

DNA Oligonucleotides used with SYBR Green-based real-time PCR.

Camk2-F	5'- GAG GAA CTG GGA AAG GGA G -3'
Camk2-R	5'- GGT AAC CTA CCT CTG GCT G -3'
Cbln2 F	5’- AGA CAA ACT ATC CAG GTC AGC -3’
Cbln2 R	5’- CCT GGT AAC ATC CTG GTC TC -3’
Cbln4 F	5- TTTGATCAGATCCTGGTTAACG -3’
Cbln4 R	5- ACTATATTCCTTTCCTCGGT -3’
ErbB4-F	5'- ATC CCT GTG GCT ATA AAG ATC C -3'
ErbB4-R	5'- CAT GAT CAG AGC CTC ATC CA -3'
Gfap-F	5'- CTC GTG TGG ATT TGG AGA G -3'
Gfap-R	5'- AGT TCT CGA ACT TCC TCC T -3’
Gad67-F	5'- GTA CTT CCC AGA AGT GAA GAC -3'
Gad67-R	5'- GAA TAG TGA CTG TGT TCT GAG G -3'
Pvrl3-F	5'- GTG ACT GTG TTA GTT GAA CCC -3'
Pvrl3-R	5'- TGC TAC TGT CTC ATT CCC TC -3'
Pv-F	5'- CATTGAGGAGGATGAGCTG
Pv-R	5'- AGTGGAGAATTCTTCAACCC
Vglut1-F	5'- ACC CTG TTA CGA AGT TTA ACA C -3'
Vglut1-R	5'- CAG GTA GAA GGT CCA GCT G -3'
SAM 68 F	5'- GGG AAG GGT TCA ATG AGA GA -3’
SAM 68 R	5'- AAT GGG CAT ATT TGG GGT CT -3’
SLM1 F	5'- GAC CAA GAG GAA ACT CCT TGA A -3’
SLM1 R	5'- GGC ATG ACT CAT CCG TGA ATA -3’
SLM2 F	5'- GGT CCG CGT GGC AAT TC-3’
SLM2 R	5'- CAT CCG GGC ATA TGC TTC T-3’
Wsf1-F	5'- CATCATTCCCACCAACCTG -3'
Wsf1-R	5'- TAC TTC ACC ACC TTC TGG C -3'

4.11. Radiolabelled semi-quantitative PCR

Radioactive semi-quantitative PCR was performed with γ-^{32} P 5' end-labelled primers (Hartmann) using 5X Firepol mastermix (Solis Biodyne). The gel image was acquired with Typhon FLA 700 (GE healthcare) phosphoimager. The PCR band intensity was analyzed using Fiji software. The background intensity was substracted to mean intensity of each PCR band and then normalized by the number of CTP and GTP in PCR product.

DNA Oligonucleotides used for radioactive semi-quantitative PCR

*Nrxn1 AS2*_F	5'- TGG GAT CAG GGG CCT TTG AAG CA-3'
*Nrxn1 AS2*_R	5'- GAA GGT CGG CTG TGC TGG GG -3'
*Nrxn2 AS2*_F	5'- GCA CGA CGT CCG GGT TAC CC-3'
*Nrxn2 AS2*_R	5'- GGT CGG CTG TGT TGG GGC TG -3
*Nrxn3 AS2*_F	5'- TCC GGG GCC TTT GAG GCC AT-3'
*Nrxn3 AS2*_R	5'- GCG GTA CTT GGG CTT CCA CCA-3'
*Nrxn1 AS3*_F	5'- TGG AGC TAG ATG CAG GAC GTG TGA A -3'
*Nrxn1 AS3*_R	5'- TTC CTC GCC GAA CCA CAC GC -3'
*Nrxn2 AS3*_F	5' – CCC ACT CGC ATG CAC ACG GA -3'
*Nrxn2 AS3*_R	5'- TGC CCC GCA AAC AGT GTC TCG -3'
*Nrxn3 AS3*_F	5'- TGT CAC AGC GAG CCT ATG GGC -3'
*Nrxn3 AS3*_R	5'- TCT CCG CAC TAC CCG GAC GG -3'
*Nrxn1 AS4*_F	5'- CTG GCC AGT TAT CGA ACG CT -3'
*Nrxn1 AS4*_R	5'- GCG ATG TTG GCA TCG TTC TC -3'
*Nrxn2 AS4*_F	5'- CAA CGA GAG GTA CCC GGC -3'
*Nrxn2 AS4*_R	5'- TAC TAG CCG TAG GTG GCC TT -3
*Nrxn3 AS4*_F	5'- CCA GGA ATG GGG GAA ATG CT -3'
*Nrxn3 AS4*_R	5'- TTG TCC TTT CCT CCG ATG GC -3'
*Nrxn1 AS6*_F	5'- CTG GCC AGT TAT CGA ACG CT -3'
*Nrxn1 AS6*_R	5'- GCG ATG TTG GCA TCG TTC TC -3'
*Nrxn1 AS6*_F	5'- CTG GCC AGT TAT CGA ACG CT -3'
*Nrxn1 AS6*_R	5'- GCG ATG TTG GCA TCG TTC TC -3'

4.12. Electron microscopy analysis

Animals (postnatal day 24-25, single and double knock-out and control littermates) were transcardially perfused with fixative (2% paraformaldehyde, 2% glutaraldehyde in 100mM phosphate buffer [pH 7.4] and brains were postfixed for 1 hr. Tissues were sectioned coronally at 60 um thickness in PBS on a vibratome. Sections from the same front-caudal brain region were analyzed for each genotype. Sections were washed in 0.1M cacodylate buffer [pH 7.4], postifexed in 0.1M reduced osmium (1.5% K4Fe(CN)6, 1% OsO4 in water) and embedded in Epon resin. Images were

acquired on a Transmission Electron Microscope (Fei Morgagni, 268D). Quantification of the number and distribution of vesicles was performed using ReconstructTM software (http://synapses.clm.utexas.edu/tools/reconstruct/reconstruct.stm). All image acquisition and analysis was done blinded with respect to the genotype of the animals. Independent data sets were collected from 4 KO and 4 control animals). Parvalbumin terminals were identified by their localization on the neuron plasma membrane and the presence of large mitochondria. The vesicles and the active zones were manually drawned. The shortest distance from the vesicle membrane to the active zone membrane was then calculated and all vesicles at distances of less than 200 nm were taken into account.

4.13. In situ hybridization

In situ hybridizations were performed on 20 microns sections using digoxigenin-labelled mRNA probes as previously described (Schaeren-Wiemers and Gerfin-Moser, 1993). For in situ probes preparation DNA fragments containing SP6-promoter, target, and T7-promoter sequences synthesized as gBlock-fragments (Intergrated DNA technologies) were amplified by PCR: SP6-for: CTATCGATTTAGGTGACACTATAGAAG and T7-rev: GAATTGTAATACGACTCACTATAGGGA, and subsequently used as templates for in vitro transcription, using SP6-Polymerase for sense probe, or T7-Polymerase for anti-sense probe, respectively. The labeling with rabbit anti-RFP (homemade) followed the probes hybridization.

The probe sequences are for

-Neurexin :

AAGGGGAATAACCAGGCAGATTTCTGAGTTCTTATAAACGTCAAAATAAAATCAA
AATGCATCACCAACATACAACCAACTGACATGCTGGAGTCTTAGGGTGGCCTTG
CAGAGACAGAAAAAAGAAGAGTTTGAGGGATTGATTTCACCATCTAACAGCTTCT
GGCTACTTCACAGCAGGGTTTGAGACCTACCTACAGGGCTCCTAAACATAAAGC
GAATCAGCCTGGGAGGGCATGCACAGGAAATTTGGCCTTGGCTTTAGTGGTGC
TGGAAGCCCATGATATGACAGAAGTAGGCCTCTGAAGCTATTCTGGTGTCTCAC
TCTGTCCTTTCTCCTTCTGTGCTTGGAGCCAACATCTGGAGGGGCCTCGAGGCC

TGCCAAGCAGCCAAAGATCCTGGCTCAGTGTTGACTTCGTGTTCCTCTCCGAGA
AAAGTGTGTTTCT

-Neurexin 1β:

GCTCTTTCATCTGCCCCTGCTTTTCCTCCGCTCGCTTTCCCCAGTTCGATCCCTG
CTGTCTTCACGAGGGTGCCCACTTCCCTCTGAACCCATCGTCGGGCGTAGTGT
CAGGAGGCGGCGGACTCGGAGATTGCCTCTGGAGCAGGCGATGCGCGCCGCT
GCTCTGCGCGCTGCCCGGGTGAGGCTGGCGGGAGCTGGAGAGCTGGCCAGG
GCTGAATGGAGGGACAGGGTGCCTTGCGTCCATGGGGTCTGCTTCTTTCCTGA
AAGGAGGCTGGACCGGCGAAGTGGTCTCCCAGTTCCCCGCGCACAATGCTAAA
TGGATTTACCTAGTGGATTCCCGGTGGATGGCTGTCATGTAGAAGTGAAGACCC
TCCGGGAGGAGCTTTAAACAATTTCCAGGCTCCCCAACCCCGGCACACACTCTC
GCCCGAAACTCTTGGGGAGTA,

-Neurexin 2α :

ACCAGGAGGCGCGAGGCAGCCGATATCGCTGGCCCAGGATCTGTTACCTGCC
GTAGACCCAGCGGTCTCTAGGCTCGGATCCCTACCCTTCAGCTCCTGGCGCCC
CCAAAACCAGGCGTCCCTCCCCCACCTTCCATACGAGCCCGCCGCGGGGGAG
GGGCTCCACCACCGCAGCCGCCGTCGTTGCCTTCCGGGGACGTGGACACGTG
AGCCCCGGCTACTGAGTCCATGGCACTGTGAATCGGCGAGG

-Neurexin 2β:

TGAGGGGGGACCCCTAGCCGCCCGCGATGGATCCAGGCTTCACGGACCTTGG
CCTTCCCGCTGCGCGTACCCCGGATTCCCCGGCGGGATCCAGTTGATTTGCTT
GGCTCCGGACTGAGGCTCGGGCTCTGGTTTTCCTTCGCTTCACCCCTACCCCC
CTCTCGGAGCTCGCAACCGGAGGGGGGCTT

-Neurexin 3α :

GAAGTCTGAATCTGCTTCCGCTCTGCTCTGGGCCTCACTCCACCTGAGTCCTCA
GTTGTTTGCGGTTCCCCTTCCCAGGGTCTGCTGCTAGACCGTCAAACCTCAGCA
CTGGGCCTTGGCTTGGGCCTGCCTTTTGCCTGGCTCACCTCCCGATTACTCCTC
CTCCATTACAGCACCCTGAGCCCCAGCCCTGTCCTTGGTCTTCCTGGCTAGGAC
GCATTTGCCGGGAGGAAGACATTACGGAAGGCTTATTCCCACCCTGGGCTCCTT
CTCCTCCTTGAATCAAGGCCTCCGGATCCACATGGATAGCTGAGATCTTTTCTT
GGAGAAAGATACTTCTTCCTCGCCTCATCCCTGATTTGCCTCACCCGACAAATC
CCCTGTCTGTTTCGTCTCCCTCTTTATGGGATTTCTTGCTTGTGTGCCTATCTAG
GGCCGTGTTGTCC

-Neurexin 3β:

CTGCTCCTCTCCACCTTCTGCTACGTTGGTCTGGGTGGCTAGCTCAGTGCTGTT
TCTTTTCCTCTGGCCCTTCTTGATCCCTTTCTCTGGCTACTGCTGCTGGCTGATT
TTCAACCTATTGGGAACTCAGGACTTAAGGCGGCTGCACCGTGGCGCTCATCCA
GGACACTCAGGGTTAACAGCCTCCGCGCCCATCCACAGAGACTCCCGGGAGCA
GAACTCTTCCACCTGCAGCCCCCTTTTGCCTGGCAGTTCTGCATTGCATCGCTT
GGAAGTCGAAACAAGAAAGAAAGAAAGAAAGAAAAATGTCCAAACTCCTTGGAT
GTTGGGAAAAACTAGCGTGAATTTACTTGGTTTTTTCCTGCTCTGTCTTCTCTCT
CCGTTTCCACCTTTCCCCAGTGGCTTTCCAGAGTATGCAGCTAGTACATCGGAC
TTGAAGTACCAAG

4.14. Behavioral analysis

Behavioral testing was done with control and *Nrxn1/3 ex21Δ*^{PV} male littermates which were aged between 6 and 15 weeks. Behavioral tests were done with two mice cohorts. Before each behavioral test, mice were allowed to acclimate in the behavioral room for at least 30 min. In each tasks, arena and objects were rinsed with 70% ethanol between trials.

4.14.1. Open field

Open field was performed in a squared arena (50x50x25) and served simulstanously as habituation time before the novel object recognition test. Mice were allowed to explore freely 7 min the arena. Explorative behaviors were recorded by a Noldus Camera. Using the video tracking software Ethovision 10 of Noldus, the distance traveled, velocity and time spent in the center of arena were determined.

4.14.2. Elevated plus maze

Mice were placed at the junction of four arms of the maze and the behavior was recorded by a camera (Canon) for 5 min. Entries and duration in each arm were measured by stopwatch by the experimenter.

4.14.3. Novel object recognition test

Novel object recognition was performed in the same square arena, as described previously. The recording were perform by a camera (Canon). In the arena animals were allowed to explore for 5 min two identical small Falcon tissue culture flasks filled with sand. After a 1 hour inter-trial interval, one flask was replaced with a tower of Lego bricks and duration of interaction was assessed in a 5 min trial. Exploration time for each object were measured by stopwatch by the experimenter. Preference for the novel object was expressed as Discrimination index: ($time_{novel\ object}$- $time_{familiar\ object}$)/($time_{novel\ object}$+$time_{familiar\ object}$). If a mouse exhibits less than 2 second in the total time exploring the objects ($time_{novel\ object}$+$time_{familiar\ object}$), it was excluded from the analysis. Object exploration was defined as the orientation of the mouse snout toward the object, sniffing or touching with the snout within 2 cm proximity. Not considered as exploration time were leaning, climbing, looking over or biting the object. The position of the objects in the test was counterbalanced between the animals in a group.

5. Appendix

5.1. Index of figures

5.2. Index of abbreviations

AS	Alternative spliced segment
bp	base pair
CA	Cornu ammonis
Camk2	Ca2+/calmodulin-dependent protein kinase 2
Cbln	Cerebellin
CCK	Cholecystokinin
DG	Dentate gyrus
DSCAM	Down Syndrom cell adhesion molecule
E14.5	Embryonic stage 14.5
Elfn1	Extracellular leucine-rich fibronectin containing 1 protein
fl	Floxed
GABA	gamma-aminobutyric acid
GFP	Green fluorescence protein
mIPSC	Miniature inhibitory postsynaptic current
IPSP	Inhibitory postsynaptic potential
ISH	In Situ Hybridization
LAR	Leukocytes common antigen-related
NGL-3	Netrin-G ligand-3
NL2	Neuroligin 2
Nrxn	Neurexin
NYP	Neuropeptide Y
OLM	Oriens lacunosum moleculare
Pcdh	Protocadherin
PV	Parvalbumin
PTP	Protein tyrosine phosphatase
RT PCR	Reverse-transcribed polymerase chain reaction
SOM	Somatostatin
Syt2	Synaptotagmin 2
VSV	Vesicular stomatitis virus
qPCR	Quantitative qPCR

6. References

Agarwala, K.L., Ganesh, S., Tsutsumi, Y., Suzuki, T., Amano, K., and Yamakawa, K. (2001). Cloning and functional characterization of DSCAML1, a novel DSCAM-like cell adhesion molecule that mediates homophilic intercellular adhesion. Biochemical and biophysical research communications *285*, 760-772.

Anderson, G.R., Aoto, J., Tabuchi, K., Foldy, C., Covy, J., Yee, A.X., Wu, D., Lee, S.J., Chen, L., Malenka, R.C.*, et al.* (2015). beta-Neurexins Control Neural Circuits by Regulating Synaptic Endocannabinoid Signaling. Cell *162*, 593-606.

Ango, F., di Cristo, G., Higashiyama, H., Bennett, V., Wu, P., and Huang, Z.J. (2004). Ankyrin-based subcellular gradient of neurofascin, an immunoglobulin family protein, directs GABAergic innervation at purkinje axon initial segment. Cell *119*, 257-272.

Antunes, M., and Biala, G. (2012). The novel object recognition memory: neurobiology, test procedure, and its modifications. Cogn Process *13*, 93-110.

Aoto, J., Foldy, C., Ilcus, S.M., Tabuchi, K., and Sudhof, T.C. (2015). Distinct circuit-dependent functions of presynaptic neurexin-3 at GABAergic and glutamatergic synapses. Nature neuroscience *18*, 997-1007.

Aoto, J., Martinelli, D.C., Malenka, R.C., Tabuchi, K., and Sudhof, T.C. (2013). Presynaptic neurexin-3 alternative splicing trans-synaptically controls postsynaptic AMPA receptor trafficking. Cell *154*, 75-88.

Arlotta, P., Molyneaux, B.J., Chen, J., Inoue, J., Kominami, R., and Macklis, J.D. (2005). Neuronal subtype-specific genes that control corticospinal motor neuron development in vivo. Neuron *45*, 207-221.

Bannerman, D.M., Sprengel, R., Sanderson, D.J., McHugh, S.B., Rawlins, J.N., Monyer, H., and Seeburg, P.H. (2014). Hippocampal synaptic plasticity, spatial memory and anxiety. Nature reviews Neuroscience *15*, 181-192.

Barnes, S.A., Pinto-Duarte, A., Kappe, A., Zembrzycki, A., Metzler, A., Mukamel, E.A., Lucero, J., Wang, X., Sejnowski, T.J., Markou, A.*, et al.* (2015). Disruption of mGluR5 in parvalbumin-positive interneurons induces core features of neurodevelopmental disorders. Molecular psychiatry *20*, 1161-1172.

Barrow, S.L., Constable, J.R., Clark, E., El-Sabeawy, F., McAllister, A.K., and Washbourne, P. (2009). Neuroligin1: a cell adhesion molecule that recruits PSD-95 and NMDA receptors by distinct mechanisms during synaptogenesis. Neural Dev *4*, 17.

Bekirov, I.H., Needleman, L.A., Zhang, W., and Benson, D.L. (2002). Identification and localization of multiple classic cadherins in developing rat limbic system. Neuroscience *115*, 213-227.

Biederer, T., and Sudhof, T.C. (2000). Mints as adaptors. Direct binding to neurexins and recruitment of munc18. The Journal of biological chemistry *275*, 39803-39806.

Black, D.L. (2000). Protein diversity from alternative splicing: a challenge for bioinformatics and post-genome biology. Cell *103*, 367-370.

Black, D.L. (2003). Mechanisms of alternative pre-messenger RNA splicing. Annual review of biochemistry *72*, 291-336.

Boucard, A.A., Chubykin, A.A., Comoletti, D., Taylor, P., and Sudhof, T.C. (2005). A splice code for trans-synaptic cell adhesion mediated by binding of neuroligin 1 to alpha- and beta-neurexins. Neuron *48*, 229-236.

Buzsaki, G., and Moser, E.I. (2013). Memory, navigation and theta rhythm in the hippocampal-entorhinal system. Nature neuroscience *16*, 130-138.

Buzsaki, G., and Wang, X.J. (2012). Mechanisms of gamma oscillations. Annual review of neuroscience *35*, 203-225.

Castillo, P.E., Younts, T.J., Chavez, A.E., and Hashimotodani, Y. (2012). Endocannabinoid signaling and synaptic function. Neuron *76*, 70-81.

Chacon, P.J., del Marco, A., Arevalo, A., Dominguez-Gimenez, P., Garcia-Segura, L.M., and Rodriguez-Tebar, A. (2015). Cerebellin 4, a synaptic protein, enhances inhibitory activity and resistance of neurons to amyloid-beta toxicity. Neurobiol Aging *36*, 1057-1071.

Chen, B.E., Kondo, M., Garnier, A., Watson, F.L., Puettmann-Holgado, R., Lamar, D.R., and Schmucker, D. (2006). The molecular diversity of Dscam is functionally required for neuronal wiring specificity in Drosophila. Cell *125*, 607-620.

Chen, F., Venugopal, V., Murray, B., and Rudenko, G. (2011). The structure of neurexin 1alpha reveals features promoting a role as synaptic organizer. Structure *19*, 779-789.

Chen, M., and Manley, J.L. (2009). Mechanisms of alternative splicing regulation: insights from molecular and genomics approaches. Nat Rev Mol Cell Biol *10*, 741-754.

Chen, W.V., and Maniatis, T. (2013). Clustered protocadherins. Development *140*, 3297-3302.

Chih, B., Engelman, H., and Scheiffele, P. (2005a). Control of Excitatory and Inhibitory Synapse Formation by Neuroligins. Science (New York, NY *307*, 1324-1328.

Chih, B., Engelman, H., and Scheiffele, P. (2005b). Control of excitatory and inhibitory synapse formation by neuroligins. Science *307*, 1324-1328.

Chih, B., Gollan, L., and Scheiffele, P. (2006). Alternative splicing controls selective trans-synaptic interactions of the neuroligin-neurexin complex. Neuron *51*, 171-178.

Costa, M.R., and Muller, U. (2014). Specification of excitatory neurons in the developing cerebral cortex: progenitor diversity and environmental influences. Front Cell Neurosci *8*, 449.

de Wit, J., Sylwestrak, E., O'Sullivan, M.L., Otto, S., Tiglio, K., Savas, J.N., Yates, J.R., 3rd, Comoletti, D., Taylor, P., and Ghosh, A. (2009). LRRTM2 interacts with Neurexin1 and regulates excitatory synapse formation. Neuron *64*, 799-806.

Dean, C., Scholl, F.G., Choih, J., DeMaria, S., Berger, J., Isacoff, E., and Scheiffele, P. (2003). Neurexin mediates the assembly of presynaptic terminals. Nature neuroscience *6*, 708-716.

Donato, F., Chowdhury, A., Lahr, M., and Caroni, P. (2015). Early- and late-born parvalbumin basket cell subpopulations exhibiting distinct regulation and roles in learning. Neuron *85*, 770-786.

Donato, F., Rompani, S.B., and Caroni, P. (2013). Parvalbumin-expressing basket-cell network plasticity induced by experience regulates adult learning. Nature *504*, 272-276.

Ehrmann, I., Dalgliesh, C., Liu, Y., Danilenko, M., Crosier, M., Overman, L., Arthur, H.M., Lindsay, S., Clowry, G.J., Venables, J.P.*, et al.* (2013). The tissue-specific RNA binding protein T-STAR controls regional splicing patterns of neurexin pre-mRNAs in the brain. PLoS genetics *9*, e1003474.

Eid, J., Fehr, A., Gray, J., Luong, K., Lyle, J., Otto, G., Peluso, P., Rank, D., Baybayan, P., Bettman, B.*, et al.* (2009). Real-time DNA sequencing from single polymerase molecules. Science *323*, 133-138.

English, A.C., Richards, S., Han, Y., Wang, M., Vee, V., Qu, J., Qin, X., Muzny, D.M., Reid, J.G., Worley, K.C.*, et al.* (2012). Mind the gap: upgrading genomes with Pacific Biosciences RS long-read sequencing technology. PloS one *7*, e47768.

Ennaceur, A., and Delacour, J. (1988). A new one-trial test for neurobiological studies of memory in rats. 1: Behavioral data. Behavioural brain research *31*, 47-59.

Esumi, S., Kakazu, N., Taguchi, Y., Hirayama, T., Sasaki, A., Hirabayashi, T., Koide, T., Kitsukawa, T., Hamada, S., and Yagi, T. (2005). Monoallelic yet combinatorial expression of variable exons of the protocadherin-alpha gene cluster in single neurons. Nature genetics *37*, 171-176.

Etherton, M.R., Blaiss, C.A., Powell, C.M., and Sudhof, T.C. (2009). Mouse neurexin-1alpha deletion causes correlated electrophysiological and behavioral changes consistent with cognitive impairments. Proceedings of the National Academy of Sciences of the United States of America *106*, 17998-18003.

Fairless, R., Masius, H., Rohlmann, A., Heupel, K., Ahmad, M., Reissner, C., Dresbach, T., and Missler, M. (2008). Polarized targeting of neurexins to synapses is regulated by their C-terminal sequences. The Journal of neuroscience : the official journal of the Society for Neuroscience *28*, 12969-12981.

Fu, Y., and Huang, Z.J. (2010). Differential dynamics and activity-dependent regulation of alpha- and beta-neurexins at developing GABAergic synapses. Proc Natl Acad Sci U S A *107*, 22699-22704.

Fuccillo, M.V., Foldy, C., Gokce, O., Rothwell, P.E., Sun, G.L., Malenka, R.C., and Sudhof, T.C. (2015). Single-Cell mRNA Profiling Reveals Cell-Type-Specific Expression of Neurexin Isoforms. Neuron *87*, 326-340.

Fuchs, E.C., Zivkovic, A.R., Cunningham, M.O., Middleton, S., Lebeau, F.E., Bannerman, D.M., Rozov, A., Whittington, M.A., Traub, R.D., Rawlins, J.N.*, et al.* (2007). Recruitment of parvalbumin-positive interneurons determines hippocampal function and associated behavior. Neuron *53*, 591-604.

Futai, K., Doty, C.D., Baek, B., Ryu, J., and Sheng, M. (2013). Specific trans-synaptic interaction with inhibitory interneuronal neurexin underlies differential ability of neuroligins to induce functional inhibitory synapses. J Neurosci *33*, 3612-3623.

Garrett, A.M., Schreiner, D., Lobas, M.A., and Weiner, J.A. (2012). gamma-protocadherins control cortical dendrite arborization by regulating the activity of a FAK/PKC/MARCKS signaling pathway. Neuron *74*, 269-276.

Gauthier, J., Siddiqui, T.J., Huashan, P., Yokomaku, D., Hamdan, F.F., Champagne, N., Lapointe, M., Spiegelman, D., Noreau, A., Lafreniere, R.G.*, et al.* (2011). Truncating mutations in NRXN2 and NRXN1 in autism spectrum disorders and schizophrenia. Hum Genet *130*, 563-573.

Gibson, J.R., Huber, K.M., and Sudhof, T.C. (2009). Neuroligin-2 deletion selectively decreases inhibitory synaptic transmission originating from fast-spiking but not from somatostatin-positive interneurons. The Journal of neuroscience : the official journal of the Society for Neuroscience *29*, 13883-13897.

Graf, E.R., Kang, Y., Hauner, A.M., and Craig, A.M. (2006). Structure function and splice site analysis of the synaptogenic activity of the neurexin-1 beta LNS domain. J Neurosci *26*, 4256-4265.

Graf, E.R., Zhang, X., Jin, S.X., Linhoff, M.W., and Craig, A.M. (2004). Neurexins induce differentiation of GABA and glutamate postsynaptic specializations via neuroligins. Cell *119*, 1013-1026.

Gurskaya, N.G., Staroverov, D.B., Zhang, L., Fradkov, A.F., Markina, N.M., Pereverzev, A.P., and Lukyanov, K.A. (2012). Analysis of alternative splicing of cassette exons at single-cell level using two fluorescent proteins. Nucleic acids research *40*, e57.

Harris, K.D., and Mrsic-Flogel, T.D. (2013). Cortical connectivity and sensory coding. Nature *503*, 51-58.

Hata, Y., Butz, S., and Sudhof, T.C. (1996). CASK: a novel dlg/PSD95 homolog with an N-terminal calmodulin-dependent protein kinase domain identified by interaction with neurexins. The Journal of neuroscience : the official journal of the Society for Neuroscience *16*, 2488-2494.

Hattori, D., Chen, Y., Matthews, B.J., Salwinski, L., Sabatti, C., Grueber, W.B., and Zipursky, S.L. (2009). Robust discrimination between self and non-self neurites requires thousands of Dscam1 isoforms. Nature *461*, 644-648.

Hefft, S., and Jonas, P. (2005). Asynchronous GABA release generates long-lasting inhibition at a hippocampal interneuron-principal neuron synapse. Nature neuroscience *8*, 1319-1328.

Heiman, M., Kulicke, R., Fenster, R.J., Greengard, P., and Heintz, N. (2014). Cell type-specific mRNA purification by translating ribosome affinity purification (TRAP). Nature protocols *9*, 1282-1291.

Heine, M., Thoumine, O., Mondin, M., Tessier, B., Giannone, G., and Choquet, D. (2008). Activity-independent and subunit-specific recruitment of functional AMPA receptors at neurexin/neuroligin contacts. Proceedings of the National Academy of Sciences of the United States of America *105*, 20947-20952.

Hippenmeyer, S., Vrieseling, E., Sigrist, M., Portmann, T., Laengle, C., Ladle, D.R., and Arber, S. (2005). A developmental switch in the response of DRG neurons to ETS transcription factor signaling. PLoS Biol *3*, e159.

Hirano, K., Kaneko, R., Izawa, T., Kawaguchi, M., Kitsukawa, T., and Yagi, T. (2012). Single-neuron diversity generated by Protocadherin-beta cluster in mouse central and peripheral nervous systems. Front Mol Neurosci *5*, 90.

Hu, H., Gan, J., and Jonas, P. (2014). Interneurons. Fast-spiking, parvalbumin(+) GABAergic interneurons: from cellular design to microcircuit function. Science *345*, 1255263.

Hughes, M.E., Bortnick, R., Tsubouchi, A., Baumer, P., Kondo, M., Uemura, T., and Schmucker, D. (2007). Homophilic Dscam interactions control complex dendrite morphogenesis. Neuron *54*, 417-427.

Ichtchenko, K., Hata, Y., Nguyen, T., Ullrich, B., Missler, M., Moomaw, C., and Sudhof, T.C. (1995). Neuroligin 1: a splice site-specific ligand for beta-neurexins. Cell *81*, 435-443.

Iijima, T., Iijima, Y., Witte, H., and Scheiffele, P. (2014). Neuronal cell type-specific alternative splicing is regulated by the KH domain protein SLM1. The Journal of cell biology *204*, 331-342.

Iijima, T., Miura, E., Matsuda, K., Kamekawa, Y., Watanabe, M., and Yuzaki, M. (2007). Characterization of a transneuronal cytokine family Cbln--regulation of secretion by heteromeric assembly. The European journal of neuroscience *25*, 1049-1057.

Iijima, T., Wu, K., Witte, H., Hanno-Iijima, Y., Glatter, T., Richard, S., and Scheiffele, P. (2011). SAM68 regulates neuronal activity-dependent alternative splicing of neurexin-1. Cell *147*, 1601-1614.

Ito-Ishida, A., Miyazaki, T., Miura, E., Matsuda, K., Watanabe, M., Yuzaki, M., and Okabe, S. (2012a). Presynaptically released Cbln1 induces dynamic axonal structural changes by interacting with GluD2 during cerebellar synapse formation. Neuron *76*, 549-564.

Ito-Ishida, A., Miyazaki, T., Miura, E., Matsuda, K., Watanabe, M., Yuzaki, M., and Okabe, S. (2012b). Presynaptically released Cbln1 induces dynamic axonal structural changes by interacting with GluD2 during cerebellar synapse formation. Developmental Cell.

Kalinovsky, A., Boukhtouche, F., Blazeski, R., Bornmann, C., Suzuki, N., Mason, C.A., and Scheiffele, P. (2011). Development of axon-target specificity of ponto-cerebellar afferents. PLoS biology *9*, e1001013.

Kaneko, R., Kato, H., Kawamura, Y., Esumi, S., Hirayama, T., Hirabayashi, T., and Yagi, T. (2006). Allelic gene regulation of Pcdh-alpha and Pcdh-gamma clusters involving both monoallelic and biallelic expression in single Purkinje cells. The Journal of biological chemistry *281*, 30551-30560.

Kelemen, O., Convertini, P., Zhang, Z., Wen, Y., Shen, M., Falaleeva, M., and Stamm, S. (2013). Function of alternative splicing. Gene *514*, 1-30.

Kepecs, A., and Fishell, G. (2014). Interneuron cell types are fit to function. Nature *505*, 318-326.

Kim, H.G., Kishikawa, S., Higgins, A.W., Seong, I.S., Donovan, D.J., Shen, Y., Lally, E., Weiss, L.A., Najm, J., Kutsche, K.*, et al.* (2008). Disruption of neurexin 1 associated with autism spectrum disorder. American journal of human genetics *82*, 199-207.

Kirov, G., Rujescu, D., Ingason, A., Collier, D.A., O'Donovan, M.C., and Owen, M.J. (2009). Neurexin 1 (NRXN1) deletions in schizophrenia. Schizophr Bull *35*, 851-854.

Klausberger, T., Magill, P.J., Marton, L.F., Roberts, J.D., Cobden, P.M., Buzsaki, G., and Somogyi, P. (2003). Brain-state- and cell-type-specific firing of hippocampal interneurons in vivo. Nature *421*, 844-848.

Klausberger, T., and Somogyi, P. (2008). Neuronal diversity and temporal dynamics: the unity of hippocampal circuit operations. Science *321*, 53-57.

Ko, J., Fuccillo, M.V., Malenka, R.C., and Sudhof, T.C. (2009). LRRTM2 functions as a neurexin ligand in promoting excitatory synapse formation. Neuron *64*, 791-798.

Koehnke, J., Jin, X., Trbovic, N., Katsamba, P.S., Brasch, J., Ahlsen, G., Scheiffele, P., Honig, B., Palmer, A.G., 3rd, and Shapiro, L. (2008). Crystal structures of beta-neurexin 1 and beta-neurexin 2 ectodomains and dynamics of splice insertion sequence 4. Structure *16*, 410-421.

Koehnke, J., Katsamba, P.S., Ahlsen, G., Bahna, F., Vendome, J., Honig, B., Shapiro, L., and Jin, X. (2010). Splice form dependence of beta-neurexin/neuroligin binding interactions. Neuron *67*, 61-74.

Krueger, D.D., Tuffy, L.P., Papadopoulos, T., and Brose, N. (2012). The role of neurexins and neuroligins in the formation, maturation, and function of vertebrate synapses. Current opinion in neurobiology *22*, 412-422.

Kuroyanagi, H., Kobayashi, T., Mitani, S., and Hagiwara, M. (2006). Transgenic alternative-splicing reporters reveal tissue-specific expression profiles and regulation mechanisms in vivo. Nature methods *3*, 909-915.

Kuroyanagi, H., Watanabe, Y., and Hagiwara, M. (2013). CELF family RNA-binding protein UNC-75 regulates two sets of mutually exclusive exons of the unc-32 gene in neuron-specific manners in Caenorhabditis elegans. PLoS genetics *9*, e1003337.

Kuwako, K., Nishimoto, Y., Kawase, S., Okano, H.J., and Okano, H. (2014). Cadherin-7 regulates mossy fiber connectivity in the cerebellum. Cell Rep *9*, 311-323.

Lefebvre, J.L., Kostadinov, D., Chen, W.V., Maniatis, T., and Sanes, J.R. (2012). Protocadherins mediate dendritic self-avoidance in the mammalian nervous system. Nature *488*, 517-521.

Levi, S., Grady, R.M., Henry, M.D., Campbell, K.P., Sanes, J.R., and Craig, A.M. (2002). Dystroglycan is selectively associated with inhibitory GABAergic synapses but is dispensable for their differentiation. The Journal of neuroscience : the official journal of the Society for Neuroscience *22*, 4274-4285.

Li, Q., Lee, J.A., and Black, D.L. (2007). Neuronal regulation of alternative pre-mRNA splicing. Nature reviews Neuroscience *8*, 819-831.

Lohmann, C., and Bonhoeffer, T. (2008). A role for local calcium signaling in rapid synaptic partner selection by dendritic filopodia. Neuron *59*, 253-260.

Matthews, B.J., Kim, M.E., Flanagan, J.J., Hattori, D., Clemens, J.C., Zipursky, S.L., and Grueber, W.B. (2007). Dendrite self-avoidance is controlled by Dscam. Cell *129*, 593-604.

McGlincy, N.J., and Smith, C.W. (2008). Alternative splicing resulting in nonsense-mediated mRNA decay: what is the meaning of nonsense? Trends in biochemical sciences *33*, 385-393.

Miles, R., Toth, K., Gulyas, A.I., Hajos, N., and Freund, T.F. (1996). Differences between somatic and dendritic inhibition in the hippocampus. Neuron *16*, 815-823.

Miller, M.T., Mileni, M., Comoletti, D., Stevens, R.C., Harel, M., and Taylor, P. (2011). The crystal structure of the alpha-neurexin-1 extracellular region reveals a hinge point for mediating synaptic adhesion and function. Structure *19*, 767-778.

Missler, M., Hammer, R.E., and Sudhof, T.C. (1998). Neurexophilin binding to alpha-neurexins. A single LNS domain functions as an independently folding ligand-binding unit. The Journal of biological chemistry *273*, 34716-34723.

Missler, M., Sudhof, T.C., and Biederer, T. (2012). Synaptic cell adhesion. Cold Spring Harb Perspect Biol *4*, a005694.

Missler, M., Zhang, W., Rohlmann, A., Kattenstroth, G., Hammer, R.E., Gottmann, K., and Sudhof, T.C. (2003). Alpha-neurexins couple Ca2+ channels to synaptic vesicle exocytosis. Nature *423*, 939-948.

Miura, S.K., Martins, A., Zhang, K.X., Graveley, B.R., and Zipursky, S.L. (2013). Probabilistic splicing of Dscam1 establishes identity at the level of single neurons. Cell *155*, 1166-1177.

Molyneaux, B.J., Arlotta, P., Menezes, J.R., and Macklis, J.D. (2007). Neuronal subtype specification in the cerebral cortex. Nature reviews Neuroscience *8*, 427-437.

Mondin, M., Labrousse, V., Hosy, E., Heine, M., Tessier, B., Levet, F., Poujol, C., Blanchet, C., Choquet, D., and Thoumine, O. (2011). Neurexin-neuroligin adhesions capture surface-diffusing AMPA receptors through PSD-95 scaffolds. The Journal of neuroscience : the official journal of the Society for Neuroscience *31*, 13500-13515.

Neves, G., Zucker, J., Daly, M., and Chess, A. (2004). Stochastic yet biased expression of multiple Dscam splice variants by individual cells. Nature genetics *36*, 240-246.

Newman, E.A., Muh, S.J., Hovhannisyan, R.H., Warzecha, C.C., Jones, R.B., McKeehan, W.L., and Carstens, R.P. (2006). Identification of RNA-binding proteins that regulate FGFR2 splicing through the use of sensitive and specific dual color fluorescence minigene assays. Rna *12*, 1129-1141.

O'Connor, V.M., Shamotienko, O., Grishin, E., and Betz, H. (1993). On the structure of the 'synaptosecretosome'. Evidence for a neurexin/synaptotagmin/syntaxin/Ca2+ channel complex. FEBS letters *326*, 255-260.

Ohno, G., Hagiwara, M., and Kuroyanagi, H. (2008). STAR family RNA-binding protein ASD-2 regulates developmental switching of mutually exclusive alternative splicing in vivo. Genes & development *22*, 360-374.

Orengo, J.P., Bundman, D., and Cooper, T.A. (2006). A bichromatic fluorescent reporter for cell-based screens of alternative splicing. Nucleic acids research *34*, e148.

Pan, Q., Shai, O., Lee, L.J., Frey, B.J., and Blencowe, B.J. (2008). Deep surveying of alternative splicing complexity in the human transcriptome by high-throughput sequencing. Nature genetics *40*, 1413-1415.

Petrenko, A.G., Kovalenko, V.A., Shamotienko, O.G., Surkova, I.N., Tarasyuk, T.A., Ushkaryov Yu, A., and Grishin, E.V. (1990). Isolation and properties of the alpha-latrotoxin receptor. The EMBO journal *9*, 2023-2027.

Pettem, K.L., Yokomaku, D., Luo, L., Linhoff, M.W., Prasad, T., Connor, S.A., Siddiqui, T.J., Kawabe, H., Chen, F., Zhang, L.*, et al.* (2013). The specific alpha-neurexin interactor calsyntenin-3 promotes excitatory and inhibitory synapse development. Neuron *80*, 113-128.

Pouille, F., and Scanziani, M. (2004). Routing of spike series by dynamic circuits in the hippocampus. Nature *429*, 717-723.

Poulopoulos, A., Aramuni, G., Meyer, G., Soykan, T., Hoon, M., Papadopoulos, T., Zhang, M., Paarmann, I., Fuchs, C., Harvey, K.*, et al.* (2009). Neuroligin 2 drives postsynaptic assembly at perisomatic inhibitory synapses through gephyrin and collybistin. Neuron *63*, 628-642.

Rabaneda, L.G., Robles-Lanuza, E., Nieto-Gonzalez, J.L., and Scholl, F.G. (2014). Neurexin dysfunction in adult neurons results in autistic-like behavior in mice. Cell Rep *8*, 338-346.

Reissner, C., Runkel, F., and Missler, M. (2013). Neurexins. Genome Biol *14*, 213.

Reissner, C., Stahn, J., Breuer, D., Klose, M., Pohlentz, G., Mormann, M., and Missler, M. (2014). Dystroglycan binding to alpha-neurexin competes with neurexophilin-1 and neuroligin in the brain. The Journal of biological chemistry *289*, 27585-27603.

Rossignol, E., Kruglikov, I., van den Maagdenberg, A.M., Rudy, B., and Fishell, G. (2013). CaV 2.1 ablation in cortical interneurons selectively impairs fast-spiking basket cells and causes generalized seizures. Ann Neurol *74*, 209-222.

Rubinstein, R., Thu, C.A., Goodman, K.M., Wolcott, H.N., Bahna, F., Mannepalli, S., Ahlsen, G., Chevee, M., Halim, A., Clausen, H.*, et al.* (2015). Molecular logic of neuronal self-recognition through protocadherin domain interactions. Cell *163*, 629-642.

Rujescu, D., Ingason, A., Cichon, S., Pietilainen, O.P., Barnes, M.R., Toulopoulou, T., Picchioni, M., Vassos, E., Ettinger, U., Bramon, E.*, et al.* (2009). Disruption of the neurexin 1 gene is associated with schizophrenia. Hum Mol Genet *18*, 988-996.

Saito, T., and Nakatsuji, N. (2001). Efficient gene transfer into the embryonic mouse brain using in vivo electroporation. Dev Biol *240*, 237-246.

Sanes, J.R., and Yamagata, M. (2009). Many paths to synaptic specificity. Annu Rev Cell Dev Biol *25*, 161-195.

Sanz, E., Yang, L., Su, T., Morris, D.R., McKnight, G.S., and Amieux, P.S. (2009). Cell-type-specific isolation of ribosome-associated mRNA from complex tissues. Proc Natl Acad Sci U S A *106*, 13939-13944.

Schaeren-Wiemers, N., and Gerfin-Moser, A. (1993). A single protocol to detect transcripts of various types and expression levels in neural tissue and cultured cells: in situ hybridization using digoxigenin-labelled cRNA probes. Histochemistry *100*, 431-440.

Scheiffele, P., Fan, J., Choih, J., Fetter, R., and Serafini, T. (2000). Neuroligin expressed in nonneuronal cells triggers presynaptic development in contacting axons. Cell *101*, 657-669.

Schmucker, D., Clemens, J.C., Shu, H., Worby, C.A., Xiao, J., Muda, M., Dixon, J.E., and Zipursky, S.L. (2000). Drosophila Dscam is an axon guidance receptor exhibiting extraordinary molecular diversity. Cell *101*, 671-684.

Schneggenburger, R., and Neher, E. (2005). Presynaptic calcium and control of vesicle fusion. Current opinion in neurobiology *15*, 266-274.

Schreiner, D., Nguyen, T.M., Russo, G., Heber, S., Patrignani, A., Ahrne, E., and Scheiffele, P. (2014a). Targeted combinatorial alternative splicing generates brain region-specific repertoires of neurexins. Neuron *84*, 386-398.

Schreiner, D., Nguyen, T.M., Russo, G., Hebert, S., Patrignani, A., Arnhe, E., and Scheiffele, P. (2014b). Targeted Combinatorial Alternative Splicing Generates Brain Region-Specific Repertoires of Neurexins. Neuron *84*, 386-398.

Schreiner, D., Nguyen, T.M., and Scheiffele, P. (2014c). Polymorphic receptors: neuronal functions and molecular mechanisms of diversification. Current opinion in neurobiology *27*, 25-30.

Schreiner, D., Simicevic, J., Ahrne, E., Schmidt, A., and Scheiffele, P. (2015). Quantitative isoform-profiling of highly diversified recognition molecules. eLife *4*.

Schreiner, D., and Weiner, J.A. (2010). Combinatorial homophilic interaction between gamma-protocadherin multimers greatly expands the molecular diversity of cell adhesion. Proceedings of the National Academy of Sciences of the United States of America *107*, 14893-14898.

Shen, K., and Scheiffele, P. (2010). Genetics and cell biology of building specific synaptic connectivity. Annual review of neuroscience *33*, 473-507.

Shen, K.C., Kuczynska, D.A., Wu, I.J., Murray, B.H., Sheckler, L.R., and Rudenko, G. (2008). Regulation of neurexin 1beta tertiary structure and ligand binding through alternative splicing. Structure *16*, 422-431.

Soba, P., Zhu, S., Emoto, K., Younger, S., Yang, S.J., Yu, H.H., Lee, T., Jan, L.Y., and Jan, Y.N. (2007). Drosophila sensory neurons require Dscam for dendritic self-avoidance and proper dendritic field organization. Neuron *54*, 403-416.

Sohal, V.S., Zhang, F., Yizhar, O., and Deisseroth, K. (2009). Parvalbumin neurons and gamma rhythms enhance cortical circuit performance. Nature *459*, 698-702.

Sommeijer, J.P., and Levelt, C.N. (2012). Synaptotagmin-2 is a reliable marker for parvalbumin positive inhibitory boutons in the mouse visual cortex. PLoS One *7*, e35323.

Spafford, J.D., and Zamponi, G.W. (2003). Functional interactions between presynaptic calcium channels and the neurotransmitter release machinery. Current opinion in neurobiology *13*, 308-314.

Spellman, R., and Smith, C.W. (2006). Novel modes of splicing repression by PTB. Trends in biochemical sciences *31*, 73-76.

Sperry, R.W. (1963). Chemoaffinity in the Orderly Growth of Nerve Fiber Patterns and Connections. Proceedings of the National Academy of Sciences of the United States of America *50*, 703-710.

Stoss, O., Novoyatleva, T., Gencheva, M., Olbrich, M., Benderska, N., and Stamm, S. (2004). p59(fyn)-mediated phosphorylation regulates the activity of the tissue-specific splicing factor rSLM-1. Mol Cell Neurosci *27*, 8-21.

Sugita, S., Saito, F., Tang, J., Satz, J., Campbell, K., and Sudhof, T.C. (2001). A stoichiometric complex of neurexins and dystroglycan in brain. The Journal of cell biology *154*, 435-445.

Sylwestrak, E.L., and Ghosh, A. (2012). Elfn1 regulates target-specific release probability at CA1-interneuron synapses. Science *338*, 536-540.

Tabata, H., and Nakajima, K. (2001). Efficient in utero gene transfer system to the developing mouse brain using electroporation: visualization of neuronal migration in the developing cortex. Neuroscience *103*, 865-872.

Tabuchi, K., and Sudhof, T.C. (2002). Structure and evolution of neurexin genes: insight into the mechanism of alternative splicing. Genomics *79*, 849-859.

Tacke, R., and Manley, J.L. (1999). Determinants of SR protein specificity. Current opinion in cell biology *11*, 358-362.

Takacs, V.T., Szonyi, A., Freund, T.F., Nyiri, G., and Gulyas, A.I. (2015). Quantitative ultrastructural analysis of basket and axo-axonic cell terminals in the mouse hippocampus. Brain Struct Funct *220*, 919-940.

Takahashi, H., and Craig, A.M. (2013). Protein tyrosine phosphatases PTPdelta, PTPsigma, and LAR: presynaptic hubs for synapse organization. Trends in neurosciences *36*, 522-534.

Takahashi, H., Katayama, K., Sohya, K., Miyamoto, H., Prasad, T., Matsumoto, Y., Ota, M., Yasuda, H., Tsumoto, T., Aruga, J.*, et al.* (2012). Selective control of inhibitory synapse development by Slitrk3-PTPdelta trans-synaptic interaction. Nature neuroscience *15*, 389-398, S381-382.

Takeuchi, A., Hosokawa, M., Nojima, T., and Hagiwara, M. (2010). Splicing reporter mice revealed the evolutionally conserved switching mechanism of tissue-specific alternative exon selection. PloS one *5*, e10946.

Tasic, B., Nabholz, C.E., Baldwin, K.K., Kim, Y., Rueckert, E.H., Ribich, S.A., Cramer, P., Wu, Q., Axel, R., and Maniatis, T. (2002). Promoter choice determines splice site selection in protocadherin alpha and gamma pre-mRNA splicing. Mol Cell *10*, 21-33.

Thu, C.A., Chen, W.V., Rubinstein, R., Chevee, M., Wolcott, H.N., Felsovalyi, K.O., Tapia, J.C., Shapiro, L., Honig, B., and Maniatis, T. (2014). Single-cell identity generated by combinatorial homophilic interactions between alpha, beta, and gamma protocadherins. Cell *158*, 1045-1059.

Traunmuller, L., Bornmann, C., and Scheiffele, P. (2014). Alternative splicing coupled nonsense-mediated decay generates neuronal cell type-specific expression of SLM proteins. The Journal of neuroscience : the official journal of the Society for Neuroscience *34*, 16755-16761.

Treutlein, B., Gokce, O., Quake, S.R., and Sudhof, T.C. (2014). Cartography of neurexin alternative splicing mapped by single-molecule long-read mRNA sequencing. Proceedings of the National Academy of Sciences of the United States of America *111*, E1291-1299.

Tsien, J.Z., Chen, D.F., Gerber, D., Tom, C., Mercer, E.H., Anderson, D.J., Mayford, M., Kandel, E.R., and Tonegawa, S. (1996). Subregion- and cell type-restricted gene knockout in mouse brain. Cell *87*, 1317-1326.

Uemura, T., Lee, S.J., Yasumura, M., Takeuchi, T., Yoshida, T., Ra, M., Taguchi, R., Sakimura, K., and Mishina, M. (2010). Trans-synaptic interaction of GluRdelta2 and Neurexin through Cbln1 mediates synapse formation in the cerebellum. Cell *141*, 1068-1079.

Ullrich, B., Ushkaryov, Y.A., and Sudhof, T.C. (1995). Cartography of neurexins: more than 1000 isoforms generated by alternative splicing and expressed in distinct subsets of neurons. Neuron *14*, 497-507.

Ushkaryov, Y.A., Hata, Y., Ichtchenko, K., Moomaw, C., Afendis, S., Slaughter, C.A., and Sudhof, T.C. (1994). Conserved domain structure of beta-neurexins. Unusual cleaved signal sequences in receptor-like neuronal cell-surface proteins. The Journal of biological chemistry *269*, 11987-11992.

Ushkaryov, Y.A., Petrenko, A.G., Geppert, M., and Sudhof, T.C. (1992). Neurexins: synaptic cell surface proteins related to the alpha-latrotoxin receptor and laminin. Science *257*, 50-56.

Vaags, A.K., Lionel, A.C., Sato, D., Goodenberger, M., Stein, Q.P., Curran, S., Ogilvie, C., Ahn, J.W., Drmic, I., Senman, L.*, et al.* (2012). Rare deletions at the neurexin 3 locus in autism spectrum disorder. American journal of human genetics *90*, 133-141.

Varoqueaux, F., Jamain, S., and Brose, N. (2004a). Neuroligin 2 is exclusively localized to inhibitory synapses. Eur J Cell Biol *83*, 449-456.

Varoqueaux, F., Jamain, S., and Brose, N. (2004b). Neuroligin 2 is exclusively localized to inhibitory synapses. Eur J Cell Biol *83*, 449-456.

Vrieseling, E., and Arber, S. (2006). Target-induced transcriptional control of dendritic patterning and connectivity in motor neurons by the ETS gene Pea3. Cell *127*, 1439-1452.

Wang, E.T., Sandberg, R., Luo, S., Khrebtukova, I., Zhang, L., Mayr, C., Kingsmore, S.F., Schroth, G.P., and Burge, C.B. (2008). Alternative isoform regulation in human tissue transcriptomes. Nature *456*, 470-476.

Wang, J., Zugates, C.T., Liang, I.H., Lee, C.H., and Lee, T. (2002a). Drosophila Dscam is required for divergent segregation of sister branches and suppresses ectopic bifurcation of axons. Neuron *33*, 559-571.

Wang, X., Su, H., and Bradley, A. (2002b). Molecular mechanisms governing Pcdh-gamma gene expression: evidence for a multiple promoter and cis-alternative splicing model. Genes & development *16*, 1890-1905.

Warburton, E.C., and Brown, M.W. (2015). Neural circuitry for rat recognition memory. Behavioural brain research *285*, 131-139.

Wei, P., Pattarini, R., Rong, Y., Guo, H., Bansal, P.K., Kusnoor, S.V., Deutch, A.Y., Parris, J., and Morgan, J.I. (2012). The Cbln family of proteins interact with multiple signaling pathways. Journal of neurochemistry *121*, 717-729.

West, A.E., and Greenberg, M.E. (2011). Neuronal activity-regulated gene transcription in synapse development and cognitive function. Cold Spring Harb Perspect Biol *3*.

Williams, M.E., Wilke, S.A., Daggett, A., Davis, E., Otto, S., Ravi, D., Ripley, B., Bushong, E.A., Ellisman, M.H., Klein, G.*, et al.* (2011). Cadherin-9 regulates synapse-specific differentiation in the developing hippocampus. Neuron *71*, 640-655.

Wohr, M., Orduz, D., Gregory, P., Moreno, H., Khan, U., Vorckel, K.J., Wolfer, D.P., Welzl, H., Gall, D., Schiffmann, S.N.*, et al.* (2015). Lack of parvalbumin in mice leads to behavioral deficits relevant to all human autism core symptoms and related neural morphofunctional abnormalities. Transl Psychiatry *5*, e525.

Wojtowicz, W.M., Flanagan, J.J., Millard, S.S., Zipursky, S.L., and Clemens, J.C. (2004). Alternative splicing of Drosophila Dscam generates axon guidance receptors that exhibit isoform-specific homophilic binding. Cell *118*, 619-633.

Wonders, C.P., and Anderson, S.A. (2006). The origin and specification of cortical interneurons. Nature reviews Neuroscience *7*, 687-696.

Woo, J., Kwon, S.K., Choi, S., Kim, S., Lee, J.R., Dunah, A.W., Sheng, M., and Kim, E. (2009). Trans-synaptic adhesion between NGL-3 and LAR regulates the formation of excitatory synapses. Nature neuroscience *12*, 428-437.

Woo, J., Kwon, S.K., Nam, J., Choi, S., Takahashi, H., Krueger, D., Park, J., Lee, Y., Bae, J.Y., Lee, D.*, et al.* (2013). The adhesion protein IgSF9b is coupled to neuroligin 2 via S-SCAM to promote inhibitory synapse development. The Journal of cell biology *201*, 929-944.

Wu, L.G., Hamid, E., Shin, W., and Chiang, H.C. (2014). Exocytosis and endocytosis: modes, functions, and coupling mechanisms. Annu Rev Physiol *76*, 301-331.

Wu, L.G., Westenbroek, R.E., Borst, J.G., Catterall, W.A., and Sakmann, B. (1999). Calcium channel types with distinct presynaptic localization couple differentially to transmitter release in single calyx-type synapses. The Journal of neuroscience : the official journal of the Society for Neuroscience *19*, 726-736.

Wu, Q., and Maniatis, T. (1999). A striking organization of a large family of human neural cadherin-like cell adhesion genes. Cell *97*, 779-790.

Wu, Q., Zhang, T., Cheng, J.F., Kim, Y., Grimwood, J., Schmutz, J., Dickson, M., Noonan, J.P., Zhang, M.Q., Myers, R.M.*, et al.* (2001). Comparative DNA sequence analysis of mouse and human protocadherin gene clusters. Genome research *11*, 389-404.

Yan, J., Noltner, K., Feng, J., Li, W., Schroer, R., Skinner, C., Zeng, W., Schwartz, C.E., and Sommer, S.S. (2008). Neurexin 1alpha structural variants associated with autism. Neuroscience letters *438*, 368-370.

Yang, X., Coulombe-Huntington, J., Kang, S., Sheynkman, G.M., Hao, T., Richardson, A., Sun, S., Yang, F., Shen, Y.A., Murray, R.R.*, et al.* (2016). Widespread Expansion of Protein Interaction Capabilities by Alternative Splicing. Cell *164*, 805-817.

Yasumura, M., Yoshida, T., Lee, S.J., Uemura, T., Joo, J.Y., and Mishina, M. (2012). Glutamate receptor delta1 induces preferentially inhibitory presynaptic differentiation of cortical neurons by interacting with neurexins through cerebellin precursor protein subtypes. Journal of neurochemistry *121*, 705-716.

Yogev, S., and Shen, K. (2014). Cellular and molecular mechanisms of synaptic specificity. Annual review of cell and developmental biology *30*, 417-437.

Zhang, C., Atasoy, D., Arac, D., Yang, X., Fucillo, M.V., Robison, A.J., Ko, J., Brunger, A.T., and Sudhof, T.C. (2010). Neurexins physically and functionally interact with GABA(A) receptors. Neuron *66*, 403-416.

Zhang, W., Rohlmann, A., Sargsyan, V., Aramuni, G., Hammer, R.E., Sudhof, T.C., and Missler, M. (2005). Extracellular domains of alpha-neurexins participate in regulating synaptic transmission by selectively affecting N- and P/Q-type Ca2+ channels. The Journal of neuroscience : the official journal of the Society for Neuroscience *25*, 4330-4342.

Zhu, H., Hummel, T., Clemens, J.C., Berdnik, D., Zipursky, S.L., and Luo, L. (2006). Dendritic patterning by Dscam and synaptic partner matching in the Drosophila antennal lobe. Nature neuroscience *9*, 349-355.

Zipursky, S.L., and Grueber, W.B. (2013). The molecular basis of self-avoidance. Annual review of neuroscience *36*, 547-568.

Zipursky, S.L., and Sanes, J.R. (2010). Chemoaffinity revisited: dscams, protocadherins, and neural circuit assembly. Cell *143*, 343-353.

Acknowledgments

I would like to thank my advisor Peter Scheiffele, for his support and training during my PhD. He was a great mentor and his knowledge and expertise have often been critical for unravelling situations that looked like impasse but also for adding more depth in the projects. Moreover I am very grateful for the constructive inputs and fruitful discussions throughout the years.

I would like to thank the whole Scheiffele lab for all the advices and help and also for the nice work atmosphere. In particular, I would like to thank Dietmar Schreiner. I thank him for all the discussions about data or science and for the advices and inputs he generously always gave. Then, I am extremely grateful to Andrea Gomez and Le Xiao, who performed the electrophysiology recordings. I also thank Le for her support through stimulating discussions and inputs and for the time she spent to educate me about electrophysiology. Finally, I would like to thank Oriane Mauger for her expertise and inputs during the Ribotag project and also for her infallible optimism.

THI-MINH NGUYEN

Muespacherstrasse 44, 4055 Basel
thiminh.ng@gmail.com

Telephone +41 79 369 76 44
Swiss (born in Fribourg)

Doctoral candidate, University of Basel, Biozentrum may 2009 – april 2016
Research group: Peter Scheiffele (Neurosciences)

Master in Science of Molecular Biology, University of Basel 2011
Research group: Witold Filipowicz (Cellbiology)

Bachelor in Science of Biology, University of Basel 2009

Course: English for Natural Scientist, Sprachenzentrum, Basel Fall semester 2009

Languages:
- French (native speaker)
- English (working language C1/C2)
- German (working language C1/C2); Swiss German (Good knowledge B2)
- Vietnamiese (Good knowledge B1)

Computer Skills: MS Office Suite (PC), Adobe Illustrator and Photoshop, Graphpad, Image softwares (Metamorph and Imaris)

Award: Fellow of Biozentrum Basel international PhD program “Fellowship for Excellence”